

ISTANBUL TECHNICAL UNIVERSITY ★ GRADUATE SCHOOL OF SCIENCE
ENGINEERING AND TECHNOLOGY

**FABRICATION AND CHARACTERIZATION
OF REVERSE OSMOSIS MEMBRANES HAVING ANTIBACTERIAL
PROPERTIES**

M.Sc. THESIS

Şeyma Yılmaz

Department of Environmental Engineering

Environmental Biotechnology Programme

MAY 2015

ISTANBUL TECHNICAL UNIVERSITY ★ GRADUATE SCHOOL OF SCIENCE
ENGINEERING AND TECHNOLOGY

**FABRICATION AND CHARACTERIZATION
OF REVERSE OSMOSIS MEMBRANES HAVING ANTIBACTERIAL
PROPERTIES**

M.Sc. THESIS

**Şeyma Yılmaz
(501131806)**

Department of Environmental Engineering

Environmental Biotechnology Programme

Thesis Advisor: Doç. Dr. Derya Yüksel İMER

May 2015

Şeyma Yılmaz, a **M.Sc.** student of ITU **Graduate School of Science, Engineering and Technology** student ID **501131806**, successfully defended the **thesis** entitled “FABRICATION AND CHARACTERIZATION OF REVERSE OSMOSIS MEMBRANES HAVING ANTIBACTERIAL PROPERTIES”, which she prepared after fulfilling the requirements specified in the associated legislations, before the jury whose signatures are below.

Thesis Advisor : **Assoc. Prof. Derya Yüksel İMER**
İstanbul Technical University

Jury Members : **Prof. Dr. Ismail Koyuncu**
İstanbul Technical University

Assist. Prof. Serkan Ünal
Sabancı University

Date of Submission : 4 May 2015
Date of Defense : 27 May 2015

To my family and all beloved ones,

FOREWORD

First of all, I would like to thank my thesis supervisor Dr. Derya Yüksel İMER and Prof. Dr. İsmail KOYUNCU who shared own knowledge, supported me throughout my thesis and also appreciated for giving me the chance of working at MEMTEK as a member of his scientific research group. I am grateful to work with my project team Serkan GÜÇLÜ, Raed KHALDI, Müge BİÇER, Jalal SHARABATI. I really enjoyed work in such a great team, friends in MEMTEK. I also grateful to Tülay ERGÖR can for helping at bacterial tests.

Finally, I am especially grateful for love, support and patience of my very dear family, fiancée and friends who are always with me in my whole life. This study was financially supported by the TUBITAK-ÇAYDAG (The Scientific and Technological Research Council of Turkey) (Project No: 113Y356).

May 2015

Şeyma Yılmaz
(Environmental Engineer)

TABLE OF CONTENTS

	<u>Page</u>
FOREWORD	ix
TABLE OF CONTENTS.....	xi
ABBREVIATIONS	xiii
LIST OF TABLES	xv
LIST OF FIGURES	xvii
SUMMARY	xxi
ÖZET.....	xxiii
1.INTRODUCTION.....	1
1.1 Purpose of Thesis	2
1.2 Scope of Thesis	2
2. LITERATURE REVIEW.....	3
2.1 Membrane Technology	3
2.1.1 Role in water supply, sanitation, and reclamation	3
2.1.2 Membrane types and properties	4
2.1.3 Membrane materials.....	7
2.1.4 Membrane preparation	9
2.1.5 Membrane characterization.....	10
2.2 Reverse Osmosis Technology For Desalination	11
2.2.1 Preparation of thin film composite (TFC) membrane.....	15
2.2.2 Recent progress in the development in reverse osmosis membrane.....	16
2.2.2.1 Monomer types	16
2.2.2.2 Support layer	19
2.2.2.3 Process modification and additives	19
2.2.3 Application of RO membrane modules	21
2.3. Biofouling in RO membrane	23
2.3.1 Biofouling mechanism	25
2.3.2 Biofouling effects on membrane processes	27
2.3.3 Prevention and control of biofouling problem.....	27
2.3.3.1 Feed Pretreatment	27
2.3.3.2 Biocide application	28
2.3.3.3 Surface modification	29
2.3.3.4 Membrane cleaning	32
2.3.3.5 Improvement of interfacial polymerization process	32
2.4 Development Of Antifouling Reverse Osmosis Membrane With Bisbal Additive	33
2.4.1 Anti bacterial effects of BisBAL	33
2.4.2 Industrial applications of Bismuth-Thiols.....	35
3. MATERIALS & METHODS.....	39
3.1. Materials	39
3.1.2 Fabrication of support layer of membranes	39

3.1.3 BisBAL preparation	44
3.2. Membrane Characterization Methods	46
3.2.1 Membrane thicknesses	46
3.2.2 Viscosity.....	47
3.2.3 Permeability	47
3.2.4 Contact angle.....	50
3.2.5 Fourier transformation infrared spectroscopy (FTIR).....	50
3.2.6 Surface charge	51
3.2.7 Scanning electron microscopy (SEM).....	51
3.2.8 Optical profilometer	52
3.2.9 Mechanical stability	52
3.2.10 Porometre analysis	53
3.2.10 Salt rejection.....	54
3.3. Antibacterial Experiments	54
3.3.1 Cultivation of <i>Escherichia coli</i> (<i>E. coli</i>)	54
3.3.1.1 Preparation of growth medium	55
3.3.1.2 Preparation of solid medium	55
3.3.1.3 Optical density measurement	56
3.3.1.4 Bacterial stock preparation	56
3.3.1.5 Dilution of <i>E.coli</i>	57
3.3.1.6 Counting of <i>E.Coli</i>	58
3.3.2 Antibacterial test	58
3.3.3 Flux reduction test.....	59
3.3.4 Confocal scanning laser microscopy (CLSM)	60
4. RESULTS & DISCUSSIONS.....	61
4.1 Characterization Results Of Support Layer.....	61
4.1.1 Thicknesses	61
4.1.2 Viscosity.....	61
4.1.3 Permeability	62
4.1.4 Contact angle.....	63
4.1.5 FTIR	64
4.1.6 Surface charge of membranes	65
4.1.7 Scanning electron microscopy (SEM).....	66
4.1.8 Optical profilometer	69
4.1.2 Selection of active layer	74
4.1.2.1 Filtration tests	74
4.1.2.2 Contact angle	75
4.1.2.3 FTIR	76
4.1.2.4. Surface charge	76
4.1.2.5 SEM	77
4.1.2.6 Optical profilometer	78
4.2 Antifouling Experiments	79
4.2.1 Culvitation of <i>E. coli</i>	79
4.2.2 Antibacterial test	80
4.2.2.1.SEM	81
4.2.2.2 CSLM	83
4.2.3 Flux graphs.....	85
5. CONCLUSIONS AND RECOMMENDATIONS	87
REFERENCES.....	91
CURRICULUM VITAE.....	12

ABBREVIATIONS

BisBAL	: Bismuth dimercaptopropanol
CA	: Cellulose acetate
PVDF	: Polyvinylidene fluoride
CN	: Cellulose nitrate
CSA	: Camphor sulfonic acid
CTA	: Cellulose triacetate
PA	: Aromatic polyamides
PC	: Polycarbonate
PAN	: Polyacrylonitrile
<i>P.Aeruginosa</i>	: <i>Pseudomonas Aeruginosa</i>
ΔP	: Pressure difference
ΔC	: Concentration difference
ΔY	: Electrical potential difference
ΔT	: Temperature difference
RO	: Reverse osmosis
NF	: Nanofiltration
UF	: Ultrafiltration
MF	: Microfiltration
<i>E. coli</i>	: <i>Escherichia coli</i>
IP	: Interfacial polymerization
TFC	: Thin film composite
MPD	: Mphenylenediamine
TMC	: Trimesoyl chloride
PSF	: Polysulfon
S-BAPS	: Disulfonatedbis [4-(3- aminophenoxy)phenyl]sulfone
PTC	: Pyridine-2,4,6- tricarbonyl trichloride
TEA	: Triethylamine

LIST OF TABLES

	<u>Page</u>
Table 2.1: Membrane process configurations in the water industry	4
Table 2.2: Total dissolved salt concentrations for selected salt water bodies around the World.....	13
Table 2.3: Key differences between brackish water and seawater	13
Table 2.4: Different monomers for preparing TFC membrane.....	17
Table 2.5: Some Large Seawater Desalination Plants Utilizing RO Process in worldwide.....	22
Table 2.6: Salt rejection of commercial membranes at standard test conditions of 32,000 ppm NaCl solution at 5.5 MPa and 25 °C	22
Table 2.7 : Colloidal-organic matter complex membrane fouling mechanism.....	24
Table 2.8: Comparison chart for disinfectants used for bio-fouling control of SWRO membranes.	28
Table 3.1: Brands of materials used for the experiment.	39
Table 3.2: Prepared membranes and its properties	40
Table 3.3: Technical properties of the filtration system.....	48
Table 4.1: FTIR spectra of prepared UF PSF membranes	65
Table 4.2: Process parameters for TFC preparation.....	74
Table 4.3: Filtration Performance of prepared PA TFC membranes	75
Table 5.1: Performances of prepared membranes.....	88

LIST OF FIGURES

	<u>Page</u>
Figure 1.1: Freshwater availability.	1
Figure 2.1: Schematic diagram of the principal types of membranes.....	6
Figure 2.2: Pressure driven membranes for water and wastewater treatment	7
Figure 2.3: Historical time line in the development of reverse osmosis.....	12
Figure 2.4: The basic diagram of RO processes	12
Figure 2.5: Thin Film Composite Reverse Osmosis Membrane Layers.....	15
Figure 2.6: The schematic diagrams of TFC membrane preparation by IP technique	15
Figure 2.7: Surface modification of nascent PA RO membrane based on the unreacted acyl chloride groups on surface	16
Figure 2.8: The polyamide RO barrier layer derived from MPD and TMC via interfacial polymerization	18
Figure 2.9: Schematic representation of biofilm formation on solid surface.....	25
Figure 2.10: Microdiversity and composition of culturable heterotrophic aerobic bacteria in Marmara Sea.....	26
Figure 2.11: The major antimicrobial mechanisms	29
Figure 2.12: Microbial count protocol for identifying multiplied and adhered cells..	30
Figure 2.13.a: Confocal images of the membrane surface after P. Aeruginosa PAO1 growth: initial NF-90 membrane.....	31
Figure 2.13.b: Confocal images of the membrane surface after P. Aeruginosa PAO1 growth: modified composite membranes.....	30
Figure 2.14: Photograph of initial PVDF membrane (left) and PVDF membranewith grafted qDMAEM with degree of modification of 710 $\mu\text{g}/\text{cm}^2$ (right) after filtration of E. coli suspensionwith a concentration of 60 CFU/ cm^3 and incubation at Tergitol 7 medium at 37 °C for 24 h (Denyer et al., 1991).....	31
Figure 2.15.a: SEM images of E. coli cells incubated for 60min without SWNTs maintaining their outer membrane structure.	31
Figure 2.15.b: SEM images of E. coli cells incubated for 60min with SWNTs losing their cellular integrity.....	31
Figure 2.16: Visualization of the effects of BisBAL on planktonic biofilm formation over 3 days using phase contrast microscopy (Badireddy and Chellam, 2011). 35	35
Figure 3.1: Prepared dope solution	40
Figure 3.2: Preparation processes of the flat sheet membranes in labaratuuar scale ..	42
Figure 3.3: Preparation processes of the flat sheet membranes in pilot scale.....	44
Figure 3.4: Diagram of TFC preparation method	45
Figure 3.5: The stages of the TFC coating method.....	46
Figure 3.6: Measurement of the membrane thickness	46
Figure 3.7: Viscosimeter	47
Figure 3.8: Preparation of the filtration cell.....	49
Figure 3.9: Contact Angle Measurement Setup	50
Figure 3.10: FTIR spectrophmeter.....	50
Figure 3.11: Electrokinetic analyzer cell	51

Figure 3.12: SEM	51
Figure 3.13: Optical profilometer	52
Figure 3.14: Mechanical stability testing equipment	52
Figure 3.15: Porometer.....	53
Figure 3.16: Image of autovlave	54
Figure 3.17: Pouring of solid media.....	55
Figure 3.18: OD Spectrophotometer	56
Figure 3.19: Bacterial stock preparation	57
Figure 3.20: Example of Serial dilution of bacteria.....	57
Figure 3.21: Example of Serial dilution of bacteria.....	58
Figure 3.22: Spreading of <i>E.coli</i> on medium	59
Figure 3.23: Plating of the membranes	59
Figure 3.24: CLSM	60
Figure 4.1: The thickness values of membranes	61
Figure 4.2: Viscosity values of the dope solutions	62
Figure 4.3: Permeability of prepared UF PSF membranes	63
Figure 4.4: Hydrophilicity of prepared UF PSF membranes	74
Figure 4.5: FTIR images of prepared UF PSF membranes.....	65
Figure 4.6: Zeta potential of prepared UF PSF membranes.....	66
Figure 4.7.a: SEM images of prepared membranes %16 PSF UF membrane.....	69
Figure 4.7.b: SEM images of prepared membranes %16 PSF %8 PVP 10 UF membrane.....	69
Figure 4.7.c: SEM images of prepared membranes %18 PSF, % 4.5 PVP10 , %1.5 PVP40 UF membrane	69
Figure 4.7.d: SEM images of prepared membranes %16 PSF %8 PVP 40 UF membrane.....	69
Figure 4.7.e: SEM images of prepared membranes %16 PSF %8 PVP 360 UF membrane.....	69
Figure 4.8: Avarage roughness of prepared membrane	70
Figure 4.9.a: Optical profilometer images of prepared membranes %16 PSF membrane.....	71
Figure 4.9.b: Optical profilometer images of prepared membranes %16 PSF %8PVP10 membrane	71
Figure 4.9.c: Optical profilometer images of prepared membranes %18 PSF % 4.5 PVP10 %1.5 PVP40 membrane.....	71
Figure 4.9.d: Optical profilometer images of prepared membranes %16 PSF %8PVP40 membrane	71
Figure 4.9.e: Optical profilometer images of prepared membranes %16 PSF %8PVP360 membrane	71
Figure 4.10: Mehcnical parameters of membranes (a) Young's modulus, (b) Elongation, (c)Tensile strength	73
Figure 4.11: Avarage por size of the membranes	73
Figure 4.12: Contact angles of PA TFC RO membranes.....	75
Figure 4.13: FTIR images of prepared PA TFC membranes	76
Figure 4.14: Zeta potential values of prepared PA TFC membranes in mV.....	77
Figure 4.15: SEM images of TFC (a) pristine TFC, (b) BisBAL TFC	78
Figure 4.16: Avarage roughness of prepared PA TFC membranes	79
Figure 4.17: Images of diluted 10^{-4} with <i>E.coli</i> strain incubated plates for 18 hour at 37 ° C	80

Figure 4.18: Images of diluted 10^{-5} with <i>E.coli</i> strain incubated plates for 18 hour at 37 ° C	81
Figure 4.19: Images of diluted 10^{-6} with <i>E.coli</i> strain incubated plates for 18 hour at 37 ° C	81
Figure 4.20.a: SEM images of pristine TFC membrane surface before incubation..	82
Figure 4.20.b: SEM images of pristine TFC membrane surface after incubation (diluted 10^{-4} with <i>E.coli</i> strain).....	82
Figure 4.20.c: SEM images of pristine TFC membrane surface after incubation (diluted 10^{-5} with <i>E.coli</i> strain)	82
Figure 4.20.d: SEM images of pristine TFC membrane surface before incubation..	82
Figure 4.20.e: SEM images of pristine TFC membrane surface after incubation (diluted 10^{-4} with <i>E.coli</i> strain)	82
Figure 4.20.f: SEM images of pristine TFC membrane surface after incubation (diluted 10^{-5} with <i>E.coli</i> strain)	82
Figure 4.21.a: SEM images of BisBAL TFC membrane surface before incubation.	83
Figure 4.21.b: SEM images of BisBAL TFC membrane surface after incubation (diluted 10^{-4} with <i>E.coli</i> strain)	83
Figure 4.21.c: SEM images of BisBAL TFC membrane surface after incubation (diluted 10^{-5} with <i>E.coli</i> strain)	83
Figure 4.21.d: SEM images of BisBAL TFC membrane surface before incubation.	83
Figure 4.21.e: SEM images of BisBAL TFC membrane surface after incubation (diluted 10^{-4} with <i>E.coli</i> strain)	83
Figure 4.21.f: SEM images of BisBAL TFC membrane surface after incubation (diluted 10^{-5} with <i>E.coli</i> strain)	83
Figure 4.22.a: CLSM images of BisBAL TFC membrane surface after incubation (diluted 10^{-4} with <i>E.coli</i> strain)	84
Figure 4.22.b: CLSM images of pristine TFC membrane surface after incubation (diluted 10^{-4} with <i>E.coli</i> strain)	84
Figure 4.22.c: CLSM images of BisBAL TFC membrane surface after incubation (diluted 10^{-5} with <i>E.coli</i> strain)	84
Figure 4.22.d: CLSM images of pristine TFC membrane surface after incubation (diluted 10^{-5} with <i>E.coli</i> strain)	84
Figure 4.23: Flux of pristine TFC membrane	85
Figure 4.24: Flux of BisBAL TFC membrane	86

FABRICATION AND CHARACTERIZATION OF REVERSE OSMOSIS MEMBRANES HAVING ANTIBACTERIAL PROPERTIES

SUMMARY

Day by day, clean and potable water resources are polluted and being unavailable. As a result, the needs of existing freshwater resources are becoming unable to provide around the world. In the current situation, desalination can be solution for the water scarcity. Because seawater and saline aquifers constitute 97.5% of the all water resources on Earth, utilizing an even small amount of this resource could have a great impact on water scarcity. To increase the fresh water supply via desalination of seawater and saline aquifers is the overarching goal for the future of desalination. Desalination plants are operated in more than 120 countries around the world. To get effective results from desalination plants, there are some issues, which have to be solved. One of them, and most important is a biofouling, which effects the performance of reverse osmosis (RO) essentially. Biofouling causes some problems, such as shorter membrane life and it requires higher operating pressure and more frequent chemical cleaning. Development of antifouling RO membranes is an essential requirement for water treatment in the future.

The main objective of this study is to investigate the preparation of an antibacterial surface membrane layer with the additive Bismuth dimercaptopropanol (BisBAL), which is claimed to inhibit biofouling, and the examination of the membrane's characteristics and performance for desalination. The study includes preparation of the support layer to establish selecting of a suitable support layer for active layer. Furthermore it includes the preparation of an active layer with and without the additive BisBAL. Experiments to be carried out together with the membrane characterization and antibacterial properties achieved important results in terms of membranes fabrication at low biofouling characteristics. Antibacterial properties of the membranes were studied using with BL21 strain of *E. coli*, which was taken from Molecular Biology-Biotechnology & Genetics Research Center (MOBGAM) at ITU.

Comprehensive anti bacterial tests with *E. Coli* showed that BisBAL can be used effectively at RO membrane surface.

ANTİBAKTERİYEL ÖZELLİĞE SAHİP TERS OSMOZ MEMBRANLARIN ÜRETİMİ

ÖZET

Temiz ve içilebilir su kaynakları her geçen gün kirletilerek kullanılamaz hale getirilmektedir. Bunun bir sonucu olarak Dünya üzerindeki mevcut tatlı su kaynakları ihtiyaçları karşılayamayacak hale gelmektedir. Alternatif su kaynaklarına ilişkin teknolojilere yönelinmesi su sıkıntısının etkilerinin azaltılmak için Dünya’da gittikçe yaygınlaşmaktadır. Dünyadaki toplam suyun % 96’dan daha fazlasını tuzlu sular oluşturmaktadır, tatlı su ise Dünya’daki suyun sadece %2.5’lik kısmını oluşturur ve bunun çoğu buzullar ve buz tabakaları içerisinde donmuş haldedir.

Mevcut durum göz önünde bulundurulduğunda tuzlu sudan desalinasyon teknolojisi ile ekonomik ve güvenli bir şekilde kullanma suyu elde edilebilmesi büyük bir avantaj sağlamaktadır. Desalinasyon tesisleri Dünya’da 120’den fazla ülkede işletilmektedir ve suyun üretim maliyeti genellikle enerji tüketimi, kullanılan ekipmanın, membranların ve iş gücünün maliyeti ile orantılı olarak değişmektedir.

Desalinasyon tesislerinden etkin bir sonuç alabilmek için çözülmesi gereken bazı konular bulunmaktadır. Bunlardan birisi ve en önemlisi olan tıkanma problemleri, membran filtrasyon sistemlerinin işletilmesi esnasında sorun teşkil etmektedir. Bu problemi çözebilmek için çeşitli yollar ve yaklaşımlar geliştirilmekte ve denenmektedir. Ters osmoz membranlarında meydana gelen biyotıkanma temel olarak akıyı düşürmektedir. Akının düşmesi daha fazla enerji harcanması ve tuz tutunumunda azalma gibi olumsuz etkiler göstermektedir. Bu sebeple oluşmadan müdahale etmek biyotıkanmayı engellemek için en etkili ve iyi yol olarak düşünülmektedir. Müdahale çeşitli şekillerde yapılabilmektedir. Bunlardan birisi de membranların üretimi sırasında üretim materyallerine antibakteriyel maddelerin ilavesidir. İlave edilen maddeler ile membran filtrelerin daha dayanıklı ve biyotıkanmaya dirençli olmaları sağlanmakta, böylece kirlenme ve tıkanma oluşumunun en aza indirgenmesi sağlanmaktadır.

Bu çalışma kapsamında; içme suyu eldesi amacıyla ters osmoz membran üretimi, karakterizasyonu ve biyokirlenme özelliğinin iyileştirilmesi çalışmaları gerçekleştirilmiştir. Çalışmanın amacı su temininde ileri teknolojilerin kullanılarak, biyokirlenme performansında iyileştirme çalışmaları yapılması, membranların özelliklerinin geliştirilmesi ve halen tümüyle dışa bağımlı durumda olduğumuz membran sistemlerinin ülkemiz koşullarında üretilebilir hale getirilmesidir. Bu amaç doğrultusunda ters osmoz membranları üretimi yapılmıştır. Deneylerin ilk aşamasında destek tabakası ultrafiltrasyon düzeyinde evre dönüşümü yöntemiyle polisülfon (PSF) polimeri ile farklı polimer çözeltileri hazırlanarak destek tabaka üzerine dökülerek üretilmiştir. Membran üretiminde ilk olarak homojen dağılımı sağlanmış membran çözeltisi cam yüzey üzerine belirli hacimde dökülmüş ve dökme bıçağı (casting knife) sabit kalınlığa ayarlanarak bu çözeltinin üzerine yerleştirilmiştir. Ardından laboratuvar ölçekli dökme makinesinin gerekli ayarlamaları yapılarak belirlenen hızda cam yüzeyinde polimer film oluşturulmuştur. Bu esnada oluşturulmak istenen membranın özelliğine bağlı olarak polimer filmler belirli bir solvent buharlaşma süresinde bekletilmişlerdir. Bu çalışmada buharlaşma süresi 10 sn. olarak sabit tutulmuştur. Buharlaşmanın ardından polimer filmlerinin olduğu camlar destile suyun bulunduğu koagülasyon banyosuna daldırılmışlardır. Bu esnada en az 5 dakika membranın oluşması beklenmiş ve ardından oluşan membranlar destile suyun bulunduğu temiz bir kaba aktarılmışlardır. Biyolojik büyümenin olmaması ve reaksiyona girmeyen polimer veya solventin membrandan uzaklaşması için üretilen membranlar en az 1 hafta süre ile +40C’de soğuk odada saklanmışlardır. Üretilen bu membranlarda başta geçirgenlik deneyleri olmak üzere karakterizasyon çalışmaları yapılmıştır. Filtrasyon performanslarından önce ilk olarak literatürde sıkıştırma deneyi olarak isimlendirilen ön işleme tabi tutulmuştur. Bu işlemde, yüksek basınç altında membranların saf su ile yıkanması sağlanmış ve bu esnada reaksiyona girmemiş polimer/ıslatıcı/solvent kalıntılarının membranlardan yıkanması ve membran gözeneklerinin son halini alması sağlanmıştır. Bu deneyin ardından klasik filtrasyon deneyleri sırayla gerçekleştirilmiştir. Cihaz analizleri için membran numunelerinin hazırlanmasında sıkıştırma ön işlemi yapılmayan membranlar kullanılmıştır. Membranlara temas açısı, mekanik dayanıklılık testleri uygulanmış ve taramalı elektron mikroskobu, optik profilometre, porometre, elektrokinetik ölçer kullanarak yüzey morfolojileri tanımlanmıştır. Destek tabakası membranı olarak üretilen UF destek tabakasının yüksek basınçlara dayanıklı olması için süngerimsi yapıda olması yapılan çalışmalarla

optimize edilmiştir. Karakterizasyon testlerinin sonuçlarına bakıldığında %18PSF %4.5PVP10 %1.5 PVP40 kullanılarak üretilen membranlar aktif tabakada kullanılmak üzere destek tabakası olarak seçilmiştir. Deneylerin ikinci aşamasında ters osmoz membranı için aktif tabakası üretim çalışmaları yapılmıştır. Aktif tabaka ince film poliamid olarak ara yüzey polimerizasyon yöntemiyle üretilmiştir. Membranlara antibakteriyel özellik kazandıracak, güçlü antibakteriyel özelliğe sahip bizmut tiyollerden biri olan BisBAL maddesinin ilavesi aktif tabaka üretimi kısmında gerçekleştirilmiştir ve antibakteriyel özelliği edinmesi amaçlanmıştır. Tez çalışmasının son aşamasında membranların antibakteriyel özelliklerini belirlemek için İTÜ Moleküler Biyoloji-Biyoteknoloji ve Genetik Araştırmalar Merkezi'nden alınan E. coli suşu ile çalışmalar yapılmıştır. BisBAL ilaveli membranların üzerinde, saf membranlara nazaran daha az büyüme görülmüştür. Antibakteriyel testler karşılaştırmalı olarak incelendiğinde BisBAL ilaveli membranların antibakteriyel özellik kazandığı ve BisBAL'ın etkili olarak ters osmoz membranlarında kullanılabileceği görülmüştür.

1.INTRODUCTION

Water is primarily the basis with requirements for the survival. Moreover, water has crucial importance for the development and sustainability on the planet. Although water is foundation of life, water scarcity is one of the significant problems of the planet. While population and demand on freshwater resources are increasing, supply will always remain constant. The United Nation estimates that 1.2 billion people now live in regions facing water scarcity, and a further 600 million will encounter water scarcity by 2025 (Url-1). When countries are classified according to the presence of water; the average amount of water availability less than 1,000 cubic meters for per person per year can define water-poor countries, 1,000-3,000 m³ countries can define water-strapped countries, 3,000-10,000 m³ countries and countries with adequate water, with more than 10,000 cubic meters cand define as water-rich countries. As it is seen in Figure 1.1, the red color shows very high stress regions, orange color shows high stress region, dark yellow color shows mid stress regions, light yellow shows low stress regions and white color shows no stress regions. According to Figure 1.1 Turkey lies between the mid and very high stress region.

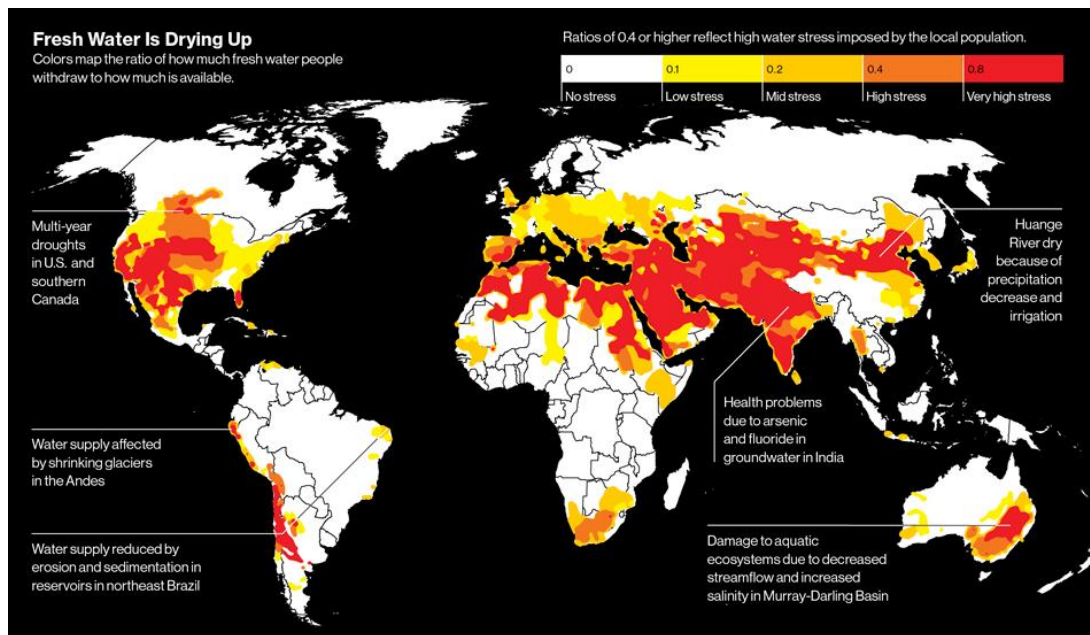


Figure 1.1: Freshwater availability (Url-1).

With the current state of Turkey and with the existing of global water scarcity, the requirement for water reuse, recycling, and development of effective water treatment processes will increase. Desalination can be a solution for the water scarcity. Because seawater and saline aquifers constitute 97.5% of the all water resources on the Earth, utilizing this resource has to be considered. The overarching goal for the future of desalination is to increase the fresh water supply via desalination of seawater and saline aquifers (M. A. Shannon et al., 2008). Today, RO membranes are outstanding for water purification applications that require high salt rejection for desalination technology. Developments in RO membranes have advanced significantly in the past decades. However, fouling due to the microorganism is an obstacle, which essentially effects RO performance.

Biofouling causes some problem, such as shorter membrane life and it requires higher operating pressure and more frequent chemical cleaning. Development of antifouling RO membranes is essential requirement in water treatment for the future.

1.1 Purpose of Thesis

The main objective of this study is to prepare and characterize the pristine RO membrane and to investigate the antibacterial surface with additive BisBAL and to examine the desalination performance of prepared membrane. However this study included the preparation of support layer. Also study includes the preparation of active layer with additive BisBAL and pristine. The membrane characterization and filtration performances of membranes were done simultaneously. Important results were achieved. Comprehensive anti bacterial tests with *E. Coli* showed the effectivity of BisBAL in the membrane surface layer.

1.2 Scope of Thesis

In this thesis study, the experiments were performed at three stages. Firstly, ultrafiltration membranes were prepared with different polymers and solvents as a support layer. Secondly, thin film composite (TFC) reverse osmosis membranes were prepared via interfacial polymerization with additive BisBAL in active layer. Finally, the characterization and performance tests of fabricated membranes were done. As a result of this thesis, RO TFC membrane with additive BisBAL contributed to literature for membrane fabrication studies.

2. LITERATURE REVIEW

2.1 Membrane Technology

Membranes can be defined as a selective barrier between two phases. Membrane technology is an emerging technology because it can be used in every separation processes with its multi-disciplinary characteristics (Mulder, 1996). Development of the membrane processes are given in Table 2.1.

Table 2.1: Historical developments of membranes (pre-1980s) (Wang et. al., 2010).

Year	Development
1784	‘Osmosis’, permeation of water
1833	Diffusion of gases law
1855	Phenomenological diffusion laws
1860-1880s	Osmotic pressure, semi permeable membranes
1907-1920	Microporous membranes
1920s	Reverse osmosis prototype
1930s	Electrodialysis membranes
1950s	Microfiltration, hemodialysis, ion exchange membranes
1963	Reverse osmosis membranes
1968	Spiral-wound reverse osmosis modules
1977	Thin film composite membranes
1970-1980	RO, UF, MF, electrodialysis membranes
1980s	Industrial gas separation membranes processes
1989	Submerged membrane (membrane bioreactor)

2.1.1 Role in water supply, sanitation, and reclamation

Especially for water and wastewater treatment technologies, membrane technology is painting a promising picture. Many types of membranes are used for water and wastewater treatment. Table 2.2 shows the membrane process configurations for the range of applications and water sources.

Table 2.2: Membrane process configurations in the water industry (Fane et al., 2011).

Source water	Membrane process	Pretreatment or hybrid	Posttreatment	Target removals
Water treatment				
Surface	MF/UF	Coagulation	Advanced treatment, oxidation, disinfection	Natural matter, organic pathogens, turbidity,
Surface	MF/UF	Powdered activated carbon	Disinfection	Taste/odor, trace organics
Surface	NF	Filtration	Disinfection	Natural organic matter
Surface	NF	Coagulation, filtration	Advanced treatment, oxidation	Trace organics, taste/odor
Ground	NF	Filtration	Disinfection	Hardness
Desalination				
Brackish ground	RO	Filtration	Disinfection	Salinity
Seawater	RO	Media filtration or MF/UF	Ca addition	Salinity
Reclamation				
Treated wastewater	RO	MF/UF	Advanced treatment, oxidation	Pathogens, trace organics
Wastewater	RO	MBR	Advanced treatment, oxidation	Pathogens, trace organics
Membrane bioreactor				
Wastewater	MF/UF	Screening	Disinfection	Biochemical oxygen demand, turbidity, pathogens

2.1.2 Membrane types and properties

Membranes can be classified by considering different aspects. The first classification is about genesis, biological or synthetic membranes. These two types of membranes differ completely from each other in structure and functionality (Mulder, 1996). Secondly, synthetic membranes can be classified into organic and inorganic membranes. The most important class of membrane material is organic (mainly polymeric materials). The inorganic membranes can be ceramic, glass or metallic. Although the inorganic membranes generally have better chemical and thermal stability than polymeric membranes, as membrane material their use are limited. Ceramic membrane is a specific genre of microporous membranes, which is used for microfiltration and ultrafiltration applications where resistance to solvent and thermal stability are necessary. Dense metal membranes are considered for the separation of hydrogen from gas mixtures, and supported liquid films are being developed for carrier-facilitated transport processes (Takao, 1983). Another classification of membranes are based on morphology or structure. Because the separation mechanism

of membranes depends on the membrane structure, this is a very revealing margin (Mulder, 1996). There are two types of membranes can be subdivided by morphology; symmetric and asymmetric membranes. Symmetric membranes can be porous or dense. As functionality and structure, symmetric microporous membrane resembles to commercial filters. It has rough, voided configuration and randomly dispersed, interdependent pores. The difference from commercial filters is the very small pore size between 0.01 to 1 micrometer in diameter (Baker, 2004). Particles that are larger than the largest pore of the membrane rejected and smaller particles than the largest pore of membrane are relatively rejected depending on the distribution of membrane's pore size. In addition, much smaller particles than smallest pore of the membrane traverse the membrane. Therefore, microporous membrane's separation of solutes depend on molecular size. Nonporous membrane compromise of a dense film. Driving forces are pressure, concentration or electrical potential that allow diffusion for transportation of permeants. Diffusivity and solubility in the membrane material determines the separation of several components of a mixture that has direct relationship with the transport rate within the membrane. Dense membranes are used mostly for gas separation, RO and pervaporation membranes for separation. Generally, these membranes have anisotropic structures to enhance flux. Another symmetric membrane type is the electrically charged membrane that can be found as microporous or dense but principally they are microporous that have positively or negatively charges ions on pore walls. A membrane with preset positively charges ions are an anion-exchange membrane that binds anions from fluid. In a similar vein, a membrane with fixed negatively charge ions are a cation-exchange membrane which bind cations from fluid. Electrically charged membranes are used for processing electrolyte solutions in electrodialysis. Schematic diagram of the principal types of membranes is shown in Figure 2.1.

Asymmetric membranes thickness and the transport rate of species are inversely proportional. Over 30 years, it was one of the major novelty for membrane technology to develop newfangled membrane fabrication techniques for anisotropic membrane structures. Anisotropic membranes are composed of intensely thin surface layer that backed on much thicker, porous basis. In a single operation, the layer and substructure can be formed or they can be formed separately. Layers are generally made of discrete polymers in composite membranes. The surface layer designate the separation features

and permeation rates and the subsurface is only for mechanical backing. For higher flows, anisotropic membranes are very advantageous that nearly all commercial processes use them (Baker, 2004).

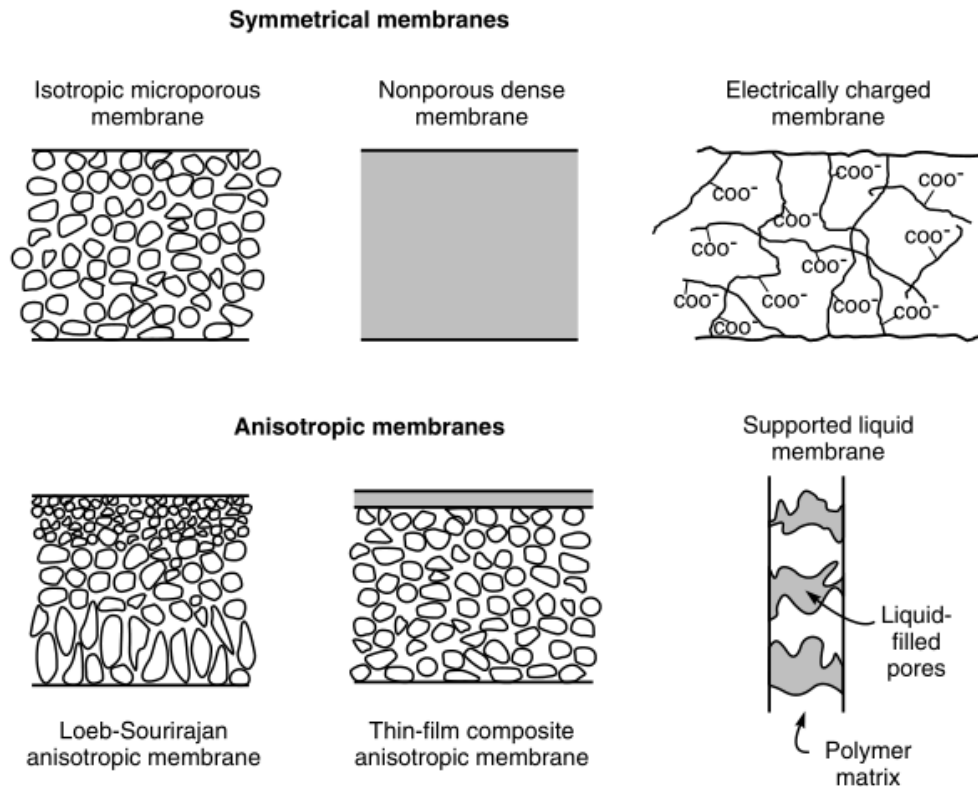


Figure 2.1: Schematic diagram of the principal types of membranes. (Mulder, 1996).

There is also composite membranes that are actually skinned asymmetric membranes but in composite membrane, the top layer and sublayer are formed of different polymeric materials (Mulder, 1996).

Membranes can be also classified as porous or nonporous. Porous membranes enable separation by differentiation between particle sizes. These membranes are used in microfiltration and ultrafiltration. Membranes can be highly selective when the pore size is greatly smaller than solute size (Mulder, 1996). Membranes that have pore size greater than 50 nm called as macroporous, membranes that have pore size 2 to 50 nm called as mesoporous and membranes that have pore size smaller than 2 nm called as microporous. Membranes, which do not have pores, also called nonporous or dense membranes. These types of membranes have the capacity of separating molecules at same size. These membranes are used in pervaporation and gas separation.

Another classification can be done by driving force. Driving force of RO, nanofiltration (NF), ultrafiltration (UF) and microfiltration (MF) membranes is pressure (ΔP). Pervaporation and dialysis membranes' driving force is concentration (ΔC). Electrodialysis and electrodialysis reversal membranes driving force is electrical potential (ΔY). In addition, there are membranes which the driving force is temperature (ΔT) (Drioli and Giorno, 2010). Pressure driven membranes for water and wastewater treatment are shown schematically in Figure 2.2.

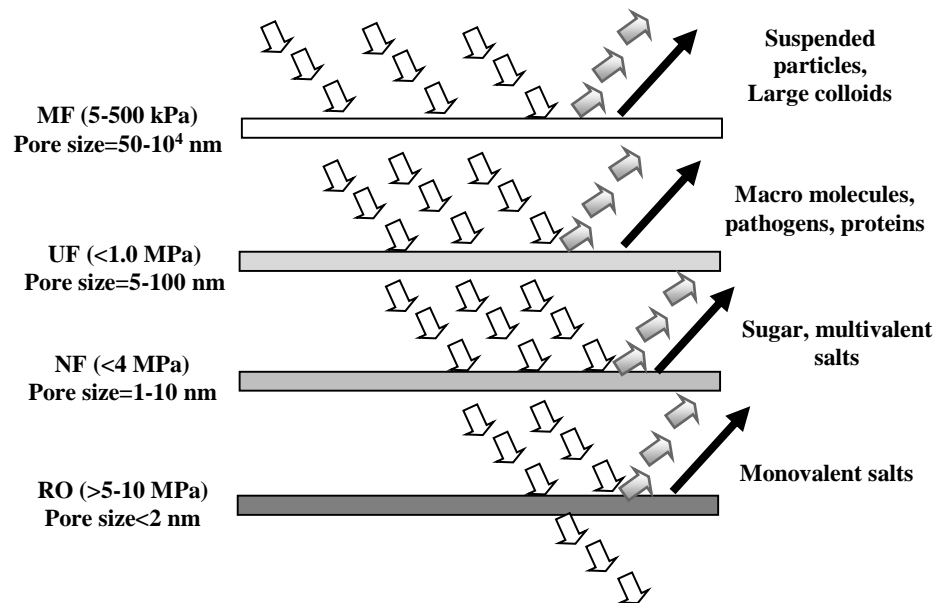


Figure 2.2: Pressure driven membranes for water and wastewater treatment (Wang and Chan, 2007).

Module types are an alternate division for membranes. Wide membrane areas are necessary to apply membranes on a technical scale. Module is the smallest unit that membrane area is packed.

2.1.3 Membrane materials

During membrane preparation, various materials are used. Generally, synthetic polymers are preferred, however, inorganic membranes known as ceramic or mineral membranes can also be used.

The most preferred polymeric membrane materials for water and wastewater treatment and their properties are as follows (Nath, 2008):

Cellulose derivatives, cellulose is the most important natural polymer used in membrane production. High structural order and hydrogen bonds between molecules

with hydroxyl groups make cellulose resistant to dissolving. The most widely used types of cellulose in membrane systems are inorganic (nitrate) and organic (acetate) esters. Cellulose nitrate (CN) was used as the first synthetic polymer during preparation of filtration material. Cellulose acetate (CA) membranes are produced as a lower cost alternative to the cellulose nitrate. The biggest advantage of cellulose acetate is the production of different pore sizes for required high fluxes. Cellulose triacetate (CTA) is a derivative of cellulose membrane the which has acetyl content greater than 42.3%. Cellulosic membranes known as hydrophilic membranes and advantageous in particular for membrane fouling. Major drawbacks of cellulosic membranes are the narrow range of operating temperature (30-40°C), low pH range (pH 3-6) and low durability of chlorinated species (Nath, 2008).

Aromatic polyamides (PA), are membranes that can be used at high temperature and have the characteristics of high resistance to organic solvents. They are characterized by the amide (-CONH-) linkage in structure. They cope with many disadvantage of cellulose acetate membranes (such as pH and temperature influence), but the resistance to chlorine species is worse than cellulosic membranes. Chlorine increase the selectivity and reduces the permeability of the membrane by damaging the the aromatic rings of polyamide (Nath, 2008).

Polysulfone (PSF), a concentrated product of bisphenol-A and diclorodifenil sulfone. These membranes contain-SO₂ group. Polysulfones and poly-ethersulfone membranes have high molecular and dimensional stability, hard and resistant structure. They are suitable for operation in a wide temperature range. Polysulfone membranes can be operated at 75°C and polietersulfon membrane can be operated at 125°C. pH ranges of these membranes is wide, can be used in the range of pH 1-10. Chlorine resistance higher than other membranes. Sulfone groups, provides the electrons that confined in the aromatic groups increases the resistance of the membranes. Electrons to provide aromatic groups, sulfone groups that membranes increase resistance in the confined. These membranes are often preferred for microfiltration, ultrafiltration and reverse osmosis systems in order to be prepared at the desired pore size and have use as the tubular or layer (Nath, 2008).

Polycarbonate (PC), these membranes contain -OCOO- group. Their structures are usually amorphous. In order to thin thickness (~10 mm) and higher molecular weight, they can also be used in the preparation of other membranes. Unlike other amorphous

polymers, they are smooth and high flexibility. Due to the nature of thermoplastic they can be prepared in different shapes and layers. With polyethylene glycol, and silicon, they especially used in the preparation of membranes used in hemodialysis (Nath, 2008).

Polyacrylonitrile (PAN), PAN membranes are membranes that have co-monomers such as methylmethacrylate. They are usually produced by the method of phase inversion and high stability membranes.

2.1.4 Membrane preparation

During membrane preparation, there exist several varied techniques to prepare synthetic membranes. Some of them can be used to prepare both organic or inorganic membranes. The most important techniques are sintering, stretching, track-etching, phase inversion and coating (Mulder, 1996).

Sintering

Sintering is a simple technique which enables porous membranes to be derived from both organic and inorganic materials. The method involves pressing a powder of sized particles. Next step is sintering at high temperature. The temperature requirement is dependent on the material used. The interface between contacting particles disappears in the course of sintering. Different materials can be used in this method such as powders of polymers, metals, ceramics, graphite or glass. Powder's particle size distribution specified the pore size of membrane. With this technique, 0.1 to 10 μm of pore size can be obtained (Mulder, 1996).

Stretching

This technique places crystalline regions to the extrusion direction by stretching an extruded film or foil made from a partially crystalline polymeric material perpendicular to that direction. Pore size 0.1 μm to 3 μm can be obtained when small ruptures occurred by mechanical stress. Only material that can be used for this method is semi crystalline polymeric material. Prepared membranes with this technique have much higher porosity than membranes manufactured by sintering (Mulder, 1996).

Track-etching

A membrane's most basic pore geometry is assembled by parallel cylindrically shaped pores of uniform dimension. The track-etching method allows this kind of structures

to be made. In this technique a film or foil is exposed to high energy particle radiation adopted perpendicular to the film and the polymer matrix is damaged by the particles to cause tracks. Then to create uniform cylindrical pores with narrow pore size distribution the film is immersed in an acid or alkaline bath and along these tracks the polymeric material is etched. The pore sizes can be obtained 0.02 to 10 μ m by this method. However, the surface porosity is not high which is about maximum 10% (Mulder, 1996).

Template leaching

Leaching out one of the components from a film is another production method for porous membranes. This technique allows to make porous glassy membranes. A three component system's homogeneous melt is heated until the system separates into two phases where one phase is soluble and the other is insoluble. The soluble phase is leached out by acid or base. Then a broad range of pore sizes can be procured. The minimum size is about 0.05 μ m (Mulder, 1996).

Phase inversion

The phase inversion technique is mainly used for production of commercially available membranes. This method is highly multipurpose and can be used for all types of morphologies (Mulder, 1996).

The phase inversion technique is used for production of membranes used for this thesis so it is explained detailed in other section.

Coating

Low fluxes are attained in dense membranes. Reduction of membrane's effective thickness is necessary to increase the flux. Preparing composite membranes can solve this problem. Composite membranes are made from two different materials. Many coating methods are possible to be used for the preparation of these kind of membranes such as dip coating, plasma polymerization, interfacial polymerization and in-situ polymerization (Mulder, 1996).

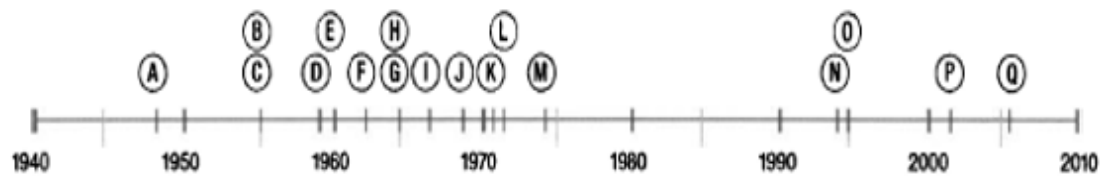
2.1.5 Membrane characterization

Membrane processes have been increasingly used for drinking water and wastewater treatment. These processes have now become an attractive option for water and

wastewater treatment and reuse of industrial and municipal wastewaters. Different polymers (Polyethersulfone (PES), polysulfone (PS), cellulose acetate (CA), polyvinylidene fluoride (PVDF) etc.) can be selected as membrane material for membrane fabrication according to its good physical and chemical characteristics such as high filtration performance, good fouling resistance and environmental endurance as well as easy processing. The ultimate goal of membrane technology is to find a proper relationship between membrane fabrication, membrane morphology and membrane performance. A rational guideline for membrane fabrication conditions is to achieve some specific membrane morphology, which enables the desired separation performance. For this reason, membrane morphology characterization is one of the indispensable components of membrane research. Physical and chemical properties of membranes can be characterized with different laboratory techniques. These techniques generally include the following aspects: pore size and porosity, surface and cross-section morphologies, hydrophilicity, mechanical strength, surface area, surface chemistry and charge. Even though these characterization techniques are not always necessary, in most cases, some of the above aspects are needed to characterize a specific type of membranes. It can be said that the ideal characterization method should be easy, accurate, and repeatable and fast and also should give a maximum possible number of data.

2.2 Reverse Osmosis Technology For Desalination

The earliest form of RO membrane for water desalination technology was discovered in the early 1950's (Wilf, 2007). The first inventor of RO membrane was Loeb and Sourirajan in 1960, he presented a method that could be used at the industrial level in actual water production plants, and cellulose-acetate-based RO membrane. After the discovered by Loeb and Sourirajan, spiral-wound membranes elements using the cellulose acetate asymmetric flat-sheet membranes were developed and manufactured by several American and Japanese companies. Since around 1964, RO technologies have been established on the market (Norman et al., 2008). Examining the RO historical timeline, one can see it's significant development and state of the art. It is the leading desalination technology (Figure 2.3).



- A. 1948 - Hassler studies osmotic properties of cellophane membranes at UCM
- B. 1955 - First reported use of the term "reverse osmosis"
- C. 1955 - Reid begins study of membranes of demineralization at University of Florida
- D. 1959 - Breton and Reid demonstrate desalination capability of cellulose acetate film
- E. 1960 - Loeb and Sourirajan develop asymmetric Cellulose acetate membrane at UCLA
- F. 1963 - First practical spiral wound module developed by General Atomics
- G. 1965 - First commercial brackish water RO facility at Coalinga, CA
- H. 1965 - Solution-Diffusion transport model described by Lonsdale, et. al
- I. 1967 - First commercially successful hollow fiber InodUle developed by DuPont
- J. 1968 - First multi-leaf spiral wound module developed by Fluid Systems
- K. 1971 - Richter-Hoehn at DuPont patents aromatic polyamide membrane
- L. 1972 - Cadotte develops interfacial composite membrane
- M. 1974 - First commercial seawater RO facility at Bermuda
- N. 1994 - TriSep introduces first "low fouling" membrane
- O. 1995 - Hydranautics introduces first 'energy saving' polyamide membrane
- P. 2002 - Koch Membrane Systems introduces first 18-inch diameter "MegaMagnum" module
- Q. 2006 - Thin-film nanocomposite membrane developed at UCLA

Figure 2.3: Historical time line in the development of reverse osmosis (Kucera, 2010).

RO is a pressure-driven process in which a semi-permeable membrane excludes dissolved constituents present in the feed. Figure 2.4. illustrates the basic diagram of RO processes. The separation mechanism depends on the size exclusion, charge exclusion and physical–chemical interactions between solute, solvent and membrane (Malaeb et al, 2011).

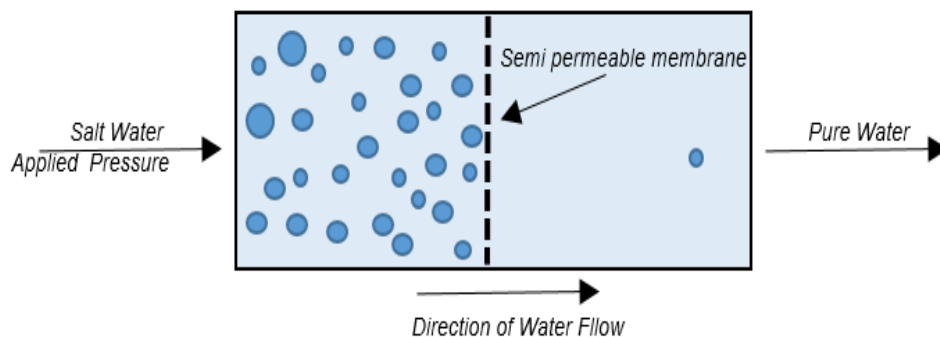


Figure 2.4: The basic diagram of RO processes.

RO is currently turned into a crucial technology that promises significant developings that provide clean water through the clarification of nontraditional water sources such as brackish, sea, and wastewater (Jeong, 2007).

Worldwide seawater concentrations lie between 35,000 mg/L to 45,000 mg/L. Different feed water sources and associated TDS concentrations around the world is shown in Table 2.3. Seawater sources generally have particulate and colloidal contaminants, as well as hydrocarbons from oil contamination and biological contaminants (algal blooms and other microorganisms) (Greenlee et al., 2009).

Table 2.3: Total dissolved salt concentrations for selected salt water bodies around the World (*Greenlee et., al, 2009 and **Url-3).

Water Body	TDS concentration (mg/L)
Tampa Bay*	18,000–31,000
Pacific Ocean*	34,000
Mediterranean Sea*	38,000–40,500
Atlantic Ocean*	38,500–40,000
Red Sea*	41,000–42,000
Gulf of Oman*	40,000–48,000
Persian Gulf*	42,000–45,000
Dead Sea*	275,000
Marmara Sea**	23,000-36,000
Black Sea**	18,000
Aegean Sea**	33,000-37,000

Brackish water sources are often groundwaters; these groundwaters can be naturally saline aquifers or groundwater that has become brackish due to seawater intrusion or anthropogenic influences (e.g., overuse and irrigation). Surface brackish waters are less common but may occur naturally or through anthropogenic activities. Brackish waters can have a wide range of TDS (1000–10,000 mg/L) and are typically characterized by low organic carbon content and low particulate or colloidal contaminants. Contaminants such as radionuclides and fluoride naturally exist in some brackish groundwater resources. Human-impacted water sources also have artificially increased levels of nitrates (fertilizers), pesticides (agricultural land use), arsenic (mining operations), and endocrine disrupters (pharmaceuticals in wastewater). Boron can also be a contaminant in brackish water RO systems (Greenlee et al., 2009). Table 2.4 main differences and comparison between brackish and seawater is exhibited.

Table 2.4: Key differences between brackish and sea water (Greenlee et al., 2009).

Component	Mediterranean Seawater –Toulon, France (mg/l)	Brackish water – Port Hueneme, USA California (mg/l)	Brackish water – Martin County, USA Florida (mg/l)
Ca ²⁺	440–670	175	179
Mg ²⁺	1400–1550	58	132
Ba ²⁺	0.010	<0.10	0.06
Sr ₂	5–7.5	–	26.4
Boron	4.9–5.3	–	–
Na ⁺	12,000	170	905
Cl ⁻	21,000–23,000	72	1867
SO ₄ ²⁻	2,400–2,670	670	384
HCO ₃ ⁻	120–142	260	146
TDS	38,000–40,000	1320	3664
DOC	<2	–	1.4

Most commercially available RO membranes are asymmetric cellulose type (cellulose acetate, triacetate, cellulose diacetate) and thin film composite (TFC) type. Preparation of the asymmetric cellulose RO membrane is done by the phase inversion method, while preparation of TFC RO membrane is done by forming a dense aromatic PA barrier layer on a microporous support such as polysulfone with interfacial polymerization process (Kang et al., 2012).

The first known published work on the TFC polyamide RO membrane is the research conducted by Cadotte et al. in 1980. The experiment performed using a patented RO membrane, codenamed FT-30, formed through interfacial polymerization of m-phenylenediamine (MPD) and trimesoyl chloride (TMC) on a polysulfone (PSF) support layer. The design variables were feedwater temperature, pressure, salt concentration, and pH level. Response performance characteristics were water flux and salt rejection. Each experiment tested a 20 liters filtration system with six serial test cells. The diameter of each of the test cell was 3 inches. Researchers minimized the recovery to 0.1 percent for each cell in order to minimize the effect of concentration polarization. This helped to achieve a more accurate intrinsic performance of the FT-30 (Cadotte et al., 1980).

To improve properties of TFC membrane, still more research is needed. TFC PA membranes consists of three layers: A nonwoven wall acting as structural support (120–150 µm thickness), microporous PSF layer (about 40µm thickness), and ultra-thin barrier layer on the upper surface (0.2 µm thickness) (Figure 2.5) (Petersen et al.,1990).

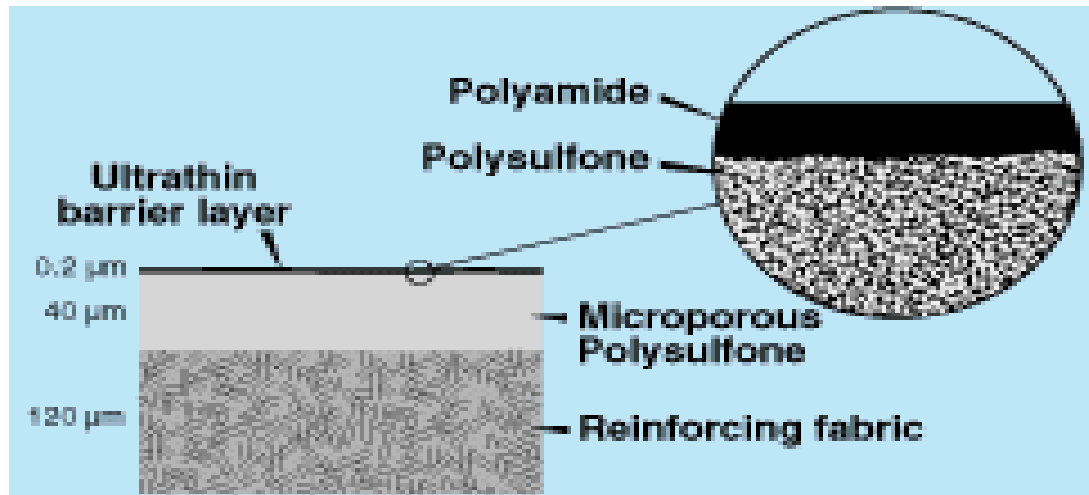


Figure 2.5: TFC RO Membrane Layers (Petersen et al.,1990).

The ultra-thin barrier is named active skin layer and controls mainly the separation properties of the membrane in RO desalination. It requires a support layer to enable to withstand high pressure compression. The polyester support web, named as nonwoven wall, can not be used directly as a support layer for the active skin layer because the structure is too irregular and porous. So, a micro-porous interlayer of PSF polymer is used as a support layer between the nonwoven wall and ultra-thin barrier (Lee et al., 2011).

2.2.1 Preparation of thin film composite (TFC) membrane

In general, TFC RO membranes are fabricated with interfacial polymerization (IP) reaction between two monomers – a polyfunctional amine dissolved in water solution and a polyfunctional acid chloride dissolved in hydrocarbon solvent. Figure 2.6 shows the schematic diagrams of the TFC membrane preparation by IP technique (Lau et al., 2011).

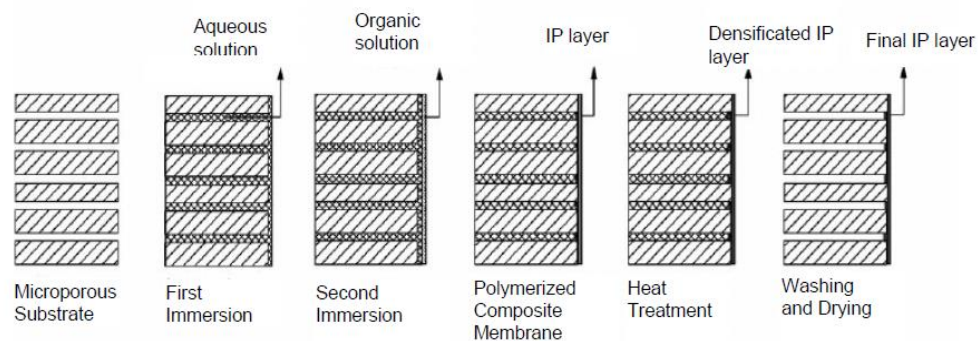


Figure 2.6: The schematic diagrams of TFC membrane preparation by IP technique (Lau et al., 2011).

When the two monomer solutions are brought into contact, both monomers partition across the liquid–liquid interface and combine to form a polymer, despite that polymerization occurs predominantly in the organic phase because of the relatively low solubility of most acid chlorides in water as it seen in Figure 2.7. Hence, a large excess of amine over acid chloride is used commonly (typically about 20:1), that drives partitioning and diffusion of the amine into the organic phase (Ghosh et al., 2008).

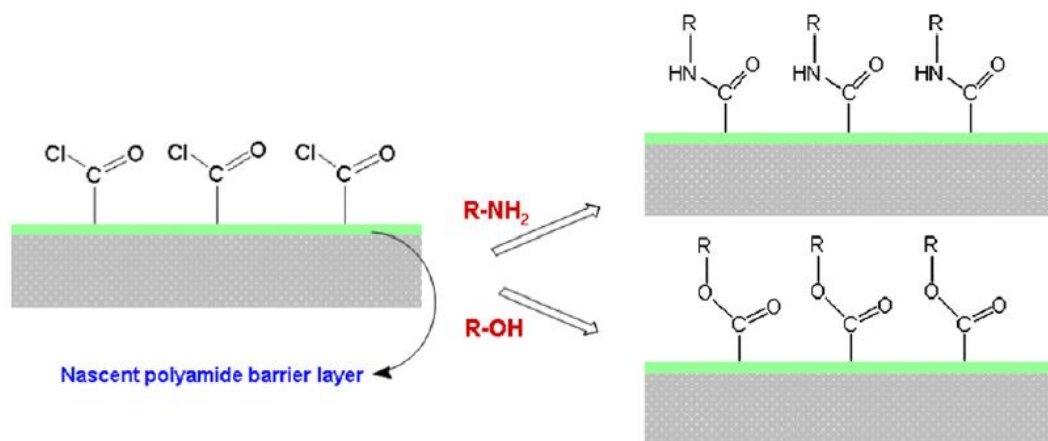


Figure 2.7: Surface modification of nascent PA RO membrane based on the unreacted acyl chloride groups on surface (Kang et al., 2012).

2.2.2 Recent progress in the development in reverse osmosis membrane

During preparation of PA-TFC membranes, there exist some important parameters such as monomer types, support layer properties, process modifications and additives.

2.2.2.1 Monomer types

During the fabrication of TFC membrane, monomers have significant importance and effect pore dimension, thickness, roughness and hydrophilicity of the thin film. In literature, there are different monomers for preparing TFC membrane (Table 2.5).

Table 2.5: Different monomers for preparing TFC membrane (Lau et al, 2012).

Amine monomer (abbreviation)	Chemical structure	Acyl chloride monomer (abbreviation)	Chemical structure
Piperazine		Trimesoyl chloride (TMC)	
m-Phenylenediamine (MPD)		Isophthaloyl chloride	
p-Phenylenediamine		5Isocyanatoisophthaloyl chloride	
Sulfonated cardopoly(arylene ether sulfone)		mm-Biphenyl tetraacyl chloride	
3,5-Diamino-N-(4-aminophenyl) benzamide		om-Biphenyl tetraacyl chloride	
Triethanolamine		op-Biphenyl tetraacyl chloride	
Methyl-diethanolamine		Cyclohexane-1,3,5- tricarboxyl chloride	
1,3-Cyclohexanebis (methylamine)		5- Chloroformyloxyisop htaloyl chloride	
m-Phenylenediamine- 4-methyl		Pyridine-2,4,6- tricarboxyl trichloride (PTC)	
Hexafluoroalcohol- mphenylenediamine			
Disulfonatedbis [4-(3- aminophenoxy)phenyl]sulfone (S-BAPS)			

Even so, MPD and TMC are most common used monomers. In addition, many commercial RO membranes are produced from MPD and TMC by altering interfacial polymerization conditions. Figure 2.8 illustrates the polyamide RO membrane dense layer based on TMC and MPD via interfacial polymerization.

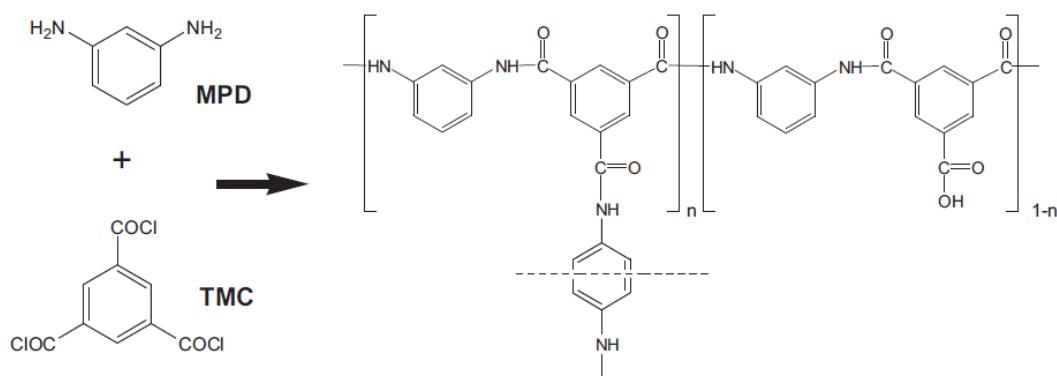


Figure 2.8: The polyamide RO barrier layer derived from MPD and TMC via interfacial polymerization (Kang et al., 2012).

Li et al. (2007) suggested to prepare TFC RO membranes on a polysulfone support layer via interfacial polymerization, using new acyl chloride monomers such as tri- and tetra-functional biphenyl acid chloride. The results of the reverse osmosis performance testing of the membranes showed that higher salt rejection compared with that prepared from TMC at the expense of some flux. The researchers believe that higher rejection is due to the higher cross-linked degree and chain stiffness, compared with TMC and MPD.

Jewrajka et al. (2013) used PTC with/without TMC in the interfacial polymerization reaction with MPD in order to produce PA TFC membrane on a PSF support. The resulted TFC membrane showed that with a combination of PTC and TMC in as much as the attachment both Grampositive (*Bacillus subtilis*) and Gram-negative (*E. coli*) bacteria were reduced by at least two orders of magnitude, the flux was higher, and salt rejection efficiency was only significantly lower than that of the conventional TFC membrane prepared under similar conditions.

Xie et al. (2012) used novel monomers for preparation of TFC membranes. The experiment was conducted at 225 psi and approximately 25°C, using cross flow system and 2000 ppm aqueous solution of NaCl. TFC membrane was prepared using MPD in TMC and a sulfone diamine and using S-BAPS in TMC via IP. Replacing MPD with S-BAPS showed that, flux increased but salt rejection decreased. In addition, novel monomer containing membranes reduced chlorine tolerance as compared to the existing TFC membrane.

2.2.2.2 Support layer

In RO TFC membranes, some polymers are used as porous support layers, these are polysulfone (PSF), polyethersulfone, polycarbonate, polyphenylene oxides, poly (styrene co-acrylonitrile), poly (phthalazinone ether sulfone ketone) (PPESK), polyacrylonitrile, polyetherimide, polypropylene. Comparing PSF with other polymers, PSF is more hydrophobic. Generally, larger, hydrophobic skin layer pores produce more permeable and rough RO TFC membranes because less PA formed within the pores (Ghosh et al., 2009).

PSF is most commonly used polymer in the fabrication of support layer. Moreover, PSF is a commercially available polymer. The main reason why PSF is widely used as a support layer is because it has excellent mechanical, chemical and thermal stability, and sustainable to bacterial attack as compared to other polymer-support layers (Misdan et al., 2012).

2.2.2.3 Process modification and additives

Ghosh et al. (2008) investigated that the impact of organic solvent properties, reaction conditions, and curing conditions on polyamide composite reverse osmosis membrane using four organic solvents to produce wide variations in MPD solubility and diffusivity. Separation performance, film structure, and interfacial properties are evaluated. During experiment, PSF was used as support membranes RO TFC membrane preparation. Prepared PSF support layer were immersed and saturated in an aqueous solution of MPD for 15 s. In order to remove excess from surface of support layer, air knife was used until surface appears dry. Then, the MPD saturated PSF support layer was immersed in an organic solution of TMC for 15 s. And lastly, the composite membranes were heat to 50°C for 10 min. Also, triethylamine (TEA) - camphor sulfonic acid (CSA) was added to the aqueous solution.

They summarized the results following:

-Properties of RO-TFC membranes having different organic solvents showed the effect of solvent type on membrane properties that the flux decreased as hexane > heptane ~ cyclohexane > isopar. On the other hand, observed salt rejection decreased in order of heptane > hexane > isopar > cyclohexane. Also, contact angle decreased in order of heptane ~ hexane > cyclohexane ~ isopar. Measured the roughness values decreased in order of cyclohexane > heptane > hexane > isopar. The thicknesses of the

membranes decreased as of cyclohexane > hexane > isopar > heptane. Diffusivity of MPD in the organic solvents was observed from highest to lowest according to hexane > heptane > cyclohexane > isopar, which strongly correlated (negatively) with solvent viscosity. Solubility of MPD in the organic solvents decreased as cyclohexane > heptane ~ isopar > hexane, which strongly correlated with surface tension. According to results, the permeability was directly proportional to hydrophilicity and roughness and inversely proportional to film thickness and crosslinking. Overall, more water permeable films were formed by enhancing MPD diffusivity and reducing MPD solubility, which also tend to increase crosslinking.

-Properties of RO TFC membranes formed with additive showed that TEA-CSA in the aqueous solution affected that the pure water permeability dramatically increased, the salt rejection was practically unchanged, contact angle was slightly reduced, and roughness was significantly reduced. According to researchers, the results of TEA in the aqueous solution might compete with MPD partitioning, diffusion, and reaction with TMC; however, the reactivity of TMC with MPD was generally much higher than tertiary amines such as TEA. It was more likely that TEA act as a catalyst, accelerating the MPD-TMC reaction by neutralizing HCl produced during amide formation. Thinner, more crosslinked MPD-TMC films appear to form, and hence, membrane permeability increases without a loss of salt rejection. Other higher order amines perform a similar role, such as trimethyl amine or piperazines, but experience has shown that TEA was most effective. Addition of CSA is generally believed to protect the microporous skin layer of the support membrane from annealing during curing, although (to our knowledge) the mechanism has not been elucidated in published literature. This is especially important when high boiling point solvents are used because they require high temperature curing.

-Properties and morphology of RO TFC membranes formed at different temperatures of TMC solution in isopar during the interfacial polymerization shows that increasing temperature of isopar, permeate flux increases, salt rejection decreases, contact angle increases, surface roughness increases, and surface area decreases. Density, surface tension, and viscosity of isopar decrease as temperature increases; therefore, MPD solubility and diffusivity in isopar increase with temperature. According to researchers, the increase in contact angle (with increasing temperature) probably results from the decrease in surface area. Increasing TMC solution temperature

produces thinner, rougher, more permeable films. However, the apparent correlation between surface roughness and water flux may be coincidental because the film layer thickness (between roughness features) and structure (crosslinking) are the most important factors in determining membrane permeability.

-Properties of RO TFC membranes formed using four organic solvents cured at different temperature and times shows that flux of the hexane and cyclohexane increases in the range of 45–60 °C, but drops off above 75 °C. This contrasts with the flux of heptane and isopar increases through 90 °C . At higher temperatures, there is a chance of pore shrinkage in the support membranes. The decrease in flux for hexane and cyclohexane membranes at 90 °C could be due to this. However, the salt rejection also increased with increasing curing temperature, which suggested the additional crosslinking occurred. Similar results were reported for hexane-based polyamide membranes formed with different coating conditions and polysulfone supports.

Hirose et al. (1996) reported that an approximately linear relationship between membrane surface roughness and permeate flux for crosslinked aromatic PA RO that permeability increased with increasing surface roughness. The linear relationship was related to surface unevenness of the RO membrane skin layer, which resulted in enlargement of the effective membrane area.

El-Aassar (2012) reported to prepare TFC RO membranes on a polysulfone support layer via interfacial polymerization with using MPD and TMC. The researcher tried to investigate the optimum synthesis conditions of PA TFC membranes and examined the effect of different parameters for the IP reaction. 1.5 wt % MPD for 5 minutes soaking time and 0.05 wt % for 30 seconds reaction time gave the best results as high salt rejection 99.81% with high water flux 36.15 L/ m² .h.

2.2.3 Application of RO membrane modules

Today, reverse osmosis membranes are the outstanding for water purification applications that require high salt rejection in desalination technology. Developments in RO membranes have advanced significantly in the past decades. The global market for RO continues to grow and is predicted to reach \$8.1 billion by 2018 (Joo and Tansel, 2015). Some large seawater desalination plants utilizing RO process worldwide is given Table 2.6. In the Gulf Region (Middle East) region , RO market is greatest installed capacity because of low cost of fossil fuel led to preferred application

of thermal desalination processes. Also, Middle East is the largest amount of desalted water supplier in the World that produces about 70% of the seawater RO membrane. The Mediterranean market follows a head of the American and Asian markets. In Europe, desalination capacities are concentrated around the Mediterranean Sea in Spain and Italy (Fritzmman et al., 2007).

Table 2.6: Some Large Seawater Desalination Plants Utilizing RO Process in worldwide (Url-4).

No.	Country	Location	Capacity (m ³ /d)	In Operation (year)
1 ^{*a}	Israel	Ashkelon	272,520	2005
2 ^{*a}	UAE	Taweelah	227,300	2006
3 ^{*a}	Algeria	Hamma	200,000	2006
4 ^{*a}	UAE	Fujairah	170,000	2003
5 ^{*a}	Trinidad & Tobago	Point Lisa	136,000	2002
6 ^{*a}	Singapore	Tuas	136,000	2005
7 ^{*a}	Saudi Arabia	Tanbu	128,000	1995
8 ^{*a}	Spain	Carponeras	120,000	2001
9 ^{*a}	Israel	Palmachim	92,250	2000
10 ^{*a}	Saudi Arabia	Al Jubail III	90,900	2000
11 ^{*b}	UAE	Fujairah 2	136,000	2010
12 ^{*b}	Cyprus	Famgusta	10,000	2009
13 ^{*b}	Algeria	Hamma	200,000	2008
14 ^{*b}	Saudi Arabia	Shuaibah	150,000	2009
15 ^{*b}	Kuwait	Shuwaikh	136,000	2010
16 ^{*b}	Algeria	Oued Sebt	100,000	2010
17 ^{*b}	Israel	Palmachim	92,250	2007

Globally, there are three major commercial seawater membrane producers supplying polyamide TFC RO membrane. as it shown Table 2.7.

Table 2.7: Salt rejection of commercial membranes at standard test conditions of 32,000 ppm NaCl solution at 5.5 MPa and 25 °C .

Supplier	Polymer	Salt Rejection (%)	pH Range	Product Flow Rate (m ³ /day)
TORAY TM810C	Polyamide	99.75	2-11	4.5
TORAY TM810V	Polyamide	99.8	2-11	7.2
NITTO DENKO SWC5 HYDRONAUTICS	Polyamide	99.7	2-11	7.2
DOW FILM TEC SW30- 2540	Polyamide	99.4	1 - 13	2.6

2.3. Biofouling in RO membrane

Fouling by microorganisms is an essential obstacle to performance of RO. In desalination membrane fouling is the most significant issues which affects negatively the performance efficiency and shorter membrane life of RO plants. Therefore, development of antifouling RO membranes is an essential requirement in water treatment for the future. According to definition of International Union of Pure and Applied Chemistry (IUPAC), membrane fouling is "a process resulting in the loss of performance of a membrane due to the deposition of suspended or dissolved substances on its external surface, at its pore openings or within its pores" (Aptel et al., 1996).

Both reversible and irreversible solute adsorption can described fouling, but irreversible portion is most problematic. Irreversible adsorption causes a long-term flux decline that cannot be fully recovered by hydraulically cleaning the membrane (Matin et al., 2011).


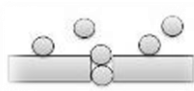


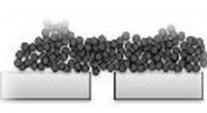

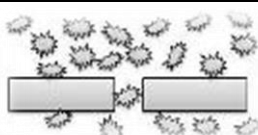

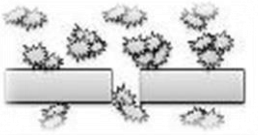
If particules are smaller than the pores, they can enter into the pores. If particle size is about same or bigger than pores, they can be adsorbed to the membrane surface and may accumulate onto it. So, pores are blocked and obviously it affects the membrane separation negatively. If these particals are cleanable by physical means, it is classified as reversible fouling. If it is not because of the adsorption, it is called as irreversible fouling (Table 2.8) (Mutamim et al., 2013).

However, RO membranes are considered essentially non-porous. Thus, the main fouling mechanism for RO membranes is surface fouling.

Membrane fouling is categorized according to the foulants (Malaeb, (2011) and Matin et al., (2011))

- 1.Crystalline: Deposition of inorganic material precipitating on a surface,
- 2.Organic: Deposition of organic substances (e.g. oil, proteins, humic substances),
- 3.Particulate and colloidal: Deposition of clay, silt, particulate humic substances, debris, silica,
- 4.Microbiological: Biofouling, adhesion and accumulation of microorganisms, forming biofilms.

Table 2.8: Colloidal-organic matter complex membrane fouling (Singh, 2006).

A. Pore versus Surface Pore versus Surface Fouling	
	Pore Adsorption ($d_{\text{solute}} \ll d_{\text{pore}}$): Colloids or solutes adsorb on the membrane walls, effective pore size is restricted and flux declines.
	Pore Plugging ($d_{\text{solute}} = d_{\text{pore}}$): Colloid or solutes of a similar size to pore diameter block pores completely, reduction in membrane porosity and severe flux decline
	Cake Formation ($d_{\text{solute}} \gg d_{\text{pore}}$): Colloid or solutes larger than the pores are retained due to sieving effects and form a cake on the membrane surface, depending on pore to particle size ratio flux decline occurs (permeability of the cake layer as well as the cake thickness are important)
B. Impact of Colloid or Solute Stability	
	Stable Colloids smaller than the pore size are not retained by membrane, unless adsorbed by the membrane material.
	Tight Aggregates are formed by slow coagulation, are retained and form a cake on the membrane. The aggregate structure may collapse depending on forces on the aggregate and the aggregate stability. Flux through the tight aggregates is usually low unless the aggregates deposit as a porous cake of large particles.
	Loose Aggregates are formed by rapid coagulation and are also retained. Such aggregates form a cake on the membrane. The aggregate structure may collapse depending on forces on the aggregate and the stability of the aggregate. Flux through the open aggregates is high if the structure is maintained during filtration.
C. Solute-Solute Interaction	
	Colloids < pores and stabilised with organics (for example) are not retained by the membrane, unless adsorbed by the membrane material or destabilised with high salt concentrations.
	Aggregates with organics adsorbed after aggregation (for example) are fully retained by the membrane, but may penetrate into the upper layer of the membrane. This could also be organics destabilised with multivalent cations.
	Colloids which are partially aggregated and destabilised such as a variety of solutes that interact with each other in heterogeneous ways in the presence of salts, colloids and dissolved organics, form small and diverse aggregates which may block pores.

With a great extent through pretreatment three types of fouling can be reduced but biofouling cannot be reduced by pretreatment alone, due to the deposited microbial cells, which can multiply and relocate. Membrane biofouling, affects many seawater desalination facilities involving the large desalination plants at Ras Abu Jarjur, Bahrain and at Saint Croix, US Virgin Islands. Also Middle East region affected especially that

largest amount of desalted water supplier in the World that produces about 70% of the seawater RO membrane (Matin et al., 2011).

2.3.1 Biofouling mechanism

Biofouling is described as the growth of microorganisms with accumulation of extracellular materials on the membrane surface (Al-Juboory and Yusaf, 2012).

Biofouling takes place on account of the transport, deposition and adhesion of cells followed by exopolymer production, and cell growth and proliferation all contributing to biofilm formation. Figure 2.9 exhibits the major events of occurring biofouling on membrane process (Matin et al., 2011).



Figure 2.9: Schema of biofilm formation on solid surface (Matin et al., 2011).

Biofouling formation is complex and many aspects must be considered to understand this process. These aspects include the following: the types of surfaces on which biofouling occur, the driving forces behind microbial adhesion, the theories that describe the interactions between microorganisms and surfaces, the factors affecting the microbial adhesion (Yusaf et al., 2012).

Microbial attachment on the membrane surface leads to the formation of biofilms, which consist of microbial cells embedded in an extracellular polymeric substances (EPS) matrix produced by the microbes (Ivnitskya et al., 2005)

Some bacteria play an important role for biofouling such as *Pseudomonas*, *Corynebacterium*, *Bacillus*, *Arthrobacter*, *Mycobacterium*, *Acinetobacter*, *Cytophaga*, *Flavobacterium*, *Moraxella*, *Micrococcus*, *Serratia*, *Lactobacillus* (Matin et al., 2011).

Altuğ et al. (2013) examined the microdiversity and composition of culturable heterotrophic aerobic bacteria in seawater. Samples were taken from the Sea of Marmara (an important basin between the Mediterranean and the Black Sea) in different periods and different areas. Research showed that in the seawater six bacterial classes are observed: Gammaproteobacteria (49%), Bacilli (34%), Alphaproteobacteria (9.09%), Betaproteobacteria (3.03%), Flavobacteria (3.03%), and Actinobacteria (3.03%). Also, diversity of culturable heterotrophic aerobic bacteria according to their isolated areas are showed in Figure 2.10. According to results, it is possible to say that heterotrophic bacteria play a key role in marine biogeochemical cycling and food webs because of the wide diversity of their metabolic properties.

Family	Species	Sampling areas						Phylum/Class
		1	2	3	4	5	6	
Enterobacteriaceae	* <i>Klebsiella pneumoniae</i> subsp. <i>pneumoniae</i> (Schroeter 1886), Trevisan 1887	+	-	-	-	+	+	Proteobacteria/ Gammaproteobacteria
	* <i>K. oxytoca</i> (Flügge 1886) Lautrop 1956	+	-	+	-	-	+	
	* <i>Citrobacter freundii</i>	+	-	+	-	-	+	
	* <i>Serratia fonticola</i> (Gavini et al. 1979)	+	-	+	+	+	+	
	<i>S. liquefaciens</i> (Grimes and Hennerty 1931) Bascomb et al. 1971	+	-	+	+	-	-	
	<i>Escherichia coli</i> (T. Escherich, 1885)	+	+	+	+	+	+	
	<i>Enterobacter cloacae</i> (Jordan 1890) Hormaeche and Edwards 1960	+	-	+	-	-	+	
	<i>E. sakazaki</i> (Farmer et. al., 1980)	+	-	+	-	-	+	
	<i>E. aerogenes</i> Hormaeche and Edwards 1960	+	-	+	-	-	-	
	* <i>Salmonella enterica</i> subsp. <i>arizonae</i> (Borman 1957) Le Minor and Popoff 1987	+	-	+	-	-	-	
Pseudomonadaceae	<i>Pseudomonas luteola</i> Kodoma, et al. 1985	+	-	+	-	-	+	Proteobacteria/ Alphaproteobacteria
	* <i>P. putida</i> Trevisan, 1889	+	-	+	+	-	-	
Xanthomonadaceae	<i>P. aeruginosa</i> (Schroeter 1872) Migula 1900	+	-	+	+	-	-	
	* <i>Stenotrophomonas maltophilia</i> Palleroni and Bradbury 1993	+	-	+	-	-	+	
Shewanellaceae	* <i>Shewanella algae</i> Simidu et al. 1990	-	+	-	+	-	-	
Brucellaceae	<i>S. putrefaciens</i> (Lee et al. 1981), MacDonell and Colwell 1986	+	-	+	-	-	+	
	* <i>Brucella melitensis</i> (Hughes 1893), Meyer and Shaw 1920	-	-	-	-	+	-	
Sphingomonadaceae	* <i>Sphingomonas paucimobilis</i> (Holmes et al. 1977), Yabuuchi et al. 1990	+	-	+	-	-	+	
Caulobacteraceae	* <i>Brevundimonas vesicularis</i> (Büsing et al. 1953) Segers et al. 1994	+	-	+	-	-	+	
Aeromonadaceae	<i>Aeromonas hydrophila</i> (Chester, 1901) Stanier, 1943	+	-	+	-	-	+	
	* <i>A. caviae</i> Eddy 1962, Popoff 1984	+	-	+	-	-	-	Firmicutes/ Bacilli
Alicyclobacillaceae	* <i>Alicyclobacillus acidoterrestris</i> (Deinhard et al. 1988) Wisotzkey et al. 1992	+	-	+	-	-	+	
Bacillaceae	* <i>Bacillus cereus</i> Frankland and Frankland 1887	+	-	+	+	+	+	Bacteroidetes/ Flavobacteria/ Actinobacteria/ Proteobacteria/ Betaproteobacteria
	* <i>B. mycoides</i> Flügge 1886	+	-	+	-	-	+	
	* <i>B. pumilus</i> Meyer and Gottheil 1901	+	-	+	-	-	+	
	* <i>B. thuringiensis</i> Berliner 1915	+	-	+	-	-	+	
	* <i>Streptococcus pneumoniae</i> (Klein 1884) Chester 1901	+	-	+	-	-	+	
Streptococcaceae	<i>E. faecalis</i> (Andrews and Horder 1906) Schleifer and Kilpper-Balz 1984	+	-	+	-	-	+	
	* <i>Staphylococcus hominis</i> Kloos and Schleifer 1975 emend. Kloos et al. 1998	-	+	-	+	-	-	
Staphylococcaceae	* <i>Virgibacillus pantothenicus</i> (Prooen and Knight 1950) Heyndrickx et al. 1998	+	-	-	-	+	+	
Flavobacteriaceae	* <i>Chryseobacterium indologenes</i> (Yabuuchi et al. 1983) Vandamme et al. 1994	+	-	+	-	-	+	
	* <i>Micrococcus luteus</i> Lehmann and Neumann 1896	+	+	+	-	-	+	
Alcaligenaceae	* <i>Alcaligenes faecalis</i> subsp. <i>faecalis</i> (King 1959) Kim et al. 2005	+	+	-	+	-	+	
Gram-negative fermenting and nonfermenting bacteria	23	23	3	3	7	15	15	
Gram-positive cocci and nonspore-forming bacilli	4	3	2	2	0	2	3	
Spore-forming gram-positive bacilli	6	6	0	5	1	6	6	
Total number of species	33	30	5	27	9	23	24	

1: Northwestern part of the Sea of Marmara, 2: eastern part of the Sea of Marmara, 3: northeastern coastal areas of İstanbul, 4: western part of the Sea of Marmara, 5: southern coastal areas of İstanbul, 6: northern coastal areas of İstanbul. *First record for the Sea of Marmara.

Figure 2.10: Microdiversity and composition of culturable heterotrophic aerobic bacteria in Marmara Sea (Altuğ et al., 2013).

2.3.2 Biofouling effects on membrane processes

Membrane systems are affected negatively by biofouling such as:

- Flux decreasing of membrane due to the formation of a low permeability biofilm on the membrane surface.
- Increasing of differential pressure and feed pressure in order to maintain the same production rate due to biofilm resistance.
- Concentrated acidic by-products due to the membrane biodegradation at the membrane surface.
- Increasing of salt passage through membrane and decreasing of quality product water due to the accumulation of dissolved ions in the biofilm at the membrane surface. Therefore, degree of concentration polarization increases.
- Increasing energy consumption, higher pressure being required to prevent biofilm and the flux decline (Nguyen et al., 2012).

2.3.3 Prevention and control of biofouling problem

2.3.3.1 Feed Pretreatment

Pretreatment is preferred by either a conventional or by MF/UF membrane processes. A conventional process consists of coagulation/flocculation, dissolved air flotation, granular media filter, and a dual media filter. Membrane pretreatment obtains a lower silt density index. So, it is known to be more effective than the conventional process to inhibit biofouling. Among this, membrane pretreatment systems need less space and chemicals compared to the conventional pretreatment systems (Matin et al., 2011).

Al-Tisan et al. (1995) evaluated the control of biofouling under different pretreatment regimes in a specially designed SWRO pilot plant in Saudi Arabia. They examined that coagulation and dual media filtration reduced bacterial number in the feed by 32–100% depending on initial chemical pretreatment of raw seawater. In most cases, the coagulation and filtration effectively removed a large portion of total bacterial mass (82%) in the feed.

Kumar et al. (2007) studied the effect of pretreatment type on SWRO performance using bench scale experiments. The researchers observed the effect of different pretreatment strategies on flux decline and using prefiltration of the feedwater using different filtration size ranges. They found that particulate matter of size greater than

1 μm (representing media filtration i.e. one of the conventional processes) caused most of the RO fouling. When membrane filtration (both MF and UF) was used significant reduction in fouling was observed. when a tight UF membrane was used, the lowest flux decline was observed.

2.3.3.2 Biocide application

Biocides are used disinfectant which prevents activity of micro-organisms. Kim et al. have summarized the chemical and physical disinfection methods that could be used for the SWRO process to prevent biofouling as it seen Table 2.9. (Matin et al., 2011).

Table 2.9: Comparison chart for disinfectants used for bio-fouling control of SWRO membranes (Matin et al., 2011).

	Disinfection	Advantage	Disadvantage
Physical	UV	<ul style="list-style-type: none"> • Easy installation and maintenance • Effective inactivation • Oxidation of organic matter 	<ul style="list-style-type: none"> • Scale formation • No residual effect
	Membrane	<ul style="list-style-type: none"> • Combined with membrane pretreated 	<ul style="list-style-type: none"> • High capital and operation cost
	Sand filtration	<ul style="list-style-type: none"> • Low installation and operation cost 	<ul style="list-style-type: none"> • Low bacterial removal efficiency
Chemical	HOCl, OC^-	<ul style="list-style-type: none"> • High inactivation efficiency • Organic matter removal • Relatively low cost 	<ul style="list-style-type: none"> • THMs, HAAs formation
	NH_2Cl	<ul style="list-style-type: none"> • Less harmful on membrane than HOCl • Residual inactivation 	<ul style="list-style-type: none"> • Relatively low efficiency
	ClO_2	<ul style="list-style-type: none"> • No damage on membrane 	<ul style="list-style-type: none"> • Chlorite toxicity
	Ozone	<ul style="list-style-type: none"> • Effective inactivation • High oxidation potential for organic matter 	<ul style="list-style-type: none"> • Damage by residual ozone • Bromate formation • Very small half life

Biocides can be applied two types in membrane systems. First, a biocide may be added continuously or intermittently (e.g., with a metering pump) to the system feedwater in an attempt to inhibit or otherwise control the unrestricted growth of biofilm microorganisms on the membrane surfaces. Second, a biocide may be added in the preservation of the polymer membranes and related module components (e.g., glues,

plastic spacers, other materials of construction) during extended periods of membrane storage or plant shutdown. This is the most general application (Matin et al., 2011).

2.3.3.3 Surface modification

Membrane surface modification is done primarily to prevent or restrict bacterial adhesion, microcolony formation, and biofilm maturation, in one or more of these stages. For instance, bacterial adhesion has been reduced significantly increasing the hydrophilicity of the surface. This can be achieved by adding negatively charged groups or decreasing the surface roughness. Similarly, the incorporation of antimicrobial nanomaterials succeeded at inactivation of irreversibly adhered microorganisms (Matin et al., 2011). Several nanomaterials have strong antimicrobial properties, such as nAg, chitosan, TiO₂ and polyethylene glycol. The major antimicrobial material's mechanisms reported in the literature are summarized in Figure 2.11. Antimicrobial materials inhibit the microbial growth with altering cell permeability, damaging DNA and inhibiting of protein synthesis.

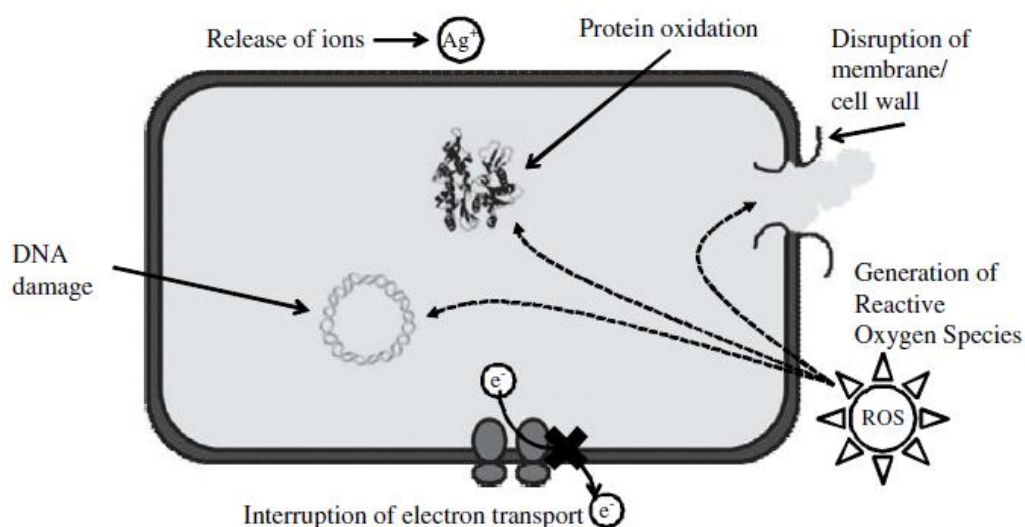


Figure 2.11: The major antimicrobial mechanisms (Li et al., 2008).

Yang et al. (2009) added nanosilver as a biocide, in a novel biofouling control approach by surface modification of the RO membrane and spacer with nanosilver coating. All the experiments were conducted using spiral-wound commercial RO membrane modules SW30-2514 FILMTECDOW. The cross flow system was operated at 800 psi with seawater approximately 20 days for long-term observation of microbial growth and to express their dynamic activity (e.g. microbial adherence and

multiplication). They developed a unique microbial counting protocol developed as it mentioned Figure 2.12. Meanwhile, reserarchers use a persistent labeling dye to stain microbes, namely Red Fluorescent Cell Linker Mini kit. The results of experiment showed that the antibacterial effect of silver-coated was observed clearly and can be used in seawater desalination plants.

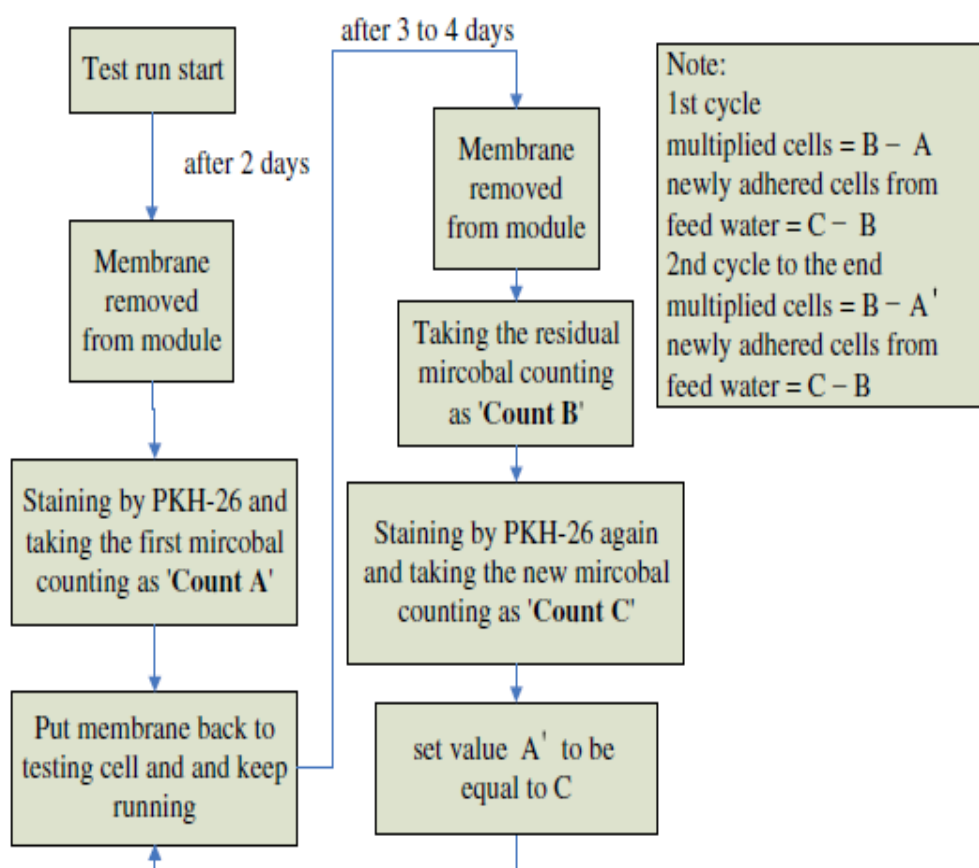


Figure 2.12: Microbial count protocol for identifying multiplied and adhered cells (Yang et al., 2009).

The antimicrobial action of composite membranes modified via layer by layer approach with PSS/polyhexamethylene biguanide have been examined using confocal imaging of the growth of *Pseudomonas Aeruginosa* bacteria on the membrane surface. It is shown at Fig 2.13 and it can be possible to say that significant difference in the number of live and dead cells on the membrane surface were found when comparing initial membrane sample and modified membranes (the live bacteria are shown in green color, while the dead bacteria are red) (Kochkodan and Hilal, 2015).

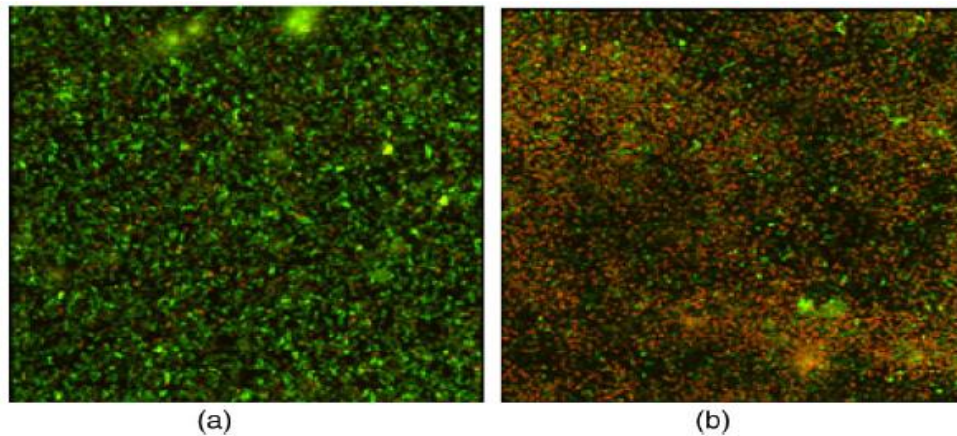


Figure 2.13: Confocal images of the membrane surface after *P. Aeruginosa* PAO1 growth: (a) initial NF-90 membrane (a) modified composite membranes (Kochkodan and Hilal, 2015).

Denyer et al. (1991) observed effect of composite membranes modified with quaternary 2-dimethyl-aminoethylmethacrylate studied with *E.coli*. Observation showed that composite membranes have strong bactericide properties. (Figure 2.14).

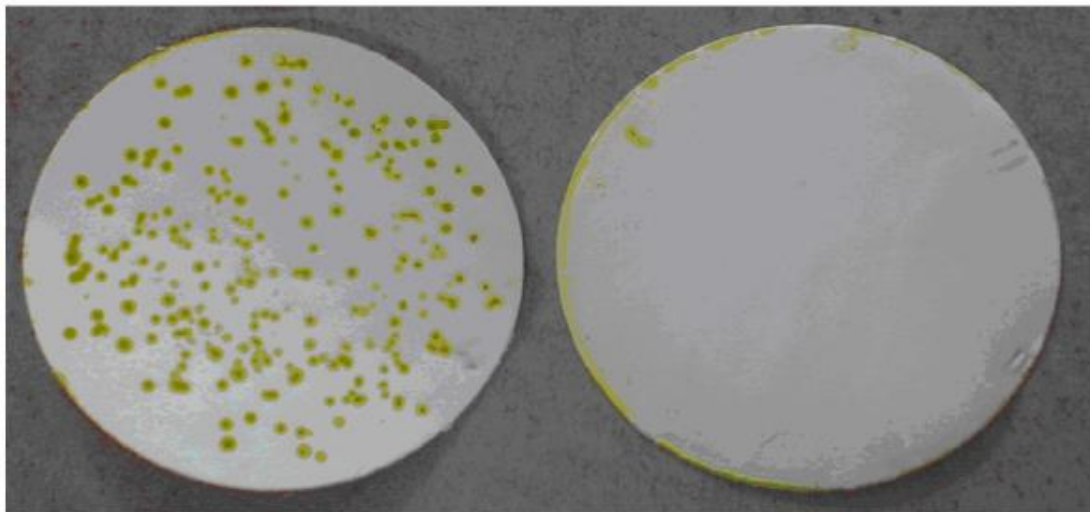


Figure 2.14: Photograph of initial PVDF membrane (left) and PVDF membrane with grafted and after filtration of *E. coli* suspension (Denyer et al., 1991).

Kang et al. (2008) showed strong antimicrobial activity of single walled carbon nanotubes. Also, they demonstrated that the likely mechanism leading to bacterial cell death is cell membrane damage resulting from direct contact with its combine (Figure 2.15). Gene expression datas show that it's displaying much stronger bacterial toxicity than their multi-walled counterparts.

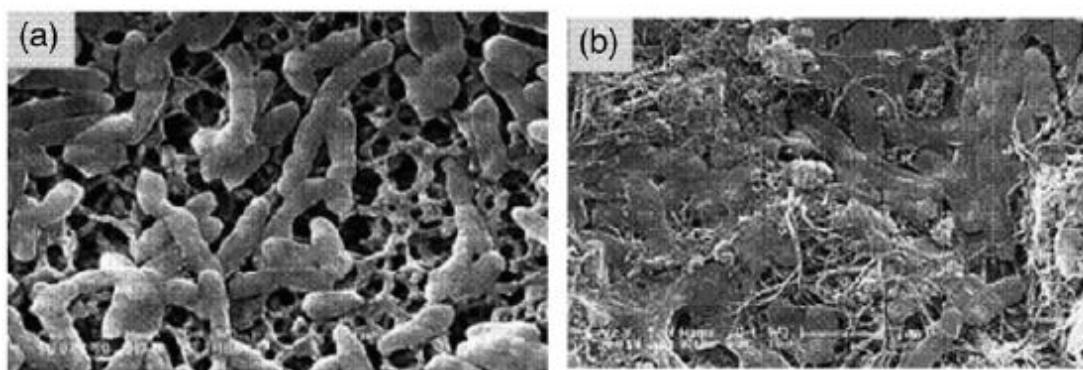


Figure 2.15: SEM images of *E. coli* cells incubated for 60min (a) without single walled carbon nanotubes maintaining their outer membrane structure. (b) SEM images of *E. coli* cells incubated for 60min with single walled carbon nanotubes losing their cellular integrity (Kang et al., 2008).

2.3.3.4 Membrane cleaning

During to clean RO membranes, acidic and/or basic (alkaline) chemicals are used in combination. Generally, hydrochloric acid, phosphoric acid, sodium hydrosulfate ($\text{Na}_2\text{S}_2\text{O}_4$) and sulfamic acid ($\text{NH}_2\text{SO}_3\text{H}$) are used for acidic solutions (pH 2) and sodium lauryl sulfate, sodium hydroxide, sodium ethylenediamine tetraacetic acid (Na_4EDTA), and proprietary cleaners for alkaline (pH 12) chemicals. Most cleaning solutions are made from stock chemical solutions to a final concentration of 0.03–2.0 % (wt). Membrane cleaning helps restore permeate flux and thus decrease salt passage (Greenlee et al., 2009)

2.3.3.5 Improvement of interfacial polymerization process

The using of novel monomers can enhance the antifouling property of prepared RO membranes since novel monomers include more functional or polar groups. Thereby the prepared TFC RO membrane shows smoother surface and better hydrophilicity that is an advantage for antifouling property of membrane. Li et al. (2007) reported to prepare TFC RO membranes on a polysulfone support layer via interfacial polymerization with using new acyl chloride monomers such as 3,4',5'-biphenyl triacyl chloride and 3,3',5,5'-biphenyl tetraacyl chloride. According to research, the atomic force microscope (AFM) images showed that the prepared with 3,4',5'-biphenyl triacyl chloride and MPD membrane exhibited a smoother surface and similar hydrophilicity compared to TMC/MPD. With using 3,3',5,5'-biphenyl tetraacyl chloride and MPD membrane had better antifouling property than TMC/MPD but it should be noted that

researchers did not conduct fouling experiments, so firm conclusion cannot be provided directly (Li et al., 2007).

Liu et al. (2006) prepared RO composite membrane using a novel monomer 5-isocyanato-isophthaloyl chloride and MPD. The antifouling performance of membranes was tested with lake water and four simulated aqueous solutions, and compared with the TMC/MPD membrane and a commercial polyamide RO membrane from Hydranautics. Results showed that prepared with monomer 5-isocyanato-isophthaloyl chloride and MPD membrane had better hydrophilicity and a smoother surface and it showed better resistance to fouling in all fouling tests (Liu et al., 2006a-b and Liu et al., 2008).

Similarly, the results probably exhibit that the antifouling properties of RO membranes were closely related with their hydrophilicity and surface roughness.

Also, the improvement of IP process can enhance the antifouling property of prepared RO membranes. Similar to using novel monomers, improvement of the interfacial polymerization process improves the membrane surface characteristics, such as increasing the hydrophilicity, reducing the roughness. With adding active organic modifiers into TMC or MPD solution, the modifiers can join the reaction and are introduced into functional barrier layer during the interfacial polymerization process. Therefore the surface property and fouling resistance of the RO membranes improves.

2.4 Development Of Antifouling Reverse Osmosis Membrane With Bisbal Additive

2.4.1 Anti bacterial effects of BisBAL

Bismuth is a chemical element with symbol Bi and atomic number 83. Bismuth is a crystalline, brittle metal and constitutes the most naturally occurring diamagnetic metal. Typically, bismuth is found as bismuthinite (bismuth sulfide), bismite (bismuth oxide) and bismuthite (bismuth carbonate) (Aptel et al., 1996). Bismuth metal has been known from ancient times but it was often confused with lead and tin. Although until the 1753, Bismuth was first shown to be a distinct element in by Claude Geoffroy the Younger (Url-5).

The heaviest member of the Pnictogen group is Bismuth and is called a “green element”, because compared with elemental bismuth and its compounds other heavy

metals are more noncarcinogenic and nontoxic . Also, they have less bioaccumulative features (Badireddy et al., 2014). Delgadillo et al. (2012) reported that bismuth nanoparticles can inhibit bacterial growth at concentrations lower than 1 mM. Elemental bismuth combined with lipophilic thiols shows antimicrobial properties even at very low ($\mu\text{mol l}^{-1}$) concentrations (Domenico et al. 1997).

Bismuth thiols can be available differently seven types as that are 1,3-propanedithiol, dimercaprol, dithiothreitol, 3-mercapto-2-butanol, b-mercaptoethanol, 1-monothioglycerol, and mercaptoethylamine in order of decreasing synergy. In particular, the antibacterial effects of bismuth- 2-3 dimercapto-1-propanol is reportedly up to 300 times higher than even other dithiol formulations over a broad range of Gram negative and Gram positive bacteria (Domenico et al. 1997). Dimercaptopropanol is also known as dimercaprol or British anti-lewisite (BAL) (Codony et al., 2003).

In addition, BisBAL exhibits extensive antifouling properties against monocultures of *Klebsiella pneumoniae*, *Pseudomonas* and *Staphylococcus spp.*, *Burkholderia cepacia*, *Escherichia coli* and *Enterobacter* and *Enterococcus spp.* (even at sub-inhibitory levels (approx. 5–15 ($\mu\text{mol l}^{-1}$)) (Badireddy and Chellam, 2011).

It is important to say that novel biocide BisBAL used for preventing biofouling at environmental systems in recent years. Badireddy and Chellam subjected to BisBAL to control floc formation in a multispecies population of micro-organisms obtained from the activated sludge unit of a wastewater treatment plant. When BisBAL at minimum inhibitory concentration ($10 \mu\text{mol l}^{-1}$), it was most effective in suppressing microbial floc formation. The study exhibits that BisBAL can also be potentially employed to control excess sludge production in wastewater treatment systems by inhibiting EPS expression (Badireddy and Chellam, 2011).

Another study indicates that BisBAL is a potential alternative to prevent biofouling with antifouling and bactericidal properties of BisBAL (Domenico, 2002).

Bismuth has significantly strong antifouling effect, when iron concentration is low. Inhibitory effects of bismuth on bacteria is negatively affected with increasing iron. In addition, insolubility properties of bismuth in aqueous solutions is one of the major problems. It has been found that ideal molar ratio of bismuth to BAL is in a ratio range of approximately 1:2 to 3:1. At a ratio of 3:1, the composition is particularly active

against microbes. However, the highest solubility in water and longest shelf life can be obtained when the molar ratio of bismuth to BAL is 1:2. It shows that differing ratios can be used depending on the desired characteristics of the composition. BisBAL can be used powerful antimicrobial agent. When compare to either Bi^{3+} or BAL alone, BisBAL activity is orders of magnitude more effective. Moreover, BisBAL inhibits biofilm organisms effectively. In particular, BisBAL was shown to be as effective against bacteria in biofilms as it is on planktonic bacteria (Domenico, 2002).

Badireddy and Chellam (2011) studied the determination of the ability of a bismuth thiol to control floc. According to the study, absence of BisBAL resulted in very dense and compact flocs, but increasing BisBAL concentrations progressively inhibited aggregation, closely resembling the initial control sample (Figure 2.16).

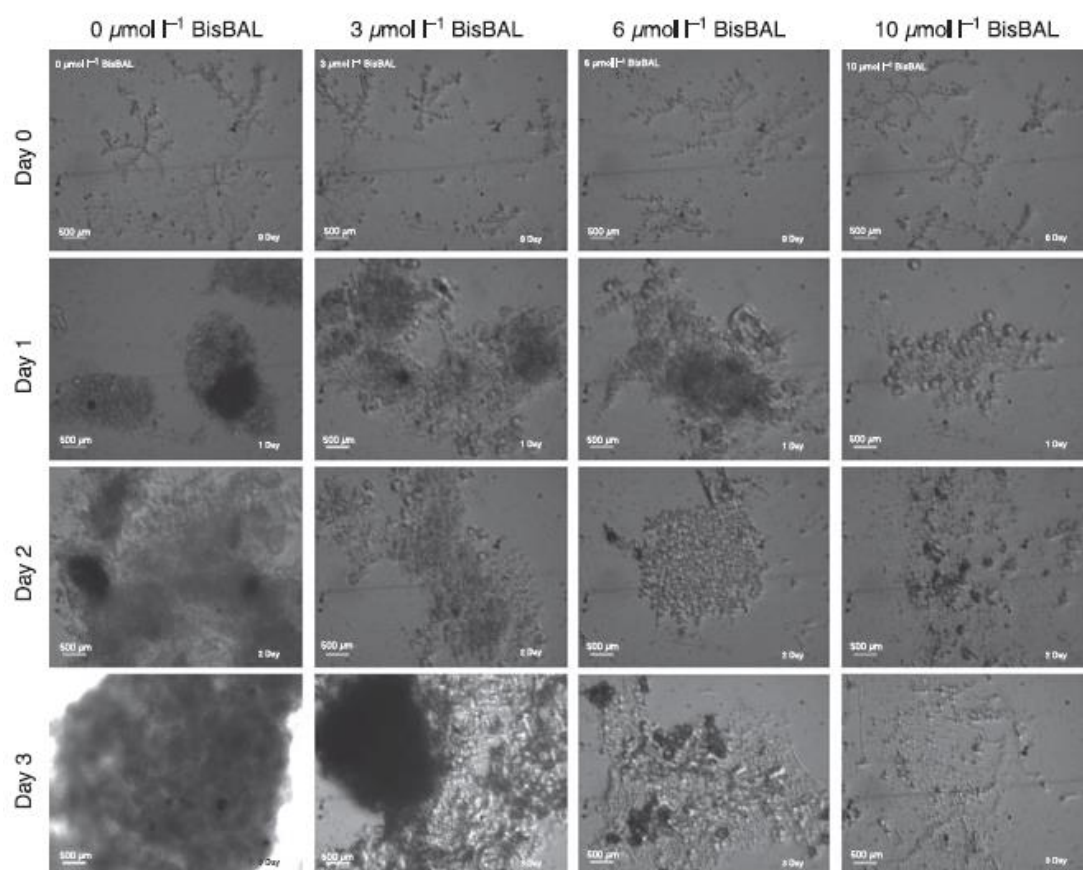


Figure 2.16: Visualization of the effects of BisBAL on planktonic biofilm formation over 3 days using phase contrast microscopy (Badireddy and Chellam, 2011).

2.4.2 Industrial applications of Bismuth-Thiols

According to Claudio and Chellam (n.d.) Bismuth nanoparticles could be used as surface disinfectant; hospitals, pediatric and geriatric clinics, food and pharmaceutical

industries, laboratories and in general all locations where microbial contamination needs to be counteracted.

Agriculture

BTs are used for preventing of crop losses.

Due to resistant microbes and their biofilms on crops, BT compounds are capable of preserving plant health and crop productivity. BTs have significant potential to provide effective new tools for combating agricultural diseases based on their unique constellation of properties:

- Broad-spectrum antimicrobial activity against agriculturally-relevant pathogens.
- Prevention of biofilm formation and ability to compromise existing biofilms .
- Low potential for development of resistance.
- Stability and functionality under a variety of environmental conditions.

Water treatment

BTs offers an overranching environmentally-friendly approach to control biofouling in water systems. BTs will be capable of reducing biofouling in drinking water treatment and distribution, and for desalinisation, wastewater treatment, and water-cooled heat exchange systems. Also, BTs have a significantly strong potential to prevent biocorrosion .

Oil & Gas

Biocorrosion on the pipelines is a major problem for oil and gas industry. The current solutions contains highly toxic chemicals which are dangerous for human health. These chemicals releases deadly hydrogen sulfide (H₂S) gas which causes deaths. Instead of these chemicals, BTs are a more environmental solution for oil and gas industry.

Pulp & Paper

BTs are very effective to prevent biofilm formation by bacteria known to contribute to biofouling in the pulp and paper industry.

Undesired microbial growth is a big problem in the pulp and paper industry. Biofilm formation is responsible for 20% of all paper machine downtime.

Current technology which is used for preventing microbial resistance has a danger for the environment and human health. BTs, instead, are safer and environmentally-friendly.

Ship's Paint

BTs have been demonstrated to be effective both against marine bacteria. Instead of toxic chemicals, BTs are more useful and safer.

Medicine

BTs are also utilized in numerous medical applications. For instance, they are used orally as an anti-diarrheal agent, for upset stomach, nausea, vomiting, and as an internal deodorant, and as skin antiseptics.

3. MATERIALS & METHODS

3.1. Materials

Brands and product codes of solvent(s), polymer(s) and the nanomaterials are indicated in Table 3.1. Chemicals are used without extra purification.

Table 3. 1: Brands of materials used for the experiment.

Chemical name	Brand
PSF (86,000 Da)	Solvey
Polyvinylpyrrolidone PVP10 (10,000 Da)	Sigma-aldrich
Polyvinylpyrrolidone PVP40 (40,000 Da)	Sigma-aldrich
Polyvinylpyrrolidone PVP360 (360,000 Da)	Sigma-aldrich
N, N-dimethylformamide (DMF)	Akkim
N-Metil-2-piroliden (NMP)	Asland
Bismuth(iii) nitrate pentahydrate; acs reagent, $\geq 98.0\%$	Sigma-aldrich
Propylene glycol $\geq 99.5\%$, fcc	Sigma-aldrich
2,3-dimercapto-1-propanol	Sigma-aldrich
Sodium hydroxide extra pure	Sigma-aldrich
MPD	Merck
Hexane	Sigma-aldrich
Trimesil klorit (TMC)	Merck
LB Broth (MILLER)	Merck
Rapid E.coli 2 Agar	Merck

3.1.2 Fabrication of support layer of membranes

For the preparation of bare polymer solutions, the amount of materials were determined according to the weight percentage (% , w/w). The ratios of the polymer, PVP and solvent for the prepared membranes are given in Table 3.2. Bottles of 200 ml solution was used to prepare the dope solution. These bottles were washed before preparing the solution with distilled water and then dried in an oven and then washed with the solvent to be used in dope solution.

DMF and NMP was used as the solvent in dope solutions. Also PVP (10,000 , 40,000 and 360,000 Da.) was used as the pore-forming agent. Commercial PSF was used as the polymer. At the first step of solution preparation, PVP was added to the solvent as

pore-forming agent and stirred for 20 min with a magnetic stirrer until it is completely dissolved.

Table 3. 2: The content of dope solutions.

Membrane code	Polyme r ratio (%)	PVP type (Da)	PVP ratio (%)	Solven t type	Solvent ratio (%)
% 16 PSF	16	-	8	NMP	84
% 16 PSF, % 8PVP10	16	10,000	8	NMP	76
% 16 PSF, % 8PVP40	16	40,000	8	NMP	76
% 16 PSF% 8PVP360	16	360,000	8	NMP	76
% 18 PSF, % 4.5 PVP10 , % 1.5 PVP40	18	10,000- 40,000	4.5-1.5	DMF	76

When exact dispersion of PVP was observed, the dried polymer was added slowly. In order to homogeneous dispersion, the prepared dope solutions were stirred for 1 day at 60 ° C at 200 rpm. Figure 3.1 shows an example of the prepared dope solution.



Figure 3.1: Prepared dope solution.

Ultrafiltration membranes were prepared using the phase inversion method. Images of the membrane preparation step are shown in the Figure 3.2 and Figure 3.3. In the first step, a specific volume (Figure 3.2-a) of homogeneous dope solution was poured on a glass surface and an aluminum casting knife which was arranged to a constant thickness (Sheen branded) was put on that solution (Figure 3.2-b,c). Then the laboratory scaled automatic film applicator machine at the MEMTEK was adjusted to

a constant velocity (80 mm/sec) and a thin film was formed on the glass surface (Figure 3.2-d). In the next step, solvent was evaporated from the polymer films for a specific time interval, in order to obtain the desired properties for produced membranes (Figure 3.2-e). Evaporation time was set to 10 seconds for this step. After the evaporation process, polymer film coated glasses were put in a coagulation bath containing distilled water (Figure 3.2-f). Polymer film coated glasses were kept in the coagulation bath at 5 min for membrane production. Thus, the solvent and the polymer replaced with water and collapsed membranes were obtained. Then, the produced membranes were transformed into a clean medium filled with distilled water (Figure 3.2-g, h). Produced membranes were kept in a cold room at +4°C at one week to prevent the biological growth and to eliminate the unreacted polymer and solvent, and then passed to the characterization process.

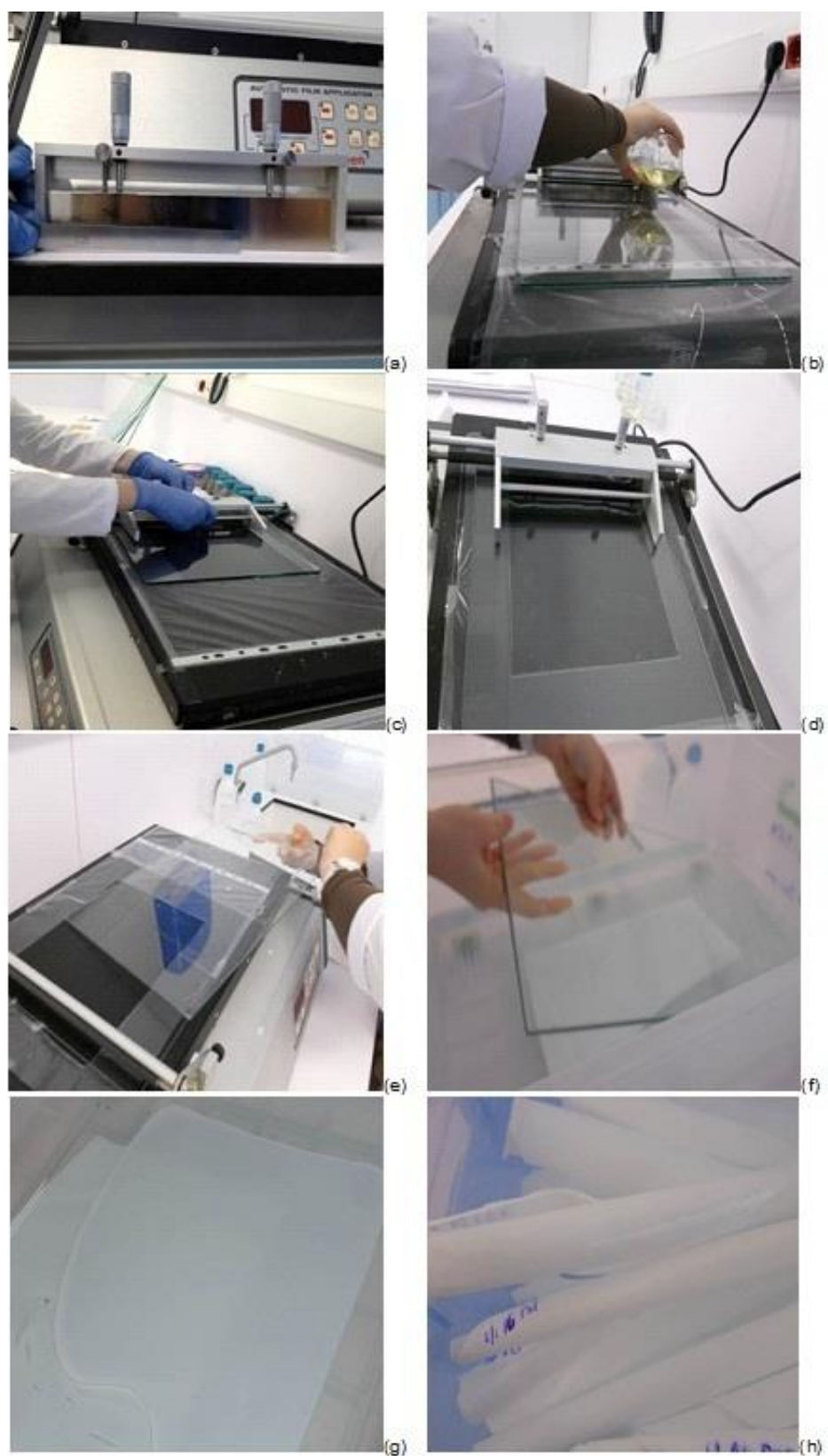
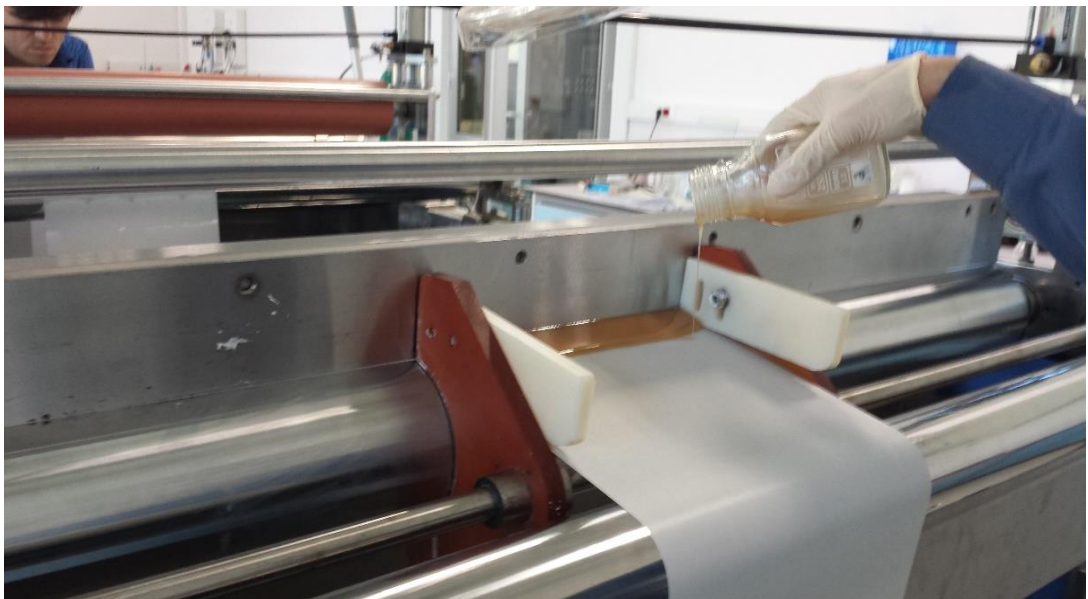


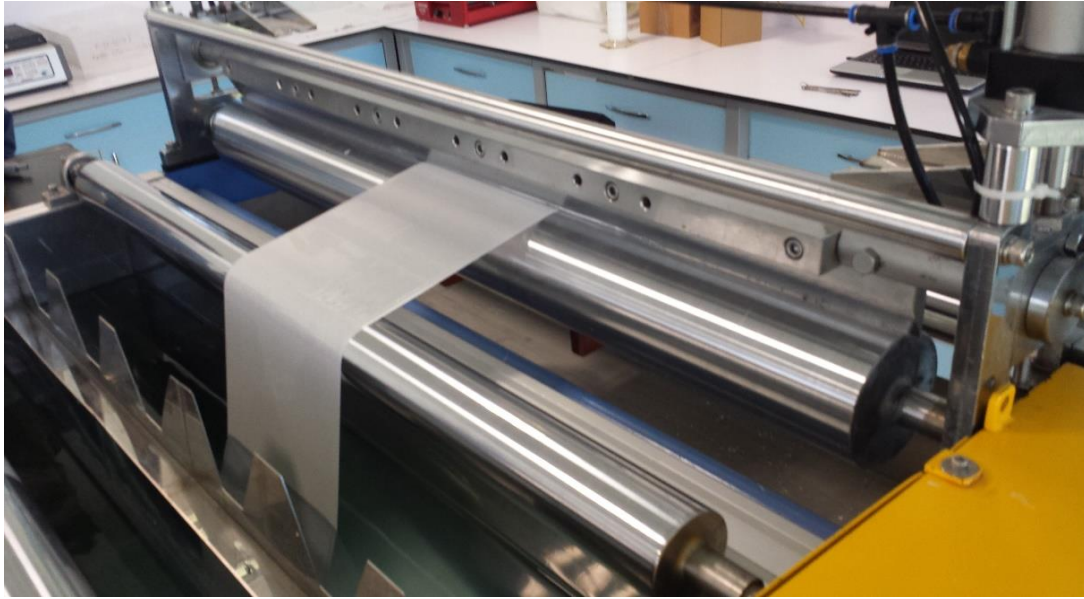
Figure 3.2: Preparation processes of the flat sheet membranes at laboratory scale.



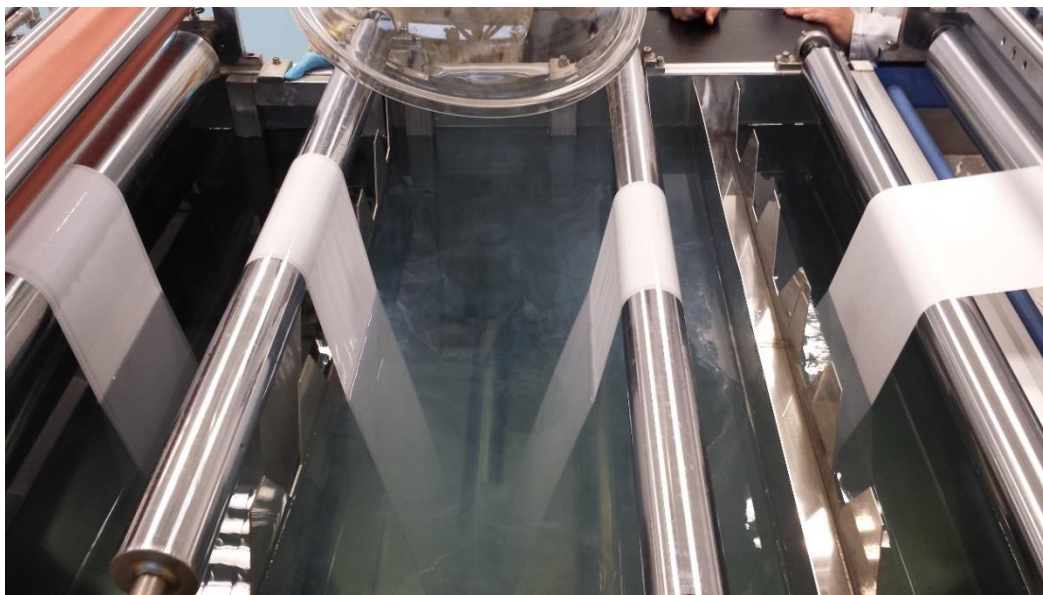
(a)



(b)



(c)



(d)

Figure 3.3: Preparation processes of the flat sheet membranes in pilot scale.

3.1.3 BisBAL preparation

First step was the preparation of stock solution for BisBAL. Main purpose of stock solution was to dissolve $\text{Bi}(\text{NO}_3)_3$ in propylene glycol. 1.21 gr Bismuth(iii) nitrate pentahydrate was solved in 50 ml propylene glycol at 40°C and it was mixed during 12 h. BisBAL was prepared using a 2 : 1 molar ratio of bismuth to BAL. 2:1 molar ratio of Bi (Bis) to 2,3-dimercapto-1-propanol (BAL) was prepared by adding $2.5 \mu\text{L}$ of 10

M BAL to 1.0 mL of 50 mM stock solution at room temperature and it was stirred. The optimum conditions were selected as 2:1 molar ratio of BisBAL and pH=4 according to the results of previous studies conducted at MEMTEK.

2:1 = Bis: 50 mM 1 mL + BAL: 10 M 2.5 μ L

3.1.4 Fabrication of active layer of membranes

The thin film composite layer was produced with using the interfacial polymerization (IP) technique. Transaction gradual expression is showed schematically in Figure 3.4. In the first step, the aqueous and organic solutions were prepared (Figure 3.5-a-b). Then the cutted support layer the size of the 25x25 cm was placed (Figure 3.5-c). Then aqueous phase (water + monomer) to about 25 ml was poured onto the support layer is immersed 30s-10 min seconds). Then the support layers were cutted as the size of the 25x25 cm and they were replaced in a frame (Figure 3.5-c). Then aqueous phase (water + monomer) was poured onto the support layer and it was immersed in 30s-10 min. Then the excess water remaining on the membrane was purged with roles (Figure 3.5-d). Once the membrane was placed again under acid chloride (dissolved phase in hexane) solution in 30s-2 min with 1-2 min was poured into the membrane surface was immersed to the selected time period. Last step, the membrane was placed an oven to 5-10 min with a temperature of 60-70°C and washed thoroughly with deionized water before storage in deionized at 5°C in a laboratory refrigerator (Figure 3.5-e-f).

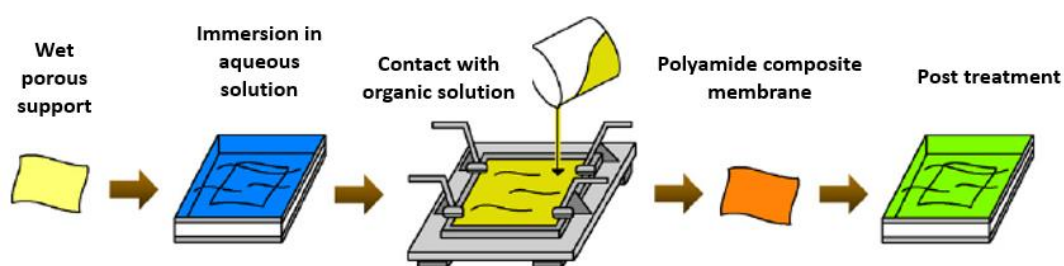
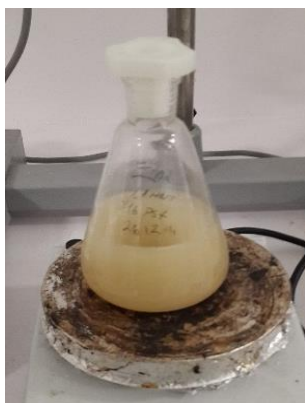


Figure 3.4: Diagram of TFC preparation method.



(a)

(b)

(c)



(d)

(e)

(f)

Figure 3.5: The stages of the TFC coating method.

3.2. Membrane Characterization Methods

3.2.1 Membrane thicknesses

Thicknesses of membrane was measured with using a micrometer before the characterization experiments as shown in the Figure 3.6.



(a)



(b)

Figure 3.6: Measurement of the membrane thickness.

3.2.2 Viscosity

Viscosity of polymer solution was measured by AND vibro viscosimeter SV-10 (UK) as it seen Figure 3.7. In the beginning calibration was done with distilled water at 25°C, then polymer solution sample (30 ml) was used to measure viscosity value was used to determine at room temperature.

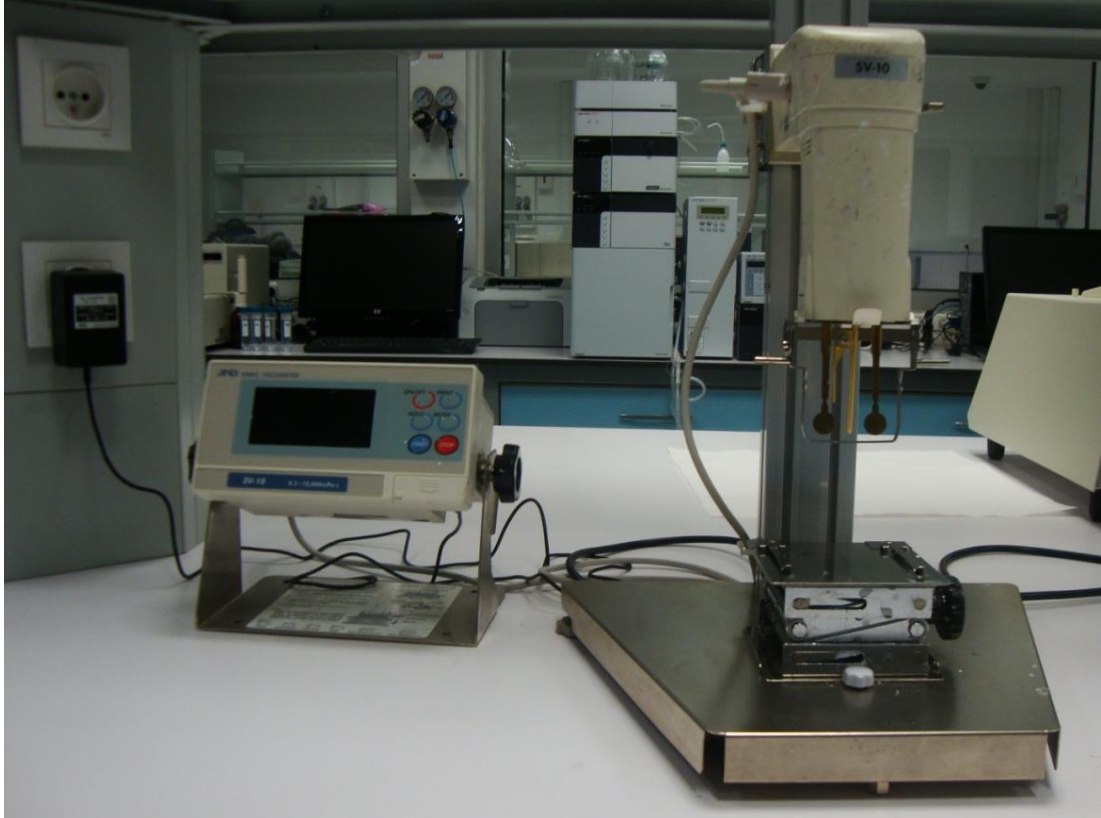


Figure 3.7: Viscosimeter.

3.2.3 Permeability

During permeability tests, pressure driven filtration cell named Sterlitech HP4750 was used with a magnetic stirrer. Technical properties of the filtration system are given in Table 3.3. Gauge of pressure was done with nitrogen gasses. Before permeability tests, compaction test were done during 1 hour at 5 bars with distilled water for removal of solvent and clearance pores. After the compaction test for 3 different pressures, filtration flux were measured during 10 minutes again with distilled water and results were transferred to an excel file. This process was repeated at least three different membrane area of cut for each membrane type. Preparation of filtration cell are given in Figure 3.8. Flux was calculated as follows.

$$J = \frac{V}{A.t}$$

where;

J: Flux (L/m².hr),

V: Volume of permeation (liter),

A: Area (m²),

t: time (hour).

Flux graphs was drawn with excel. Slope of the graphs gives permeability of membranes. Lastly, average permeability and standard deviation was calculated for each type of membrane.

Table 3.3: Technical properties of the filtration system.

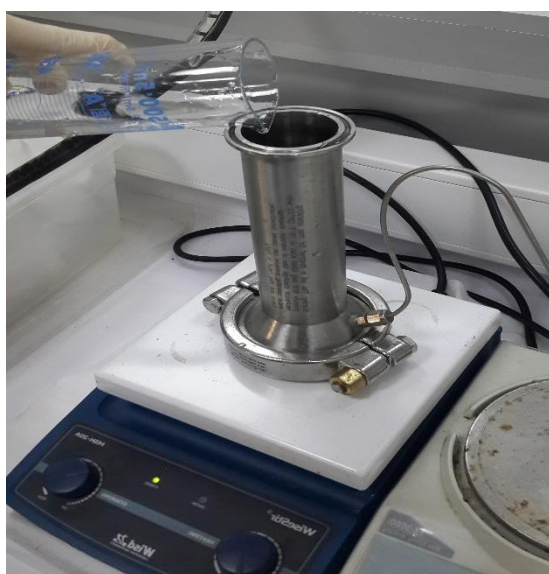
Parameter	Value
Membrane diameter	49 mm
Active membrane area	14.6 cm ²
Volume	300 ml
Maximum pressure	69 bar
Maximum temperature	121 ⁰ C



(a)



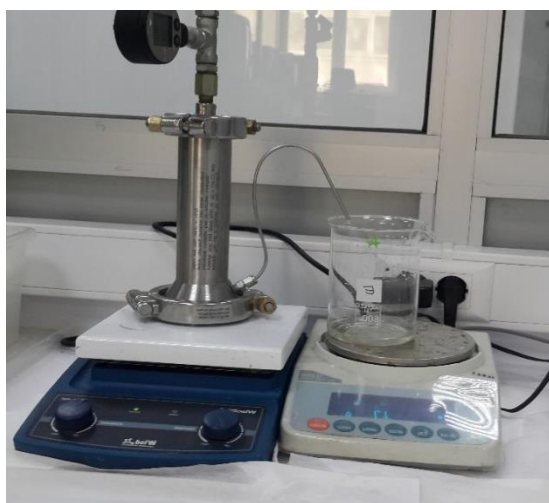
(b)



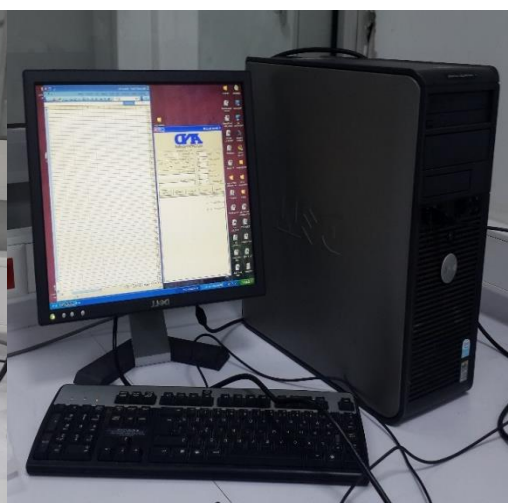
(c)



(d)



(e)



(f)

Figure 3.8: Preparation of the filtration cell.

3.2.4 Contact angle

Contact angles was measured by Attension T200 Theta (Figure 3.9). Hydrophobicity or hydrophility of membranes were determined with it. After dropped to distilled water at least 3 different surfaces of dry membranes, datas were saved.

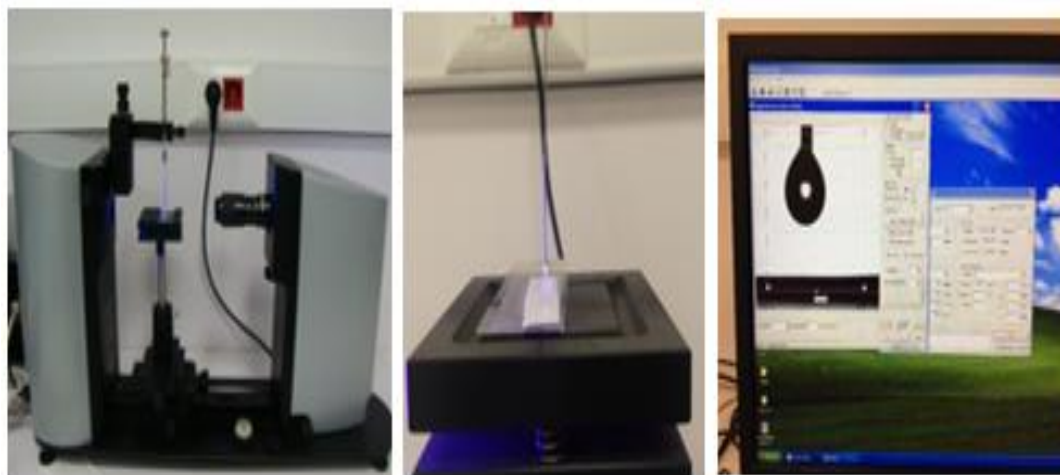


Figure 3.9: Contact angle measurement setup.

3.2.5 Fourier transformation infrared spectroscopy (FTIR)

For analysis of organic bonds in the membrane surface Perkin Elmer Spectrum 100 ATR-FTIR equipment was used (Figure 3.10). Before measuring flat sheet membranes, a background spectrum was conducted to decrease instrumental and atmospheric contributions to a minimum level.



Figure 3.10: FTIR spectrophotometer.

3.2.6 Surface charge

SurPASS electrokinetic analyzer was used for investigate the surface charge of membrane (Figure 3.11). Measurements was done with buffer solution (KCl) at different pH range.



Figure 3.11: Electrokinetic analyzer cell.

3.2.7 Scanning electron microscopy (SEM)

SEM (FEI Quanta FEG 200) (Figure 3.12). was used to examine the surface morphology of flat sheet membranes. After the preparation of membranes (dried by liquid nitrogen and cut for clean view), they were coated with 3-4 nm with Palladium and Gold (Pd-Au) by using Quorum SC7620 ion sputtering equipment.



Figure 3.12: SEM.

3.2.8 Optical profilometer

Zygo New View 7100 was used to examine the surface roughness (Figure 3.13). The samples were placed into the optical profilometer and imaged by the device. Light transmitted through or reflected from sample and formed an image of surface macrostructure with a 50x lens system.



Figure 3.13: Optical profilometer.

3.2.9 Mechanical stability

For mechanical testing of membranes SII DMS 6100 Exstar was used (Figure 3.14). Membrane should be inserted carefully to minimizing of stretching of membrane. For each sample 3 measurements were done and average was used to avoid miscalculations.



Figure 3.14: Mechanical stability testing equipment.

3.2.10 Porometre analysis

Porometer measurement for measuring the pore diameter of the membranes with 3G production was performed using a Quantachrome Poromet. Quantachrome 3G Poromet capillary flow porometer is operated by the liquid-push technique from the pores of the humidifier as the removal technique of a known fluid sample gas pressure. The pressure is inversely proportional to pore diameter in the pore space. So, the larger pores require a lower pressure than the relatively smaller pores. As a result of gap measurement is complete volumetric flow of forming gas. Washburn equation using the pore diameter is automatically calculated in the computer program.

The fact that the largest pore space (to create the low pressure stream) "bubble point" is defined. As a result, first of all pores measured on the same sample after the wet and dry (up to the maximum pressure that can be reached) is formed spaces in the pores. Various flow related parameters from the complete data set pore diameter, pore size distribution and gas permeability can be calculated.

Porometer analysis using the apparatus shown in Figure 3.15.

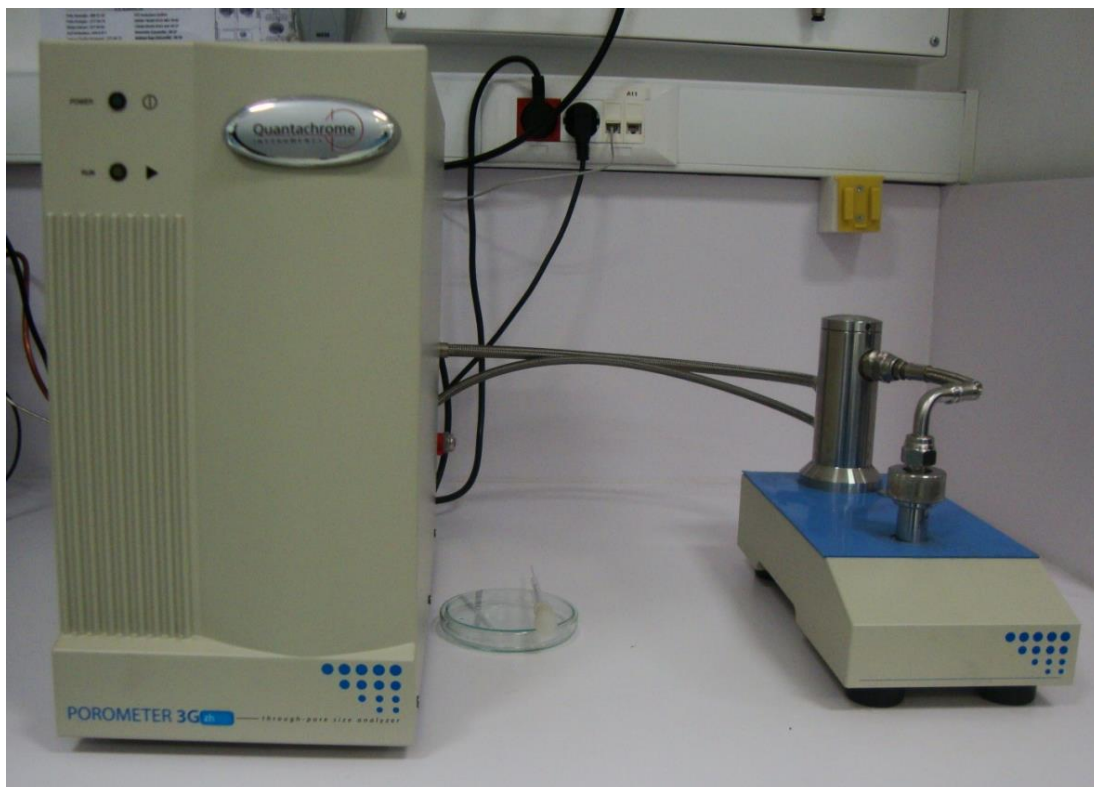


Figure 3.15: Porometer.

3.2.10 Salt rejection

Salt rejection were measured using Sterlitech filtration cell. The salt rejection (R_s %) was calculated by measuring the electric conductivity of both feed and permeate solutions using an Eutech Instruments Cyberscan CON 110 with RS232 and calculated as follows:

$$R_s\% = (C_f - C_p/C_f) \times 100$$

Where C_f and C_p are the concentrations of the feed and permeate water respectively.

Prepared TFC RO membranes are filetered with 2000 ppm NaCl under 15.5 bar pressure at 1 hour.

3.3. Antibacterial Experiments

During experiment, avoid contamination of sterile media and equipment sterile technique was used. All used disposable pieces of equipment (i.e. loops, pipette tips, plates) were autoclaved in order to minimise contamination of the experiment. Also, a laminar cabinet and bunsen burner were used during experiments.

3.3.1 Cultivation of *Escherichia coli* (*E. coli*)

During growth condition of bacteria, all the studies were performed under aseptic conditions. Glass materials, pipette tip are used after autoclaving. Autoclaving occured at 121°C, in 1.06 bar and 15 minutes .

The autoclave, vacuum-drying desktop Core brand OT032 model was used sterilizers (Figure 3.16).



Figure 3.16: Image of autovlave.

Antibacterial properties of the membranes were studied using with BL21 strain of *E. coli* which was taken from Molecular Biology-Biotechnology & Genetics Research Center (MOBGAM) at ITU.

3.3.1.1 Preparation of growth medium

150 ml distilled water was added the bottle. Then 8,5 gr LB Broth was added to the bottle. Lastly medium was autoclaved.

E. coli was inoculated into liquid medium. 200 μ l of *E. coli* was taken using the automatic pipette and added to the medium. The plates were incubated for 24 h at 37 °C from 150-170 rpm.

3.3.1.2 Preparation of solid medium

The only difference between the solid medium and liquid medium is the absence of the agar in the solid medium.

Firstly, 500 ml distilled water was added the bottle. Then 7 gr Rapid *E. coli* 2 Agar were added. After completion of solid medium with magnetic stirrer was opened. The agar dissolved completely. Purpose of mixing was prepare a transparent solution. Transparent cover the full closure of the medium was autoclaved.

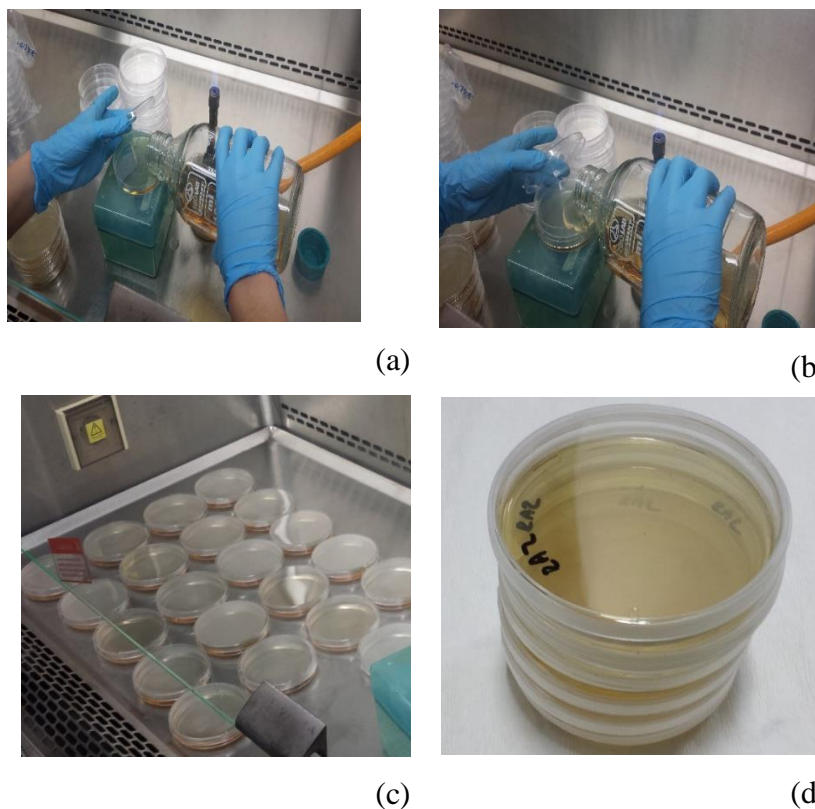


Figure 3.17: Pouring of solid media.

After autoclaving solid media and liquid media were allowed to cool. Temperature of solid medium should be 43-50 °C, because of freezing of agar at room temperature. In addition to this another reason that the experiments and the person's safety was affected by the extreme heat of the plate material. Solid medium was poured into approximately 20 ml to into every plate. Pouring occurred near to bunsen back (Figure 3.17).

3.3.1.3 Optical density measurement

Bacterial concentrations were determined by measuring optical density (OD) at 600 nm. Spectrophotometry offers an alternative method to estimate the concentration of cells in a bacterial culture. Bacterial cells are small particles capable of absorbing and scattering light. When placed in a spectrophotometer the scattering of light by bacteria can be measured as apparent absorbance at a wavelength of 600 nm. Absorbance values gained in this way are also known as Optical Density or OD600. OD measurements Pharmacia LKB-Novaspec II brand is made (Figure 3.18).



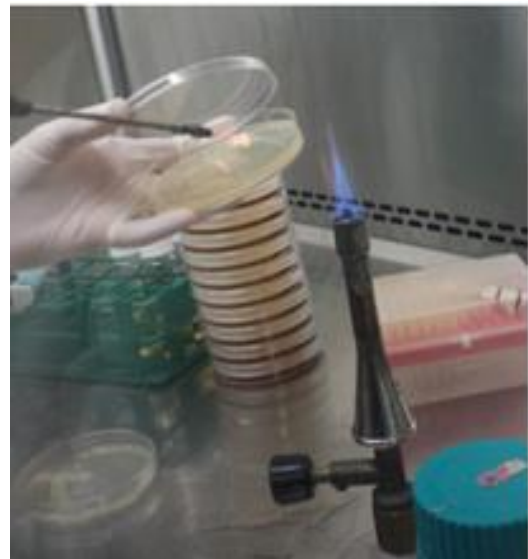
Figure 3.18: OD Spectrophotometer.

3.3.1.4 Bacterial stock preparation

Agar plates are the standard material for growing microorganisms. Growth of *E.coli* also had done under sterile conditions (Figure 3.19-a). Firstly, with sterilized loop, *E. Coli* was taken and spread to medium (Figure 3.19-b). Then, prepared medium with *E.coli* is placed in an incubator ,(16-18 hours for *E. coli*). Prepared bacterial stock was kept in a cold room at +4°C and it was used after refreshed.



(a)



(b)

Figure 3.19: Bacterial stock preparation.

3.3.1.5 Dilution of *E.coli*

A culture of microbes was diluted as it seen in Figure 3.20. For a ten-fold dilution on a 1 mL scale, vials were filled with 900 μL of sterilized water, and 100 μL of the stock microbial solution were serially transferred as it shown in Figure 3.21-a,b. New tip was used for the next step dilution. After every dilution step ,diluted *E.coli* was mixed with vorteks (Figure3.21-c). Lastly, final dilution was spread to medium using with drigalski spatula in aseptic condition as it seen Figure 3.21-d,e.

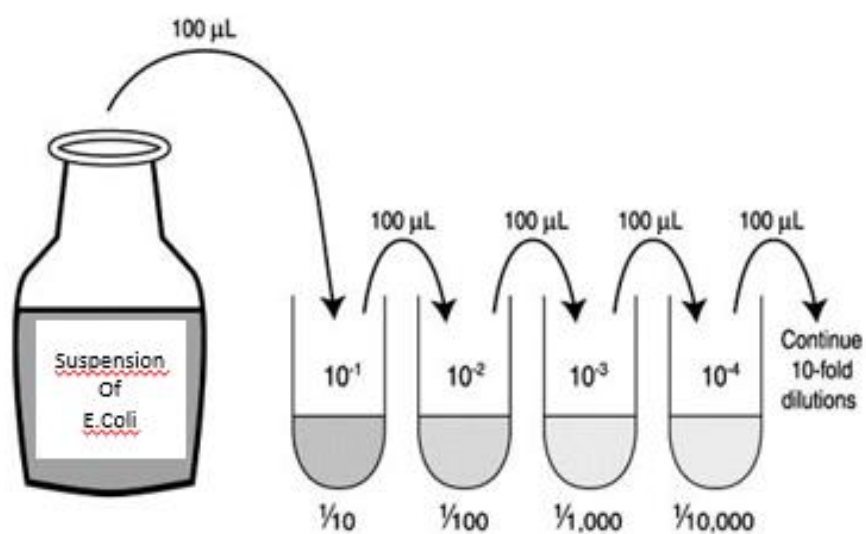


Figure 3.20: Example of Serial dilution of bacteria.

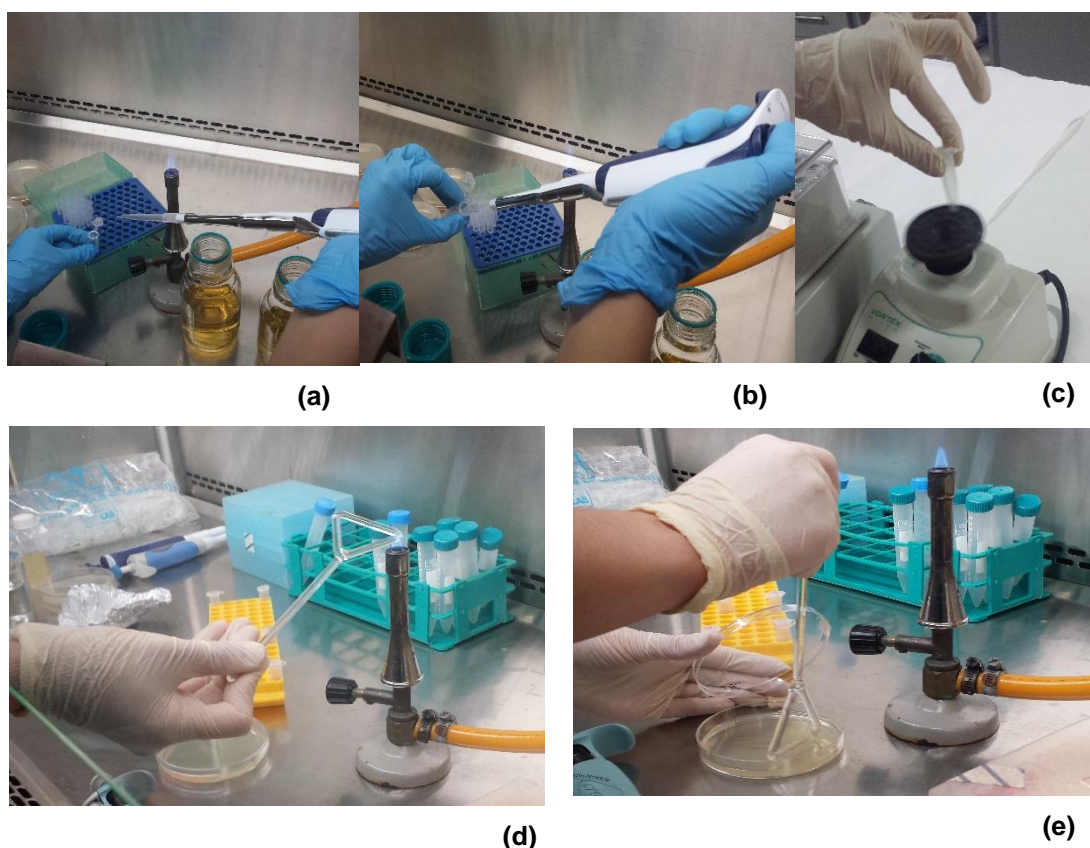


Figure 3.21: Example of Serial dilution of bacteria.

3.3.1.6 Counting of *E.Coli*

Bacterial count was estimated by standard agar plating. Dilutions of bacteria were spread on Rapid E.coli 2 Agar and incubated for 18 h at 37° C. The number of colonies are counted and then multiplied times the dilution factor to determine the number of cells/ ml in the original culture.

3.3.2 Antibacterial test

After the mentioned above, selected dilutions of bacteria were spread on medium (Figure 3.22).

TFC RO membranes pristine and with additive BisBAL are placed the plate to contact the surface of membrane (Figure 3.23). Then, all the plates are incubated for 18 hour at 37 ° C. At the end of the incubating period, *E. coli* colonies stained purple color.



Figure 3.22: Spreading of *E.coli* on medium.

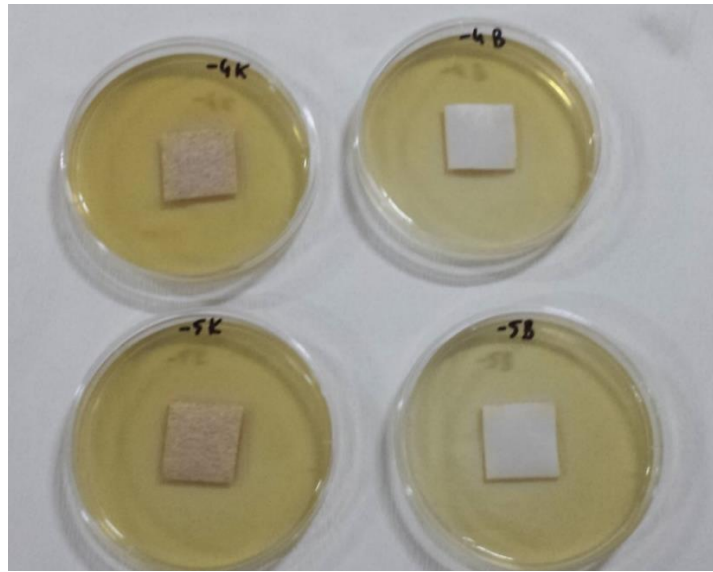


Figure 3.23: Plating of the membranes.

3.3.3 Flux reduction test

For determining of resistance capacity of membranes, firstly pristine TFC RO membrane put in a filtration cell that is filled with approximately 300 ml distilled water. Distilled water was filtrated in a filtration cell under 15.5 bar pressure for 1 h. Flux rates were recorded while this process with a computer. Then , 300 ml sample was filtrated which was taken from the Marmara Sea. Sample was filtrated in a filtration cell under 15.5 bar pressure for 6 h. Flux rates were recorded while this process with a computer. Lastly, *E.coli* suspension added to sample and sample was filtrated in a filtration cell under 15.5 bar pressure for 6 h. Flux rates were also recorded while this process with a computer.

Same procedure was repeated for additive with BisBAL TFC RO membrane. After all filtration tests, the flux graphs of membranes were drawn according to each test step.

3.3.4 Confocal scanning laser microscopy (CLSM)

In confocal scanning laser microscopy, high-resolution optical images can obtain with depth selectivity. Confocal microscopy was imaged with point-by-point and reconstructed with a computer, allowing three-dimensional reconstructions of objects topologically. After the detection of fluorescently labeled foulants on the membrane surface, images are taken by confocal microscopy to evaluate the efficiency of cleaning measures for deposit removal. In MEMTEK, Nikon brand and model C2 was used (Figure 3.24).

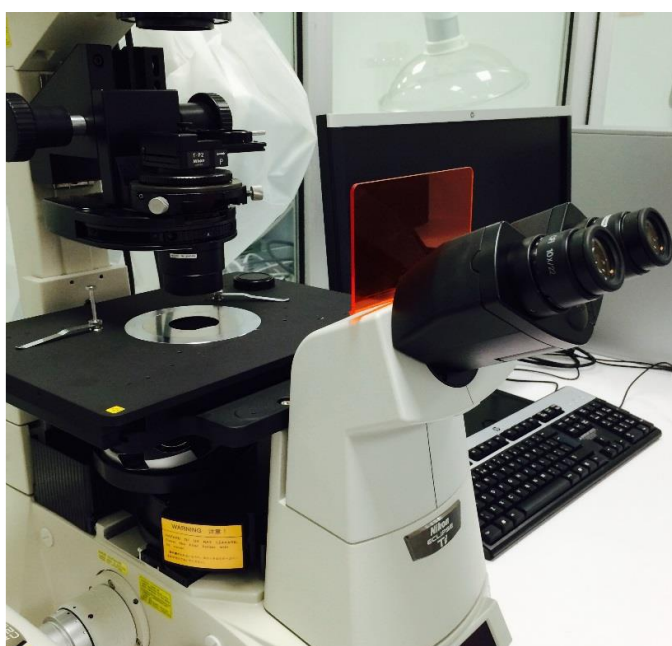


Figure 3.24: CLSM.

Bacterial Staining

SYTO 9 dye was used. SYTO 9 green-fluorescent nucleic acid stains are cell-permeant nucleic acid stains that show a large fluorescence enhancement upon binding nucleic acids. The SYTO 9 dyes can be used to stain RNA and DNA in both live and dead eukaryotic cells, as well as in Gram-positive and Gram-negative bacteria. The tested membranes were directly stained with SYTO 9, and allowed to react for 12 hours. The membranes were then directly imaged by CSLM.

4. RESULTS & DISCUSSIONS

4.1 Characterization Results Of Support Layer

After fabrication of the support layer, the characterizations (viscosity of dope solution, permeability, pore size, mechanical stability, contact angle and morphology assessment with optical profilometer, SEM) were carried out and the results are given following sections.

4.1.1 Thicknesses

Measured thickness values of support layer having ultrafiltration properties are given in Figure 4.1. The thickness values of membranes changed between 0.15 and 0.213 μm .

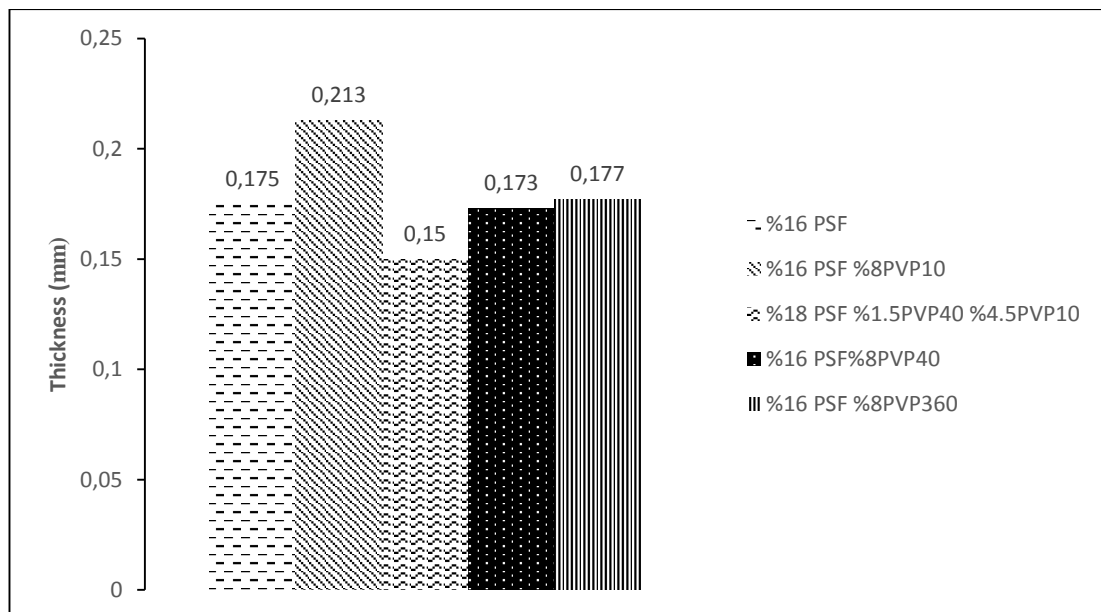


Figure 4.1: The thickness values of membranes.

4.1.2 Viscosity

Measured viscosity values of the dope solutions are given graphically in Figure 4.2. Adding PVP to the dope solution increases the overall polymer content, which increases the viscosity. The interaction between PVP and polymer plays limited influence on the increase of the viscosity. This could be due to the polymer solution undergoes the gelation at high PVP molecular weight. The gelation effect is dramatic

at high PVP molecular weight and concentration. Therefore, the viscosity values increased with increasing molecular weight of PVP.

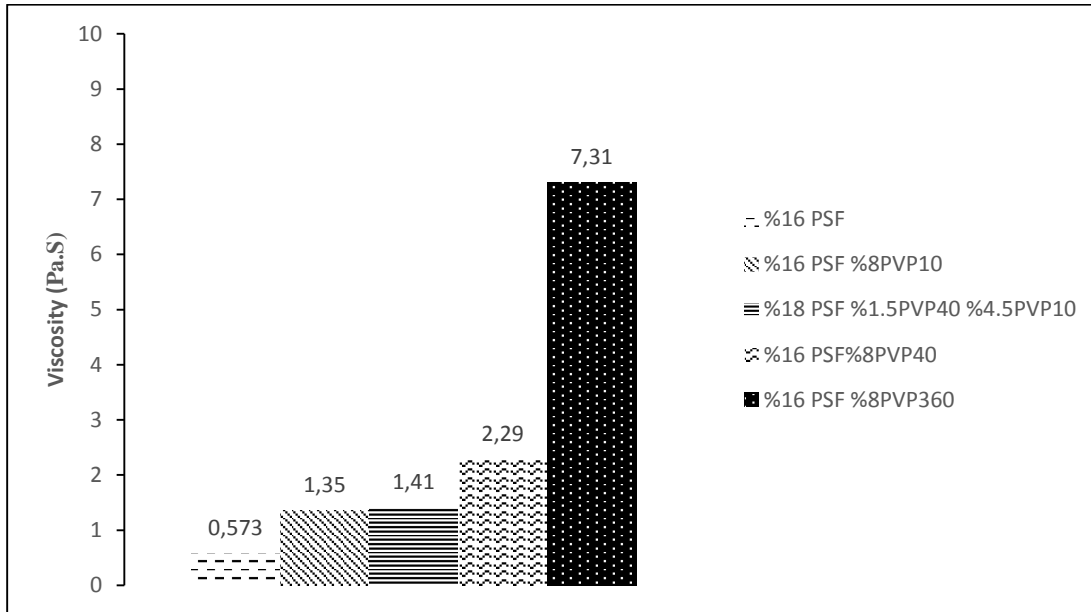


Figure 4.2: Viscosity values of the dope solutions.

4.1.3 Permeability

Permeability tests were applied for at least three times to each set of membranes. Results of the tests are shown as a graph in the Figure 4.3. Permeability of the prepared membranes are measured as; %16PSF: 109 ± 20 L/m²h.bar, %16PSF %8PVP10: 185 ± 28 L/m²h.bar, %16PSF %8PVP40: 186 ± 28 L/m²h.bar, %16PSF %8PVP360: 47 ± 2 L/m²h.bar, %18PSF %4.5PVP10 %1.5PVP40: 299 ± 29 L/m²h.bar. As can be seen from the results, %18PSF %4.5PVP10 %1.5PVP40 membrane had the highest permeability value while the %16PSF %8PVP360 membrane had the lowest permeability value. %18PSF %4.5PVP10 %1.5PVP40 had high permeability because of spongelike structure of the membrane. Permeability values increased with adding PVP. However, increasing molecular weight of PVP caused to the decrease of flux. The reason of the lowest permeability of %16PSF having %8PVP360 may be the high molecular weight of the PVP due to the clogging of pores with PVP. Also, PVP can cause an artificial obstruction due to the regeneration of PVP. According to the Idris et al., (2006) and Feng et al., (2006) though most of the additives are washed away during coagulation and washing periods, complete removal of additives from the membrane matrix becomes more and more difficult with increase in molecular weight of PVP.

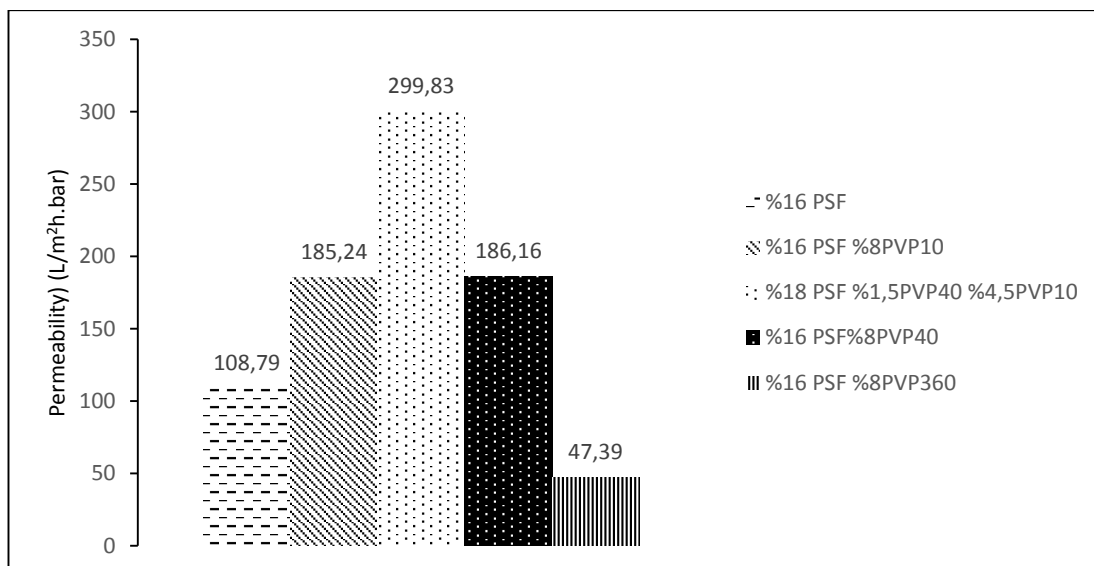


Figure 4.3: Permeability of prepared UF PSF membranes.

4.1.4 Contact angle

Contact angles of UF membranes were measured in order to examine the hydrophilicity and hydrophobicity properties of membrane surface. Contact angle values for the UF membranes are given in Figure 4.4. Contact angles of membranes were measured as; %16PSF: $80.5 \pm 3.1^\circ$, %16PSF %8PVP10: $74.4 \pm 2.2^\circ$, %16PSF %8PVP40: $82.9 \pm 2.3^\circ$, %16PSF%8PVP360: $82.3 \pm 1.8^\circ$, %18PSF %4.5PVP10 %1.5 PVP40: $68.5 \pm 2.7^\circ$.

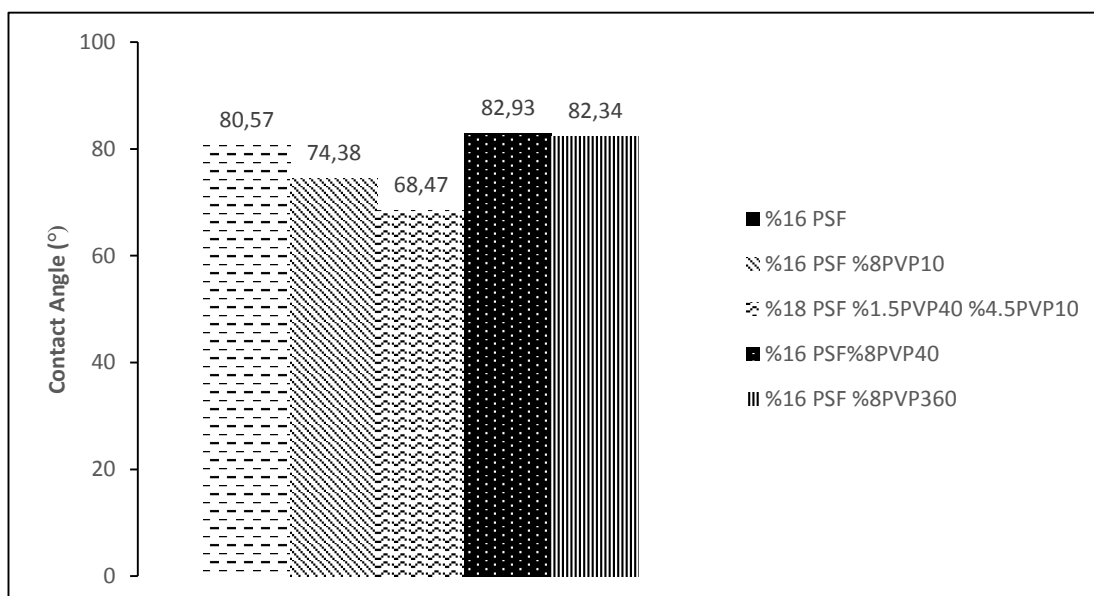


Figure 4.4: Hydrophilicity of prepared UF PSF membranes.

High hydrophilicity is an advantage for the preparation active layer of the membrane. The decrease in contact angle was observed in %18PSF %4.5 PVP10 %1.5 PVP40 due to the sponge like structure's capillary impact on membrane surface. It was appeared that measured contact angle values are similar range. Contact angle values are mainly controlled by the polymer chemistry (Deng et al., 2014).

4.1.5 FTIR

FTIR of the produced UF membranes were measured in order to examine the chemical structure of organic molecules and potential structural changes in membranes. The spectrum of the PSf membrane shows peaks in Figure 4.5. Prepared PSF UF membranes have very similar infrared absorption bands at the wave number range of 650-2000 cm^{-1}

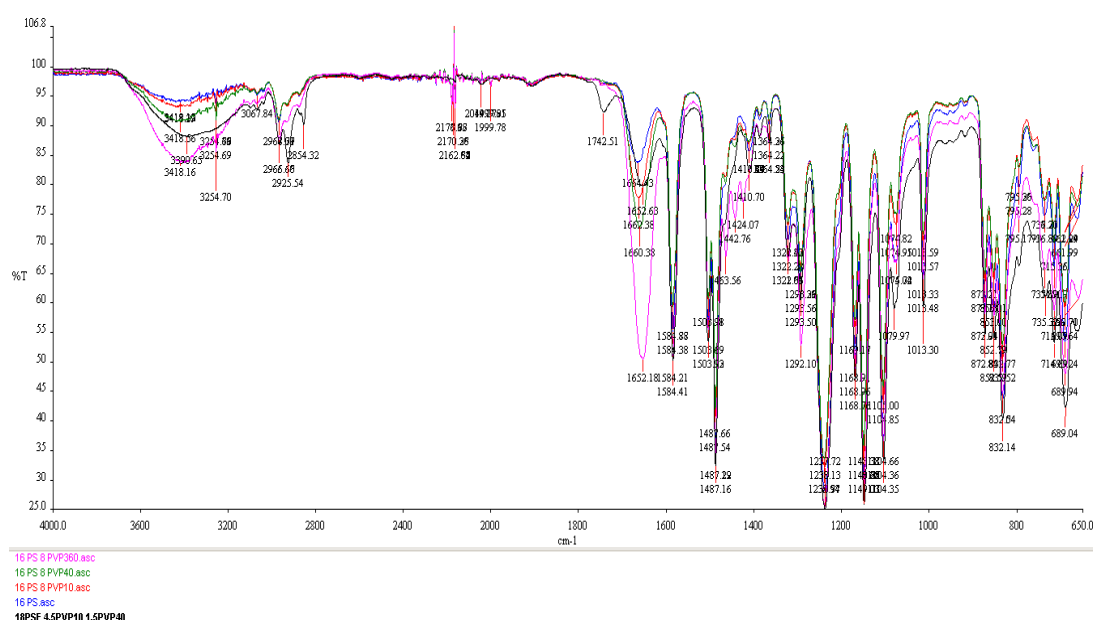


Figure 4.5: FTIR images of prepared UF PSF membranes.

The similarity of the infrared spectra over this range confirmed that the membranes had the same basic structure of PSF. The spectrum of the PSf membrane shows similar in literature (El Asaar et al., 2012). The absorption bands of the material corresponds to the polysulfone groups, being in good agreement with standard polysulfone as it seen in Table 4.1.

Table 4.1: FTIR spectra of prepared UF PSF membranes.

%16PSF	%16PSF %8PVP10	%16PSF %8PVP40	%16PSF %8PVP360	%18PSF %4.5 PVP10 %1.5 PVP10	Spectra assignments
1664	1662	1660	1652	1652	Aromatic C = C tension
1584	1584	1584	1584	1584	Aromatic C = C tension
1503	1503	1503	1503	1503	Aromatic C = C tension
1487	1487	1487	1487	1487	Aromatic C = C tension
1237	1239	1239	1238	1239	Aril eter group asymetric C-O-C tension
1168	1169	1169	1168	1169	Sulfonat group asymetric O=S=O tension
1104	1104	1104	1104	1104	Aromatic ring vibration
1013	1013	1013	1013	1013	Sulfonate group symetric O=S=O tension

4.1.6 Surface charge of membranes

Surface charge measurements were done to examine how the electrical charge membrane surface prepared with the addition of different molecular weight PVP. Lowest surface charge values were obtained for the %16 PSf membranes having 8% PVP10.

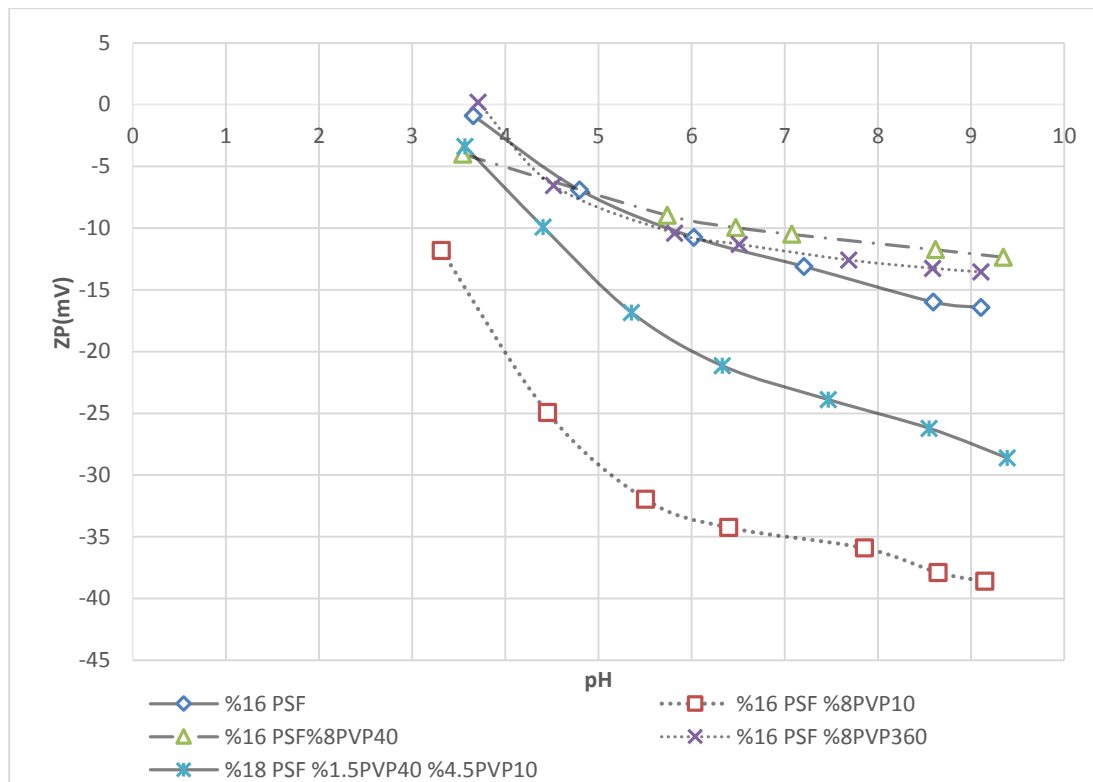
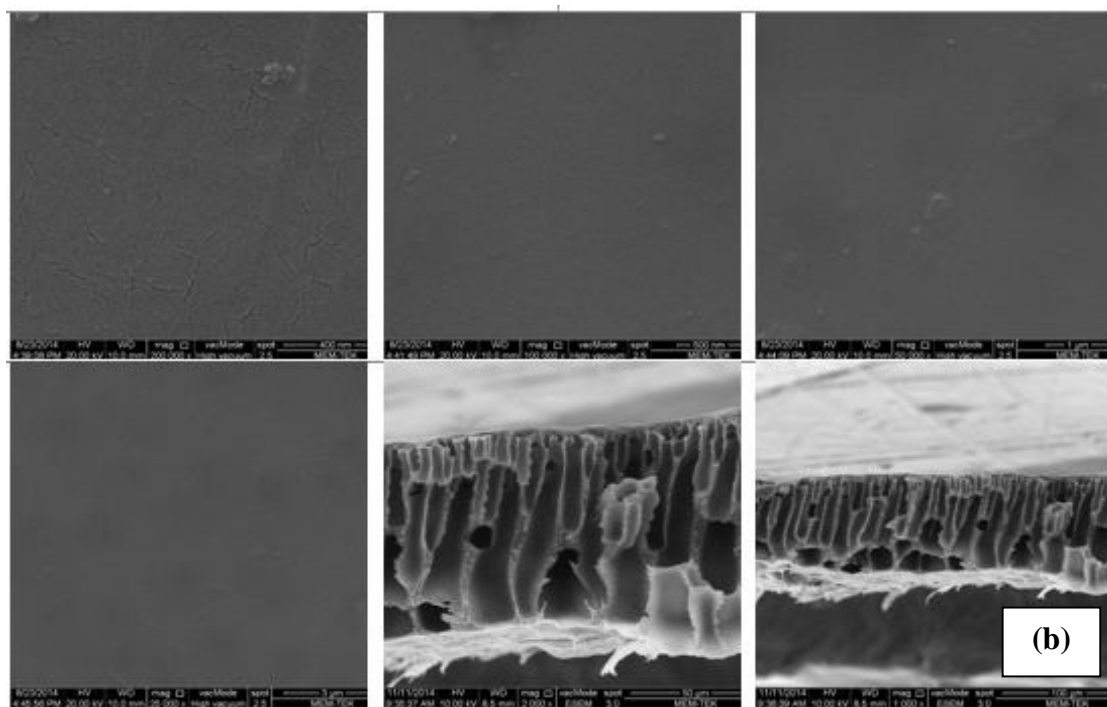
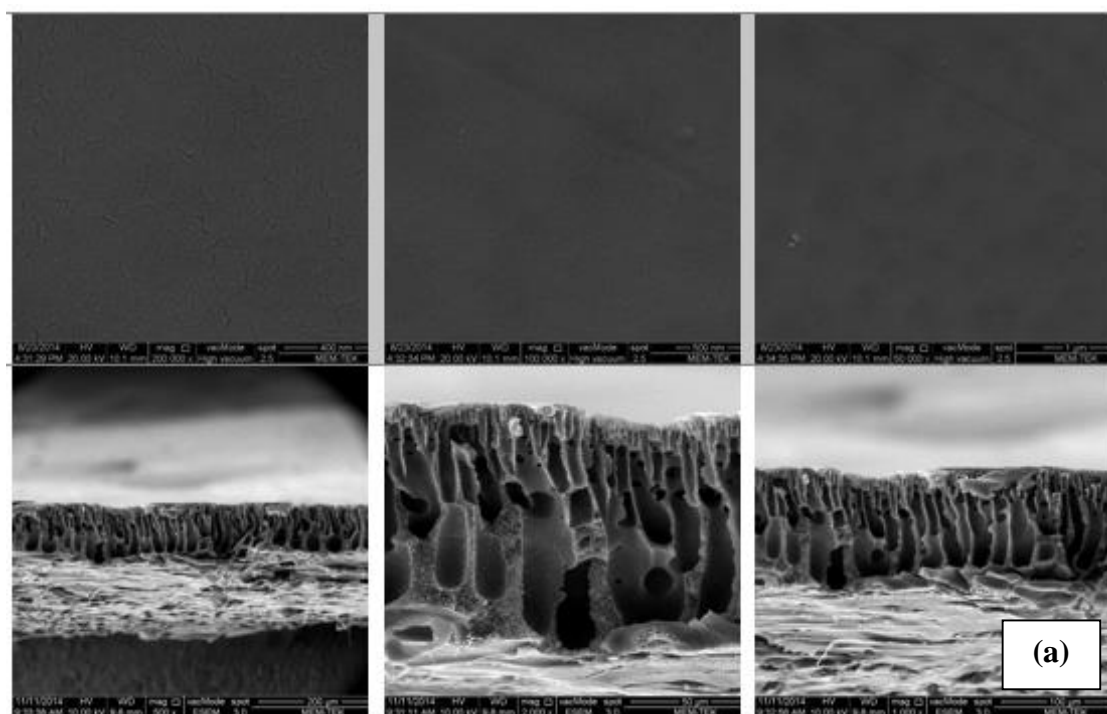
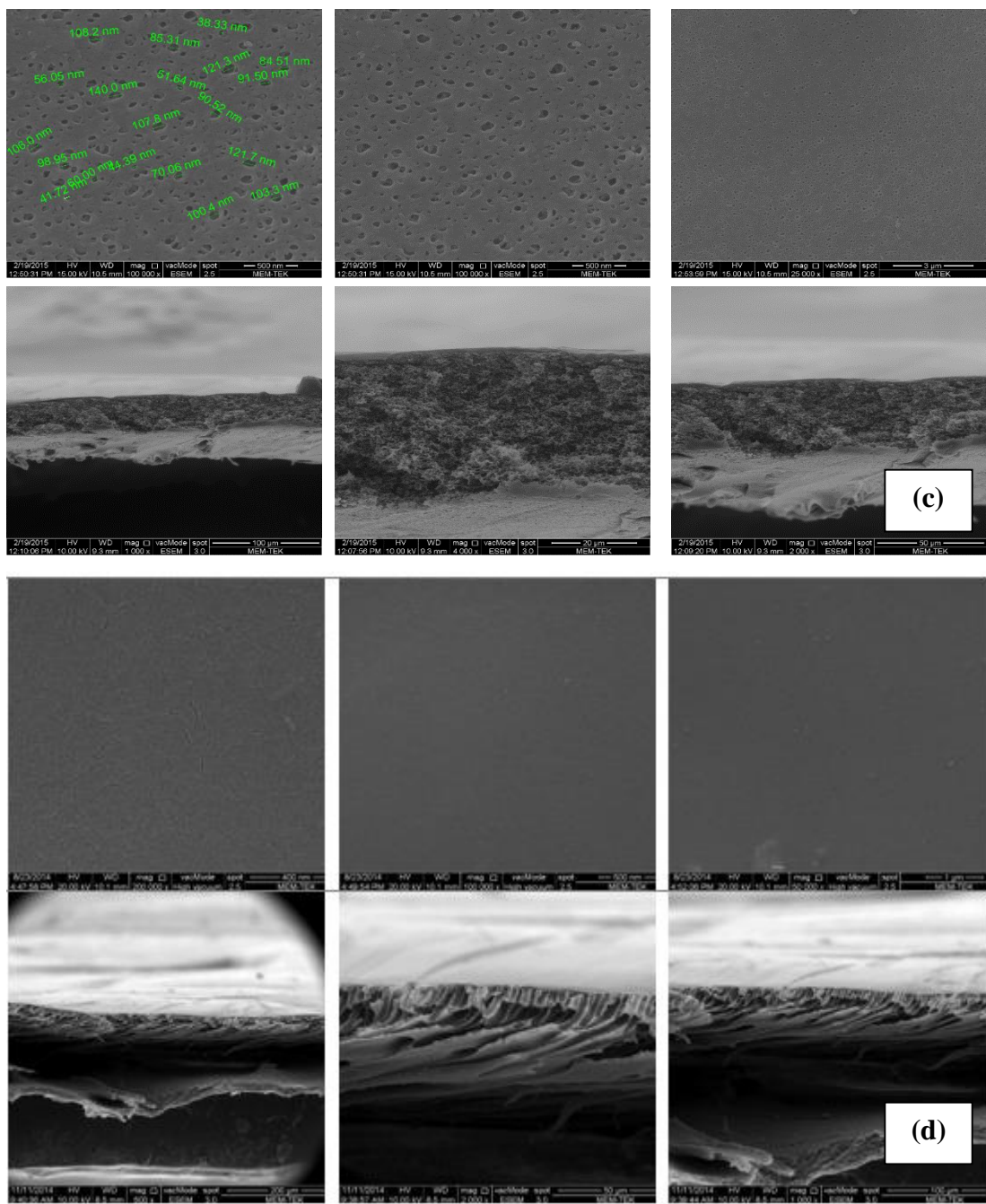


Figure 4.6: Zeta potential of prepared UF PSF membranes.

4.1.7 Scanning electron microscopy (SEM)

Images obtained from the SEM analysis of membranes are shown in Figure 4.7. While images are examined, %16 PSF, %16 PSF %8 PVP 10, %16 PSF %8 PVP 40 and %16 PSF %8 PVP 360 shows finger like structure. In the cross-sectional images, a typical asymmetric structure was observed. Also, additive PVP cause an enlargement in finger structure. Also, the fingerlike macrovoids were suppressed with increasing PVP molecular weight and structure of membrane was changed a macrovoid structure to a sponge structure. (Matsuyama et al., 2003). However, %18 PSF % 4.5 PVP10 %1.5PVP40 shows sponge like structure. The sponge like structure is an advantage for the RO membranes due to the high pressure resistance.





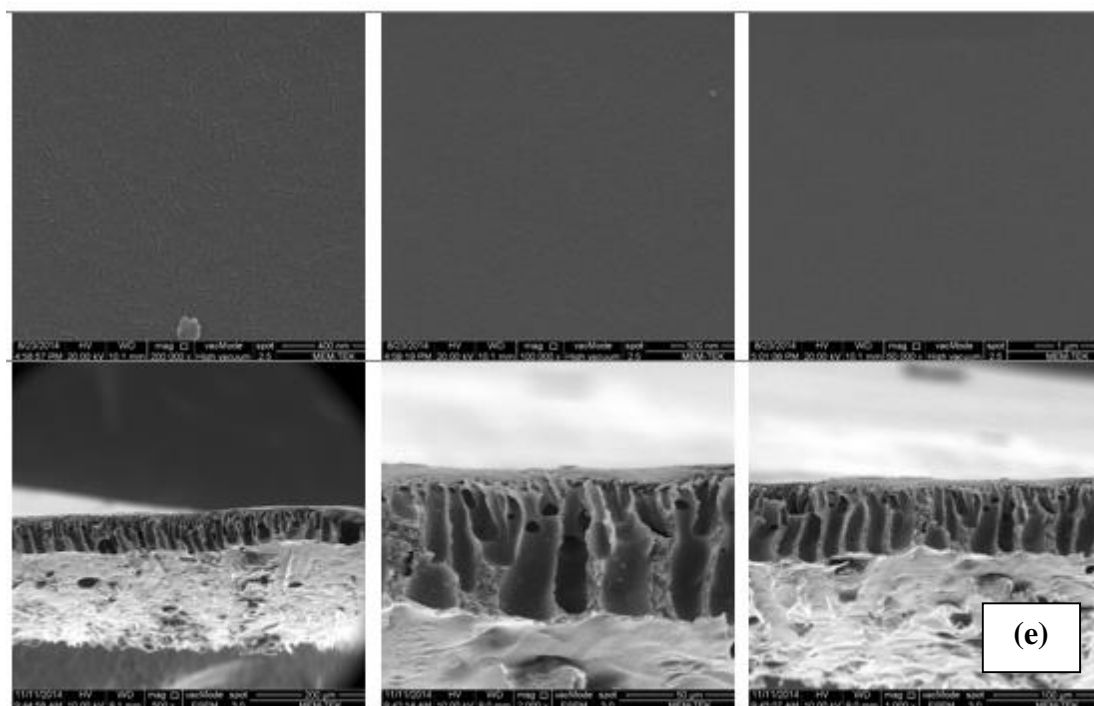


Figure 4.7: SEM images of prepared membranes: (a) %16 PSF UF membrane, (b) %16 PSF %8 PVP 10 UF membrane, (c) %18 PSF, % 4.5 PVP10, %1.5 PVP40 UF membrane, (d) %16 PSF %8 PVP 40 UF membrane, (e) %16 PSF %8 PVP 360 UF membrane.

4.1.8 Optical profilometer

Measured roughness values of the prepared support layer membranes are shown as a graph in Figure 4.8. Measured roughness values were generally decreased as the polymer solution contents of membranes were increased. In addition, Figure 4.8 showed that measured roughness values were decreasing with increasing molecular weight of PVP and polymer solution content. Lowest roughness value was measured for %18 PSF % 4.5PVP10 % 1.5 PVP40 while highest roughness value was measured for the %18 PSF. Optical profilometer images of prepared support layer membranes are given in Figure 4.9. Observed images showed parallel view with roughness values. While less line structure was observed for %18PSF % 4.5 PVP10 %1.5 PVP40 and had lowest roughness value, %16 PSF indicated density lines on the surface and had highest roughness value. Surface roughness has long been considered a cause of the high fouling propensity of modern polyamide-based composite RO membranes compared with earlier cellulose acetate-based membranes. Fouling studies have produced experimental evidences pointing at the correlation between roughness and fouling. Various mechanistic explanations have been proposed, mostly focused on

interfacial interactions and how these may be affected by surface roughness. In addition, there have been studies, which alluded to the possible correlation between higher flux and increased roughness, possibly due to an increased interfacial area between the rough membrane surface and the feed solution (Ramon et al., 2013).

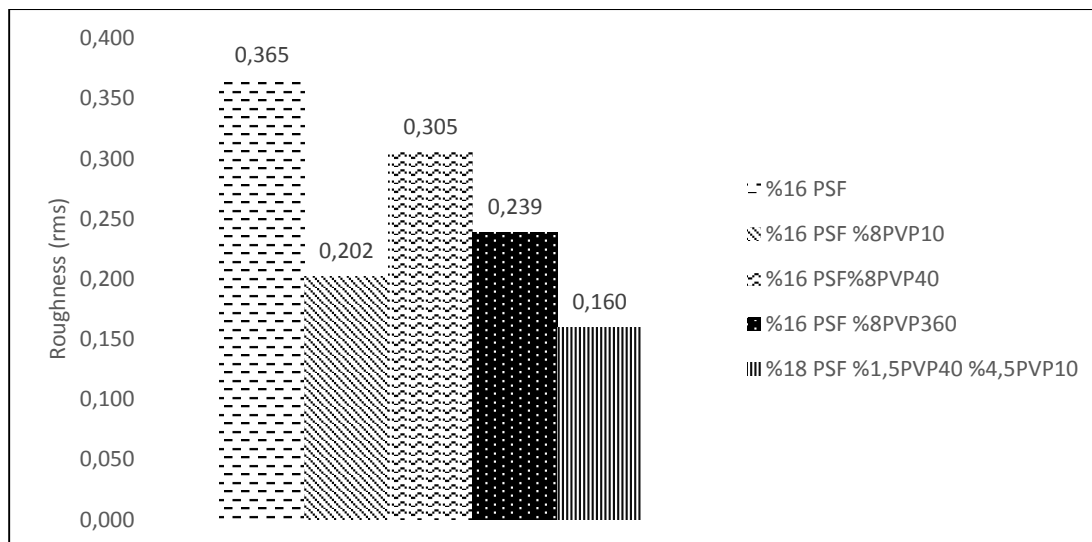
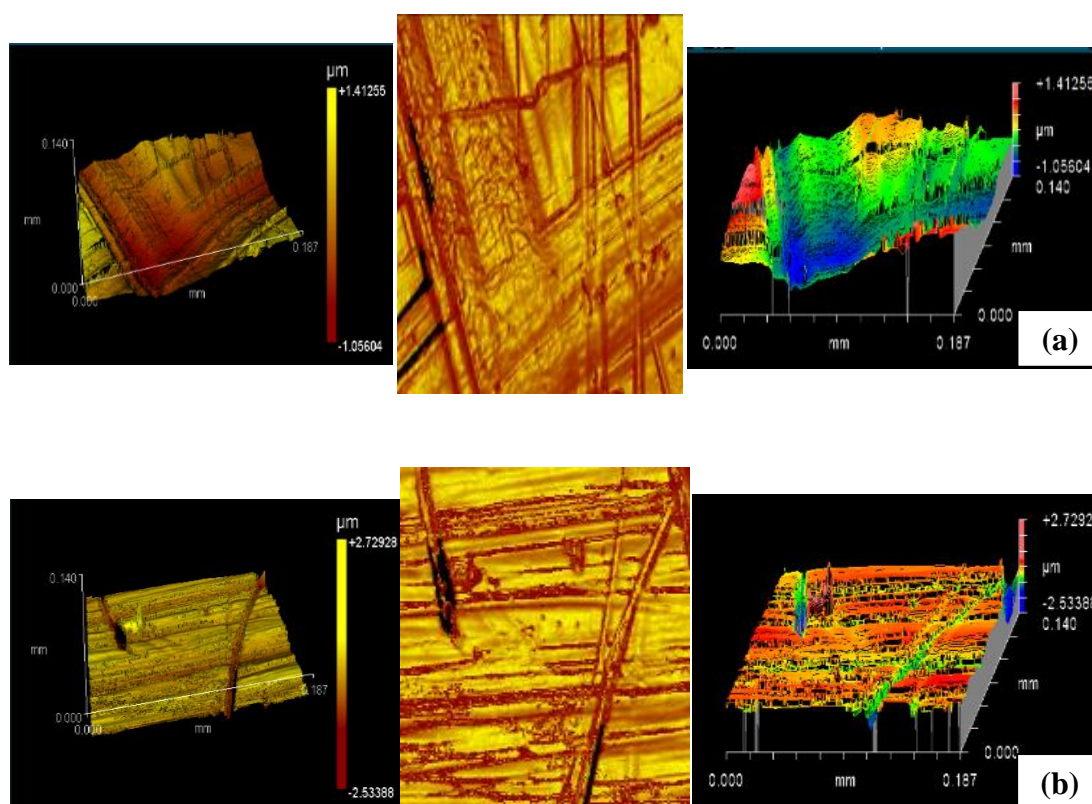


Figure 4.8: Average roughness of prepared membrane.



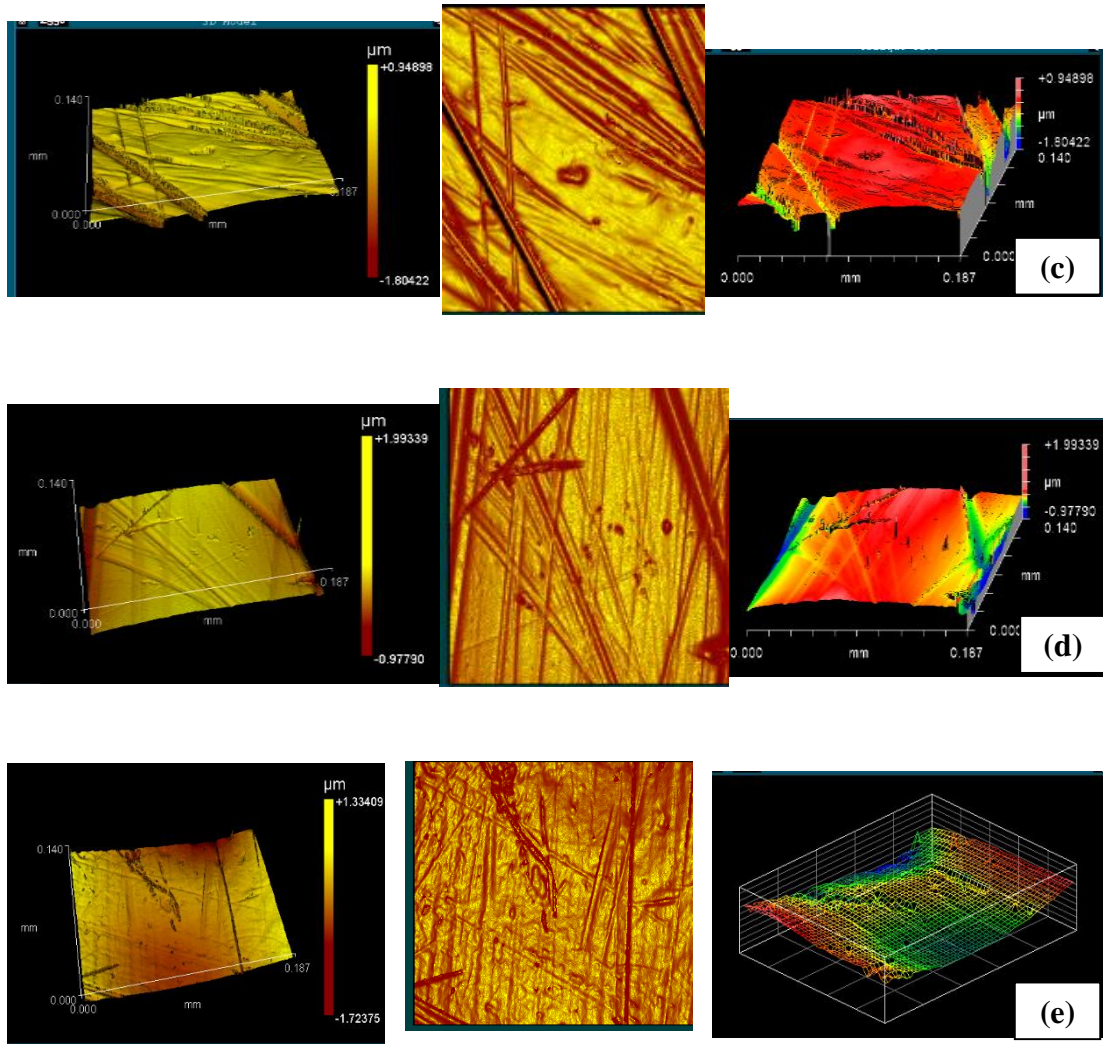


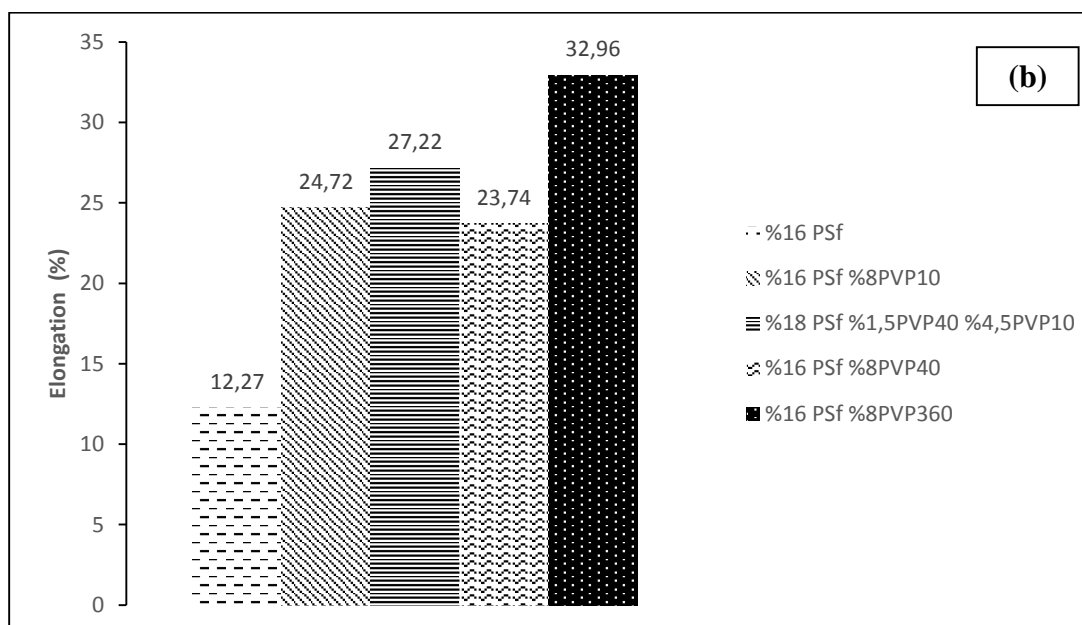
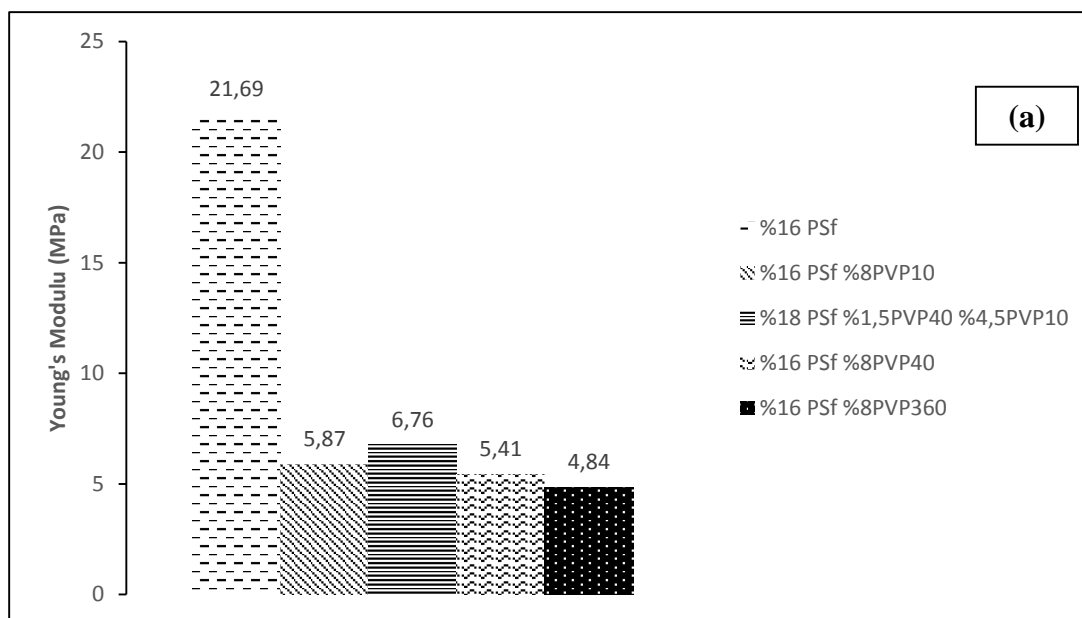
Figure 4.9: Optical profilometer images of prepared membranes: (a) %16 PSF membrane, (b) %16 PSF %8PVP10 membrane, (c) %18 PSF % 4.5 PVP10 %1.5 PVP40 membrane, (d) %16 PSF %8PVP40 membrane, (e) %16 PSF %8PVP360 membrane.

4.1.9. Mechanical stability

With the addition of having different molecular weight PVP, how mechanical properties (elongation at break, young's modulus and tensile strength) were changed was observed. Measured Young modules, elongation and tensile strength of the produced UF membranes, are shown as a graph in Figure 4.10-a,b,c. As can be seen from the results increasing of molecular weight of PVP increased the mechanical strength of the membrane.

Young's modulus values can be seen in Figure 4.10-a. The best young's modulus value observed at %16PSF. It can be said that addition of PVP decreased Young's Modulus. Elongation values can be seen in Figure 4.10-b. Increased elongation values mean

increased flexibilities of the membranes. According to the results, increasing of molecular weight of PVP increased the elongation at break. So, flexibility of the membranes were increased with adding PVP. Measured tensile strength of the produced UF membranes, are shown as a graph in Figure 4.10-c. According the results, the best tensile strength value was observed at %16 PSf %8 PVP360.



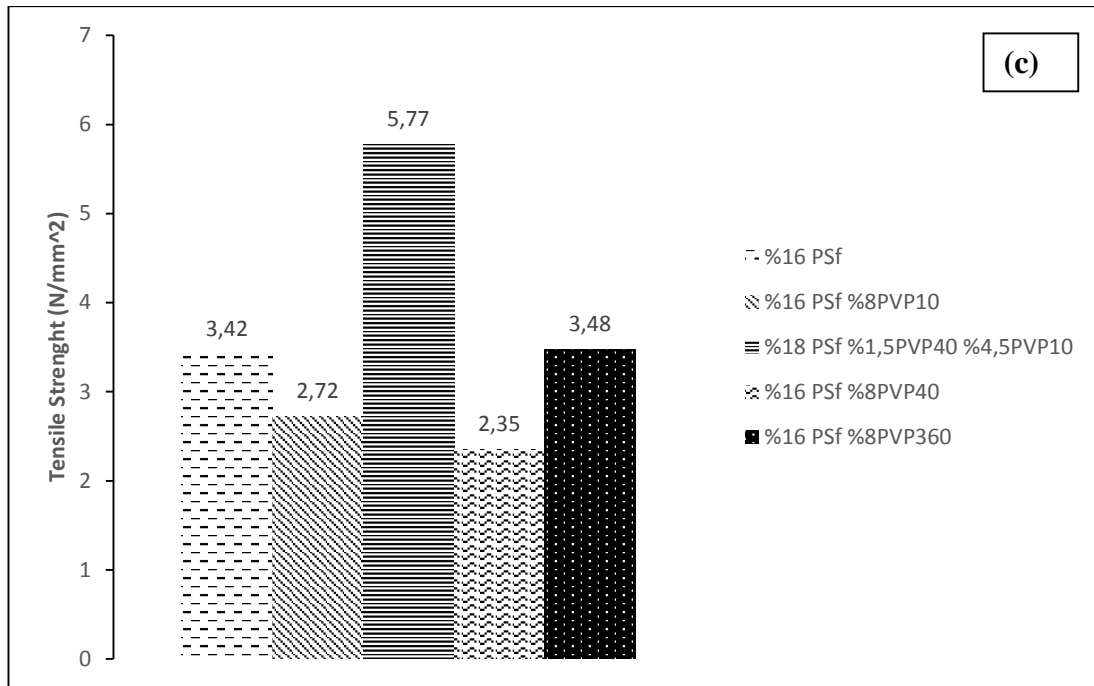


Figure 4.10: Mechanical parameters of membranes (a) Young's modulus, (b) Elongation, (c) Tensile strength.

4.1.10. Porometre analysis

Measured pore diameter of the membranes are shown as a graph in Figure 4.11. According to results, similar pore sizes were observed at all membranes. Pore diameter of the prepared membranes have suitable pore size for UF membrane level.

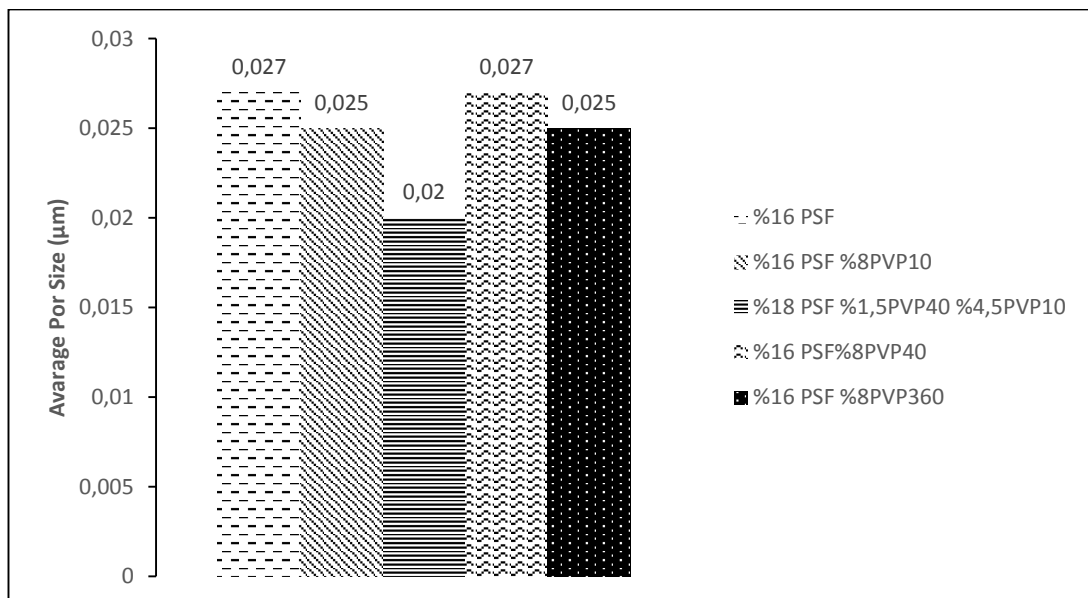


Figure 4.11: Average pore size of the membranes.

4.1.2 Selection of active layer

After characterization of support layer, most suitable one was selected. %18 PSF %4.5 PVP10 %1.5 PVP40 was selected as a support layer for the active layer preparation because of the sponge-like structure. The sponge like structure is advantage for the RO membranes due to the high pressure resistance. Also, when compare to SEM images of the commercial PA TFC membranes show sponge like structure. In additionally, flux of the selected membrane was better than the others.

In preparation TFC membranes, many trials had been done for finding the most appropriate and best result. In PA TFC membranes, high flux values and high salt rejection are important parameters. PA TFC membranes were prepared pristine and with additive BisBAL. BisBAL concentration was selected 30 mM in aqueous solution based on the results of previous studies at MEMTEK.

In order to investigate the optimum synthesis conditions of PA TFC membranes, the effect of different parameters that expected to influence the IP reaction and obtained membrane performance were studied through series of IP reactions. Finally, selected process parameters for TFC preparation as it seen Table 4.2.

Table 4.2: Process parameters for TFC preparation.

MPD Percent in Aqueous Solution	TMC Percent in Organic Solution	Immersed Time in Aqueous Solution	Drying time	Immerse d Time in Organic Solution	Oven Temperature -Time
% 2	% 0.1	5 min	1 min	1 min	70°C-7.5 min

4.1.2.1 Filtration tests

Filtration tests were done to evaluate of performance of PA TFC membranes. Filtration tests results are given in Table 4.3. Results showed that BisBAL TFC exhibited better salt rejection and also flux. It can be said that BisBAL additive may positive effect to increase membrane performance.

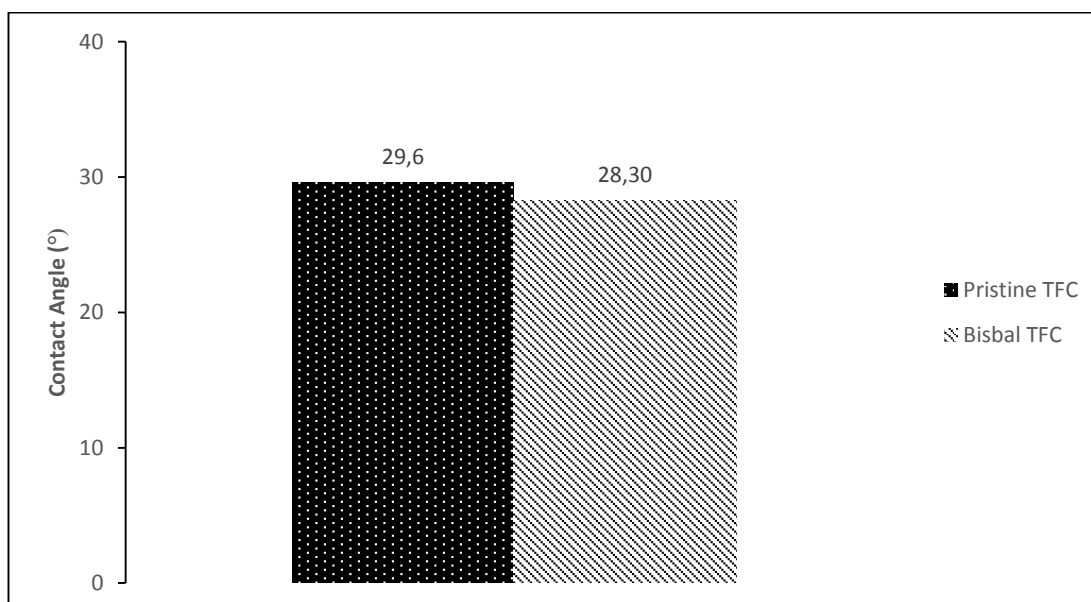
Table 4.3: Filtration Performance of prepared PA TFC membranes.

Thin Film layer	Performance Parameters	
	2000 ppm NaCl at 15 bar	
	Rejection (%)	Flux (l/m ² ·h)
Pristine TFC	%91.5±4.9	18.5±4.8
Bisbal TFC	% 94.5±3.5	24.5 ±2.1

4.1.2.2 Contact angle

Contact angles of the produced PA TFC membranes were measured in order to examine the hydrophilicity and hydrophobicity properties after drying process. Measured contact angle values for the PA TFC pristine and with additive BisBAL TFC membranes are given in Figure 4.12. Contact angles of membranes were measured as; Pristine: 29.6±1.6°, Additive BisBAL: 28.4±2.5°.

Contact angles values showed similar range. According to results, it can be said that adding BisBAL may not change the hydrophilicity effectively. In addition to this the contact angle of pristine and BisBAL TFC membranes showed the high hydrophilicity as compared to PSF support layer. The contact angle of the prepared PA TFC membranes decreased, the hydrophilicity increased due to formation of linear portion of PA which possesses free –COOH groups (El-Aassar, 2012).

**Figure 4.12:** Contact angles of PA TFC RO membranes.

4.1.2.3 FTIR

The chemical composition of both PSf support layer and synthesized PA-TFC membrane surface was investigated by FTIR as it seen in Figure 4.13.

The spectra indicated that the IP process had occurred since a strong band at 1663 cm^{-1} (amide I) was present which is the characteristic peak of the C=O band of an amide group. Other characteristic peaks of PA were also observed at 1542 cm^{-1} and (amide II, C-N stretch) and 1610 cm^{-1} (aromatic ring breathing) (Shawky et al., 2011).

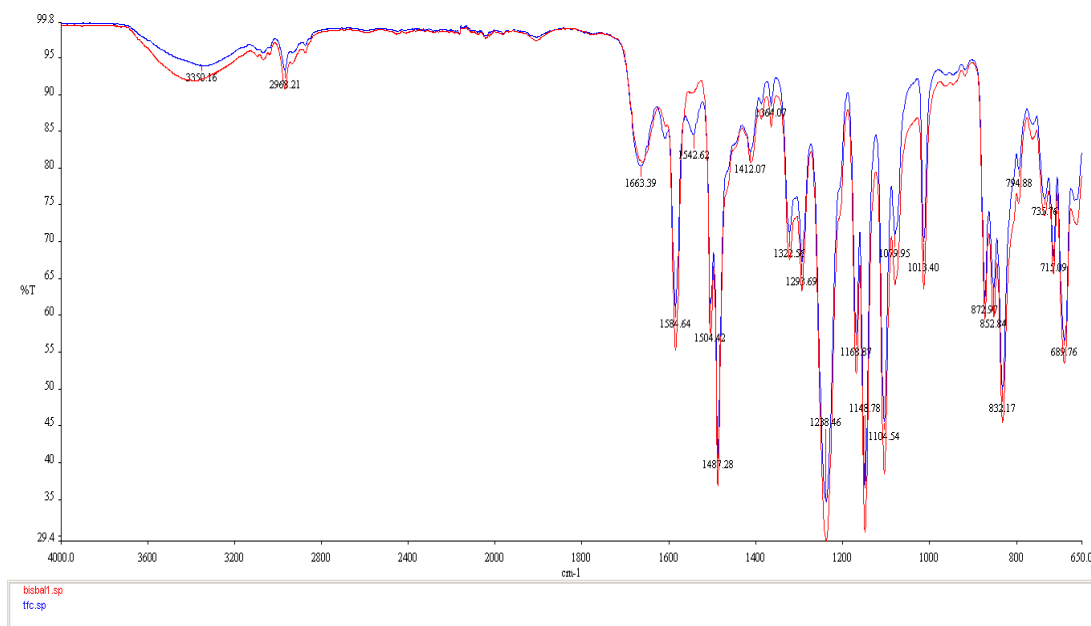


Figure 4.13: FTIR images of prepared PA TFC membranes.

4.1.2.4. Surface charge

Surface charge measurements were done to examine how the electrical charge membrane surface prepared with the additive BisBAL TFC and pristine TFC. As it seen in Figure 4.14, lowest surface charge values were obtained for the BisBAL TFC membrane.

In biomedical studies negative trends of the surface charges of the membrane is important to decrease bioadhesion due to the many bacteria have negatively electric charges (Kochkodan et al., 2015). Therefore, having a better negative trend may be advantage to prevent bacterial adhesion.

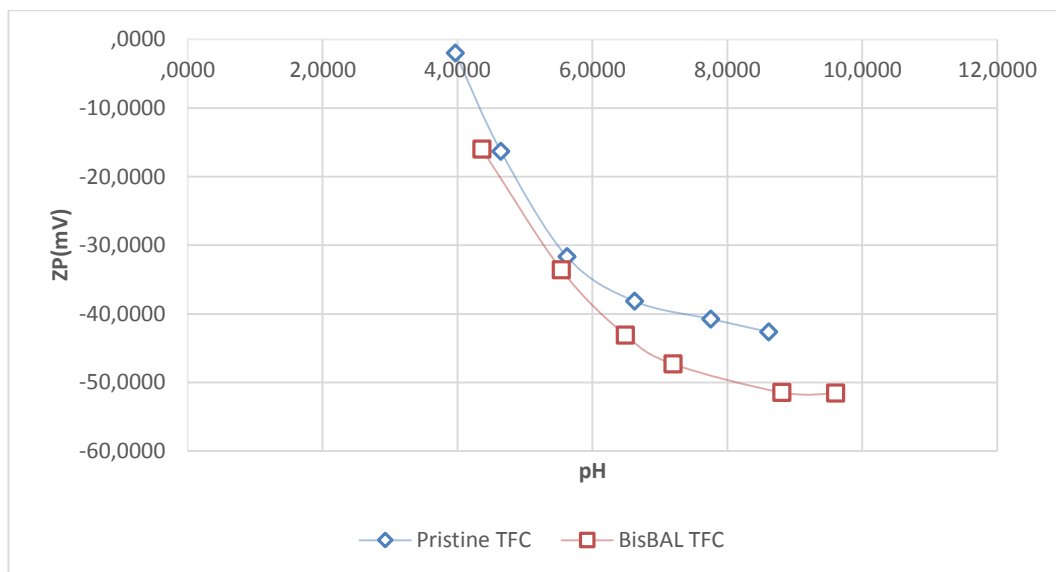


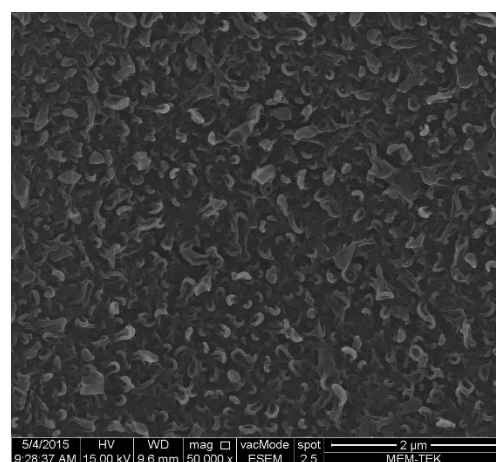
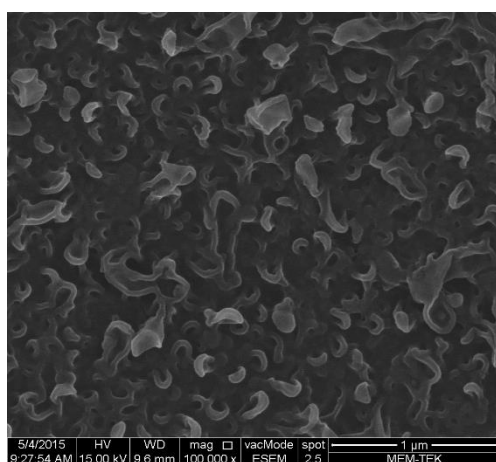
Figure 4.14: Zeta potential values of prepared PA TFC membranes in mV.

4.1.2.5 SEM

TFC membrane was analyzed by SEM in order to examine the surface morphology and structure.

SEM images of the pristine TFC membrane are shown in Figure 4.15-c. According to SEM images of prepared pristine TFC membrane, it exhibited hills and valleys morphology. Observed morphology can be reason of the TFC polyamide composites.

SEM images of the BisBAL TFC membrane are shown in Figure 4.15-b. BisBAL TFC exhibited less hills and valleys compared with pristine TFC. Also, SEM images indicated that the presence of BisBAL at discrete locations at the surface.



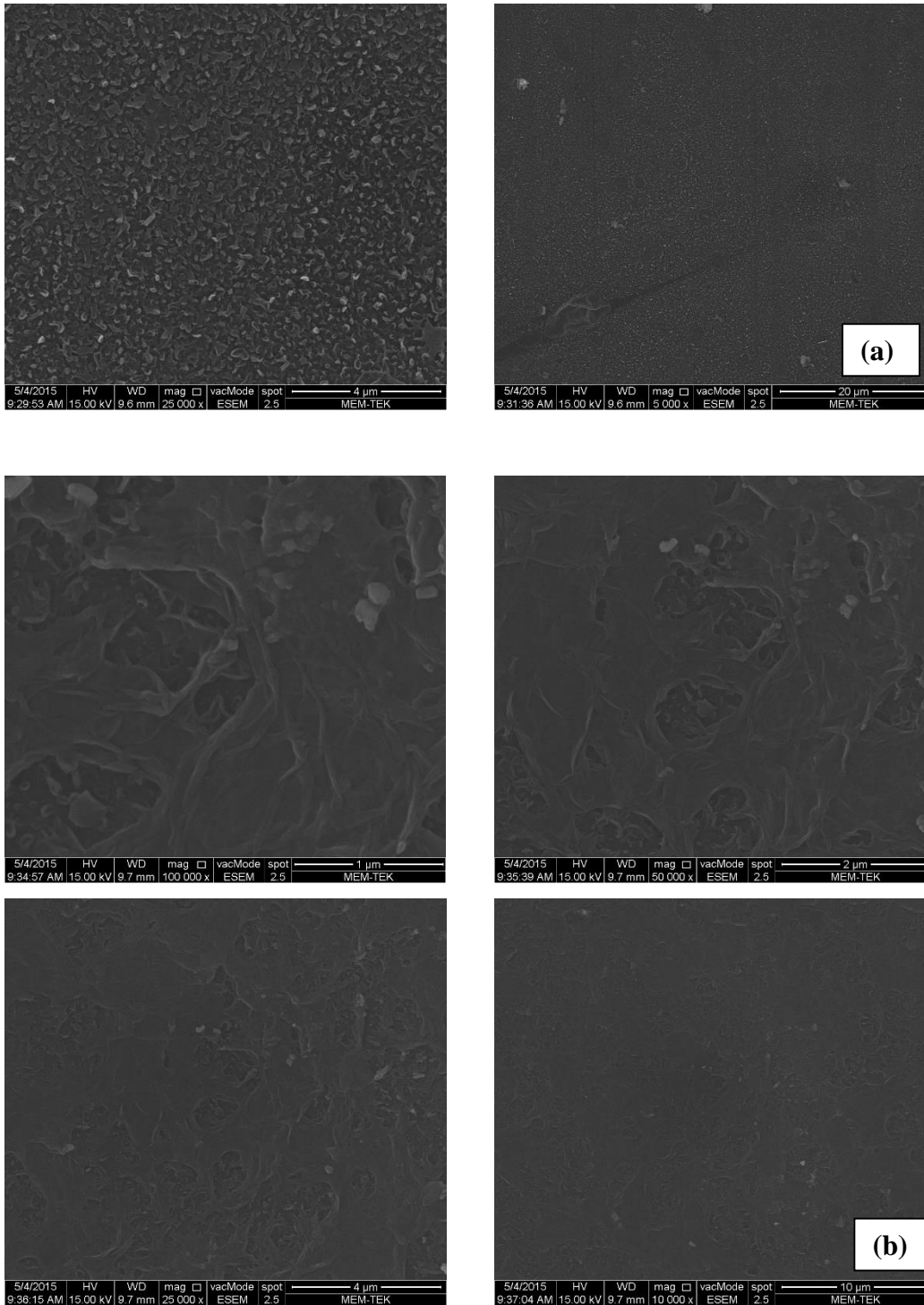


Figure 4.15: SEM images of TFC : (a) pristine TFC, (b) BisBAL TFC.

4.1.2.6 Optical profilometer

Generally, there is directly relationship between the potential of fouling and the surface roughness; smooth surfaces show less fouling as compared to rough surfaces (Matin et al., 2014). Measured roughness values of the prepared PA TFC membranes are shown as a graph in Figure 4.16. Lowest roughness value was measured for BisBAL

TFC while highest roughness value was measured for the pristine TFC. Observed optical profilometry images showed similar view with roughness values as it seen in Figure 4.17-a,b.

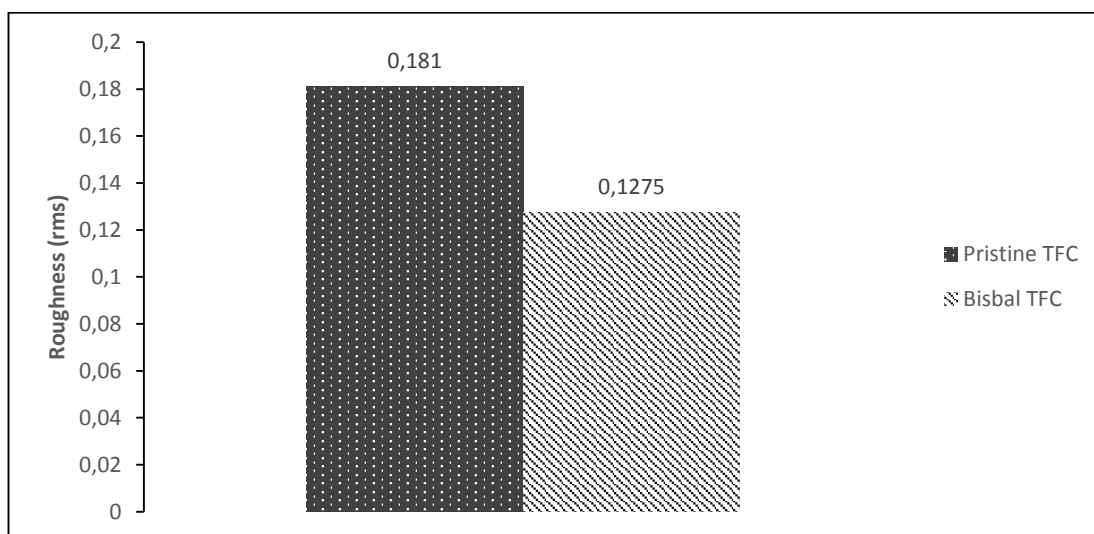


Figure 4. 16: Avarage roughness of prepared PA TFC membranes.

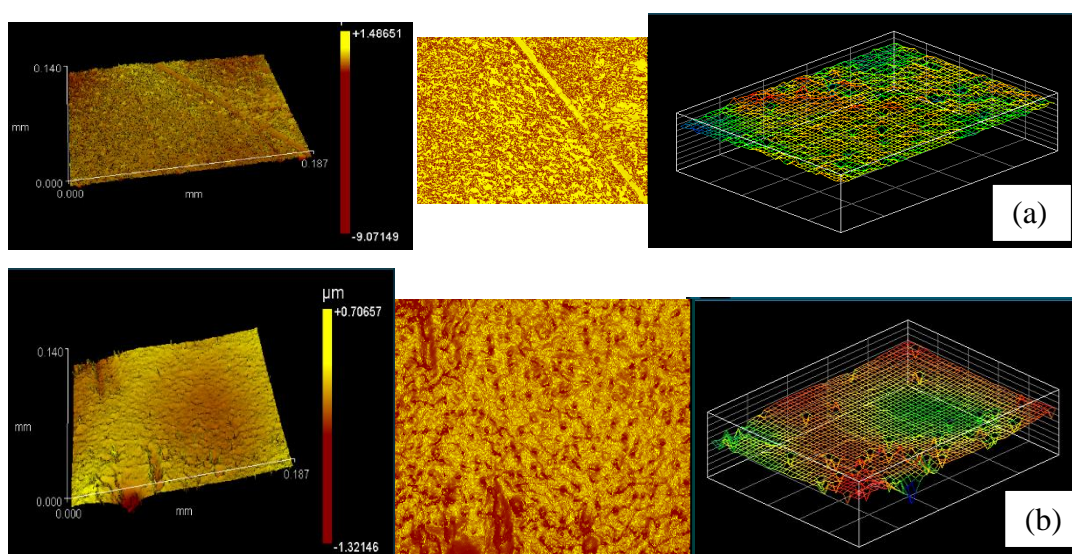


Figure 4.17: Optical profilometry images: (a) Prepared pristine TFC membrane, (b) Prepared BisBAL TFC membrane.

4.2 Antifouling Experiments

4.2.1 Culvitation of *E. coli*

Concentration of *E.coli* strain was measured 1.23 with OD at 600 nm. Strain of *E.coli* was diluted 10^{-6} , spread on agar and incubated. After incubation, it counted

approximately 140 cells in the medium. Also, suspended solids experiments was found 0.07 g/l in nondiluted *E.coli* strain.

4.2.2 Antibacterial test

E. coli was used to evaluate the antibacterial effect of BisBAL on membrane surface. The results are presented in Figure 4.18 and Figure 4.19 and Figure 4.20 using the pristine TFC membrane as a control. It can be seen that after incubation for 18 h, *E. coli* colonies was observed purple color. The images of diluted 10^{-5} and 10^{-4} with *E.coli* strain incubated plates for 18 hour at 37 ° C showed that different dilution factor of *E.coli* strain on membrane surface. The colony observed dense in diluted 10^{-4} with *E.coli* strain. Also, the colony was developed in below the pristine TFC and BisBAL TFC membranes surface. Compared to the bacterial colonies observed below the BisBAL TFC membrane surface, less bacteria can be seen. In addition to this, *E. coli* grew lower on the area surrounding the BisBAL TFC membrane. This reason may be antibacterial activity of BisBAL against. Also, *E. coli*. 10^{-6} with *E.coli* strain incubated plates for 18 hour at 37 ° C showed that approximately 50% less micrroorganism growth in the BisBAL TFC membrane.

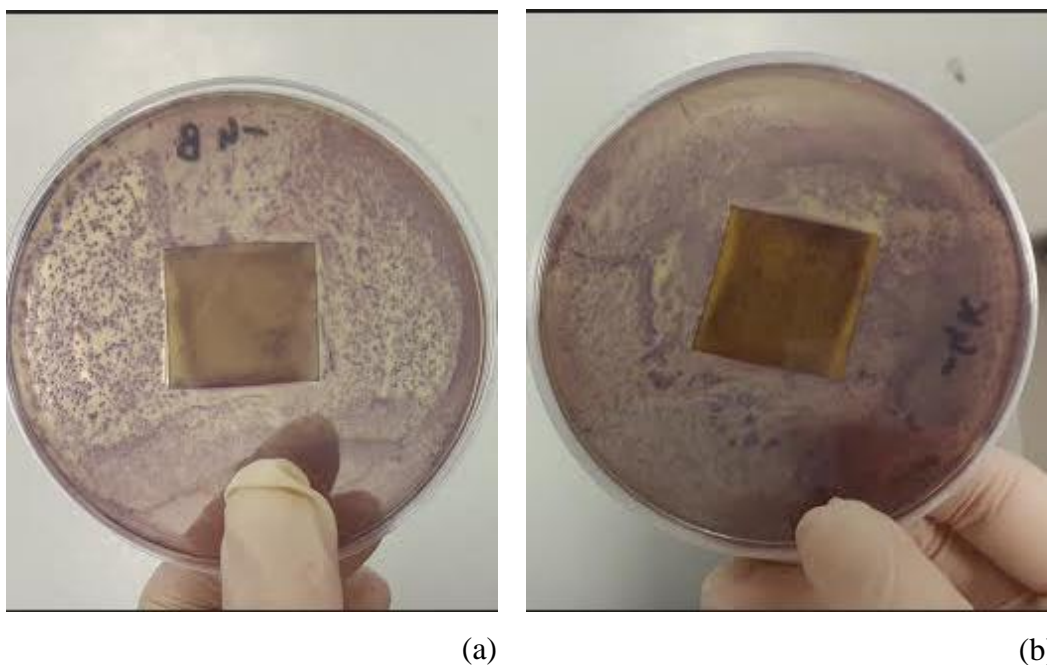
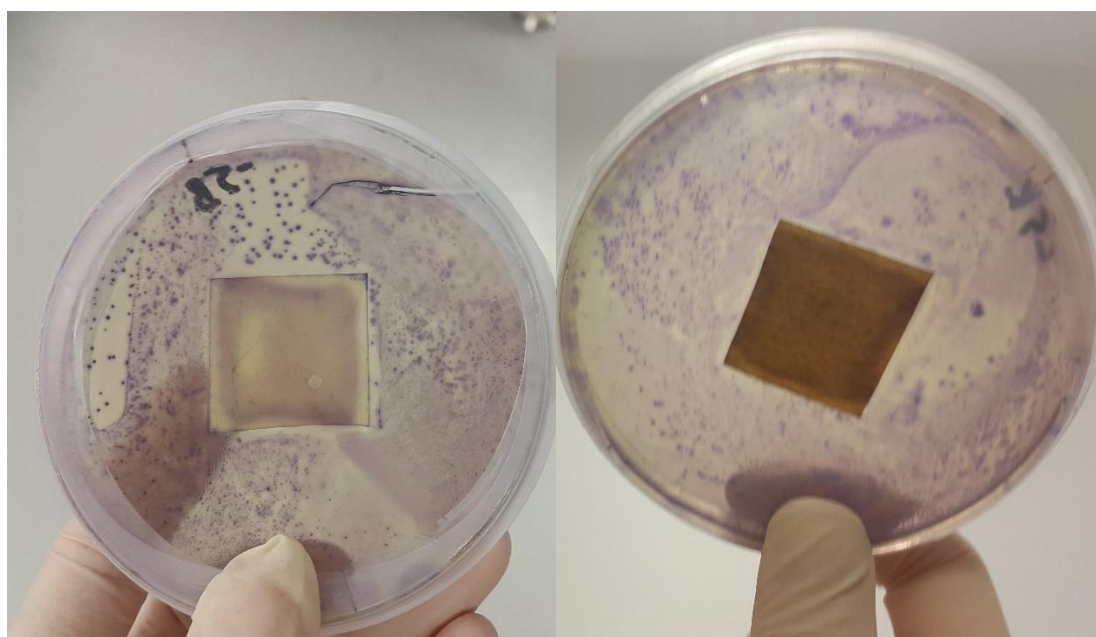


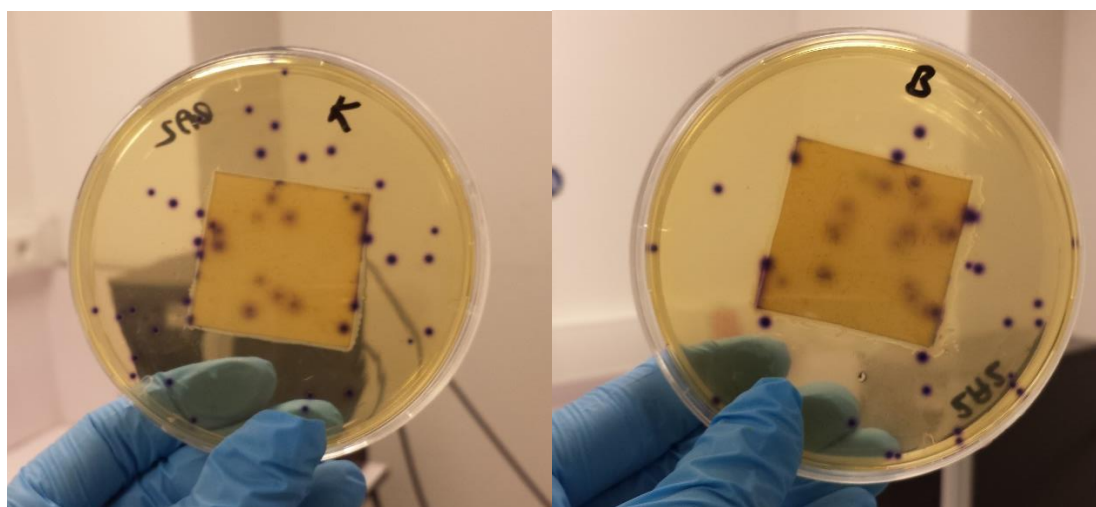
Figure 4.18: Images of diluted 10^{-4} with *E.coli* strain incubated plates for 18 hour at 37 ° C : (a) BisBAL TFC, (b) Pristine TFC.



(a)

(b)

Figure 4.19: Images of diluted 10-5 with E.coli strain incubated plates for 18 hour at 37 ° C: (a) BisBAL TFC, (b) Pristine TFC.



(a)

(b)

Figure 4.20: Images of diluted 10-6 with E.coli strain incubated plates for 18 hour at 37 ° C : (a) Pristine TFC, (b) BisBAL TFC.

4.2.2.1.SEM

SEM images were observed to compare the adhesion efficiency of the bacteria on the membrane.

SEM images of pristine TFC membrane are given in Figure 4.21 before and after diluted 10^{-4} and 10^{-5} with *E.coli* strain incubation at 37 °C for 4 h to compare the adhesion efficiency of the bacteria on the membrane. Figure 4.21-a and Figure 4.20-d shows a surface view of the pristine TFC membrane before incubation. It can be observed that pristine TFC membrane had hills and valleys morphology and TFC PA structure. Figure 4.21-b-c-d-e showed pristine TFC membrane surface after incubation. Attached contamination was observed on pristine TFC membrane surface after the membrane was incubated with the bacteria for 18 h.

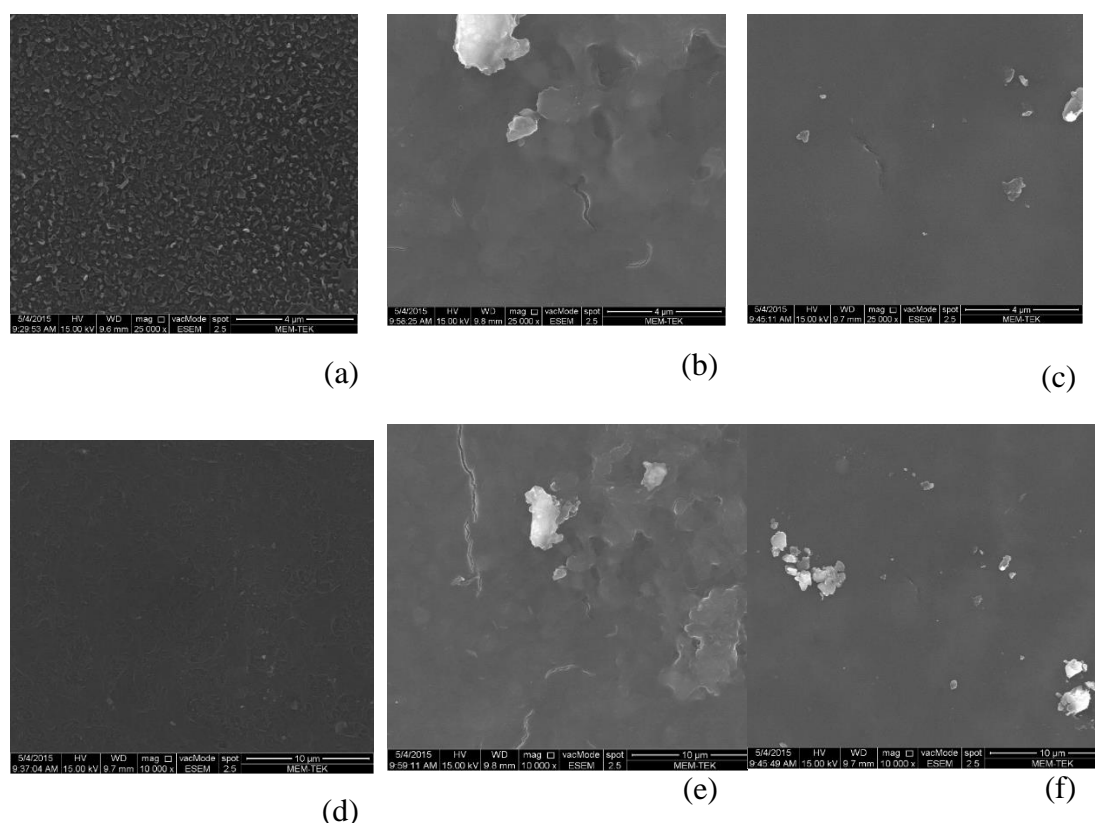


Figure 4.21: SEM images of pristine TFC membrane before and after incubation of membranes with *E.coli* at 37 °C for 18h : (a) pristine TFC membrane surface before incubation; (b) pristine TFC membrane surface after incubation (diluted 10^{-4} with *E.coli* strain); (c) pristine TFC membrane surface after incubation (diluted 10^{-5} with *E.coli* strain); (d) pristine TFC membrane surface before incubation; (e) pristine TFC membrane surface after incubation (diluted 10^{-4} with *E.coli* strain); (f) pristine TFC membrane surface after incubation (diluted 10^{-5} with *E.coli* strain).

SEM images of BisBAL TFC membrane are given in Figure 4.22 before and after diluted 10^{-4} and 10^{-5} with *E.coli* strain incubation at 37 °C for 4 h to compare the adhesion efficiency of the bacteria on the membrane. Figure 4.22-a and Figure 4.22-d

shows a surface view of the BisBAL TFC membrane before incubation with different magnitude. It can be observed that BisBAL TFC membrane had hills and valleys morphology and TFC PA structure. Figure 4.22-b-c-d-e showed BisBAL TFC membrane surface after incubation. Less attachments and hills-valleys morphology was observed on BisBAL TFC membrane surface after the membrane was diluted 10^{-4} and 10^{-5} with *E.coli* strain incubated with the bacteria for 18 h. It may be attributed to the anti adhesive effect of BisBAL TFC membrane.

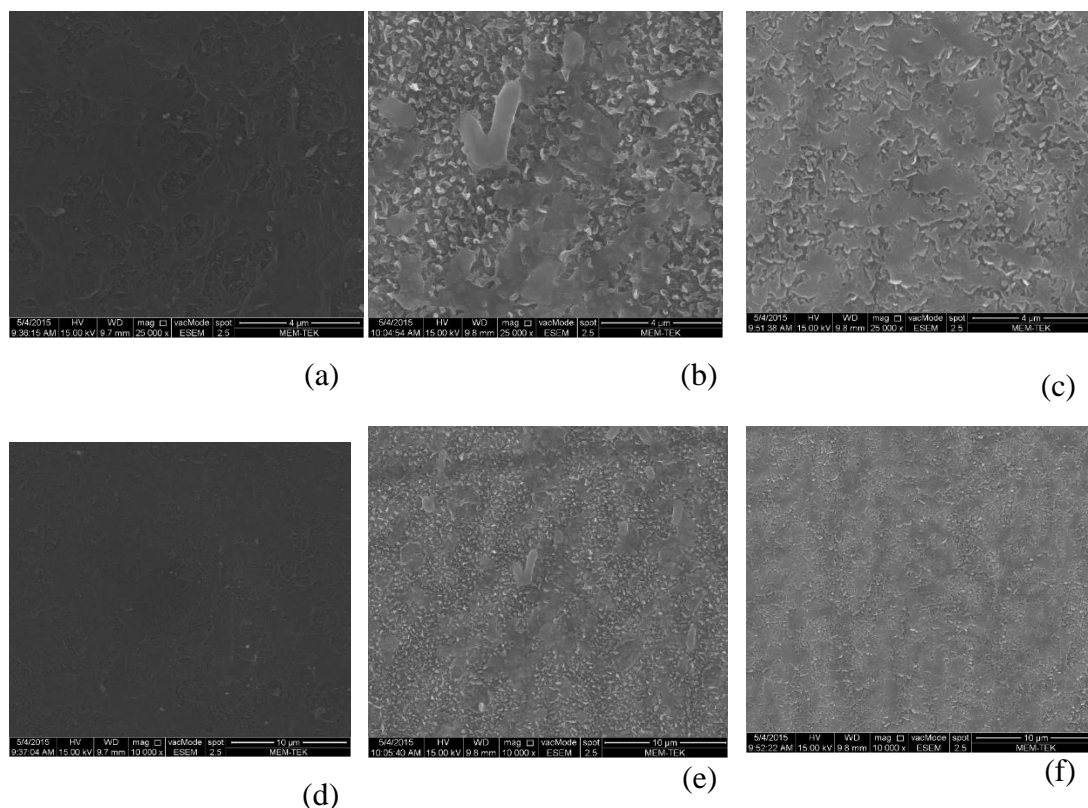


Figure 4.22: SEM images of BisBAL TFC membrane before and after incubation of membranes with *E.coli* at 37 °C for 18h (a) BisBAL TFC membrane surface before incubation; (b) BisBAL TFC membrane surface after incubation (diluted 10^{-4} with *E.coli* strain); (c) BisBAL TFC membrane surface after incubation (diluted 10^{-5} with *E.coli* strain); (d) BisBAL TFC membrane surface before incubation; (e) BisBAL TFC membrane surface after incubation (diluted 10^{-4} with *E.coli* strain); (f) BisBAL TFC membrane surface after incubation (diluted 10^{-5} with *E.coli* strain).

4.2.2.2 CSLM

The membranes from the *E.coli* tests were examined for total bacterial cell counts on the membrane surface by CLSM. Significantly higher numbers of cells were observed on the pristine TFC membrane.

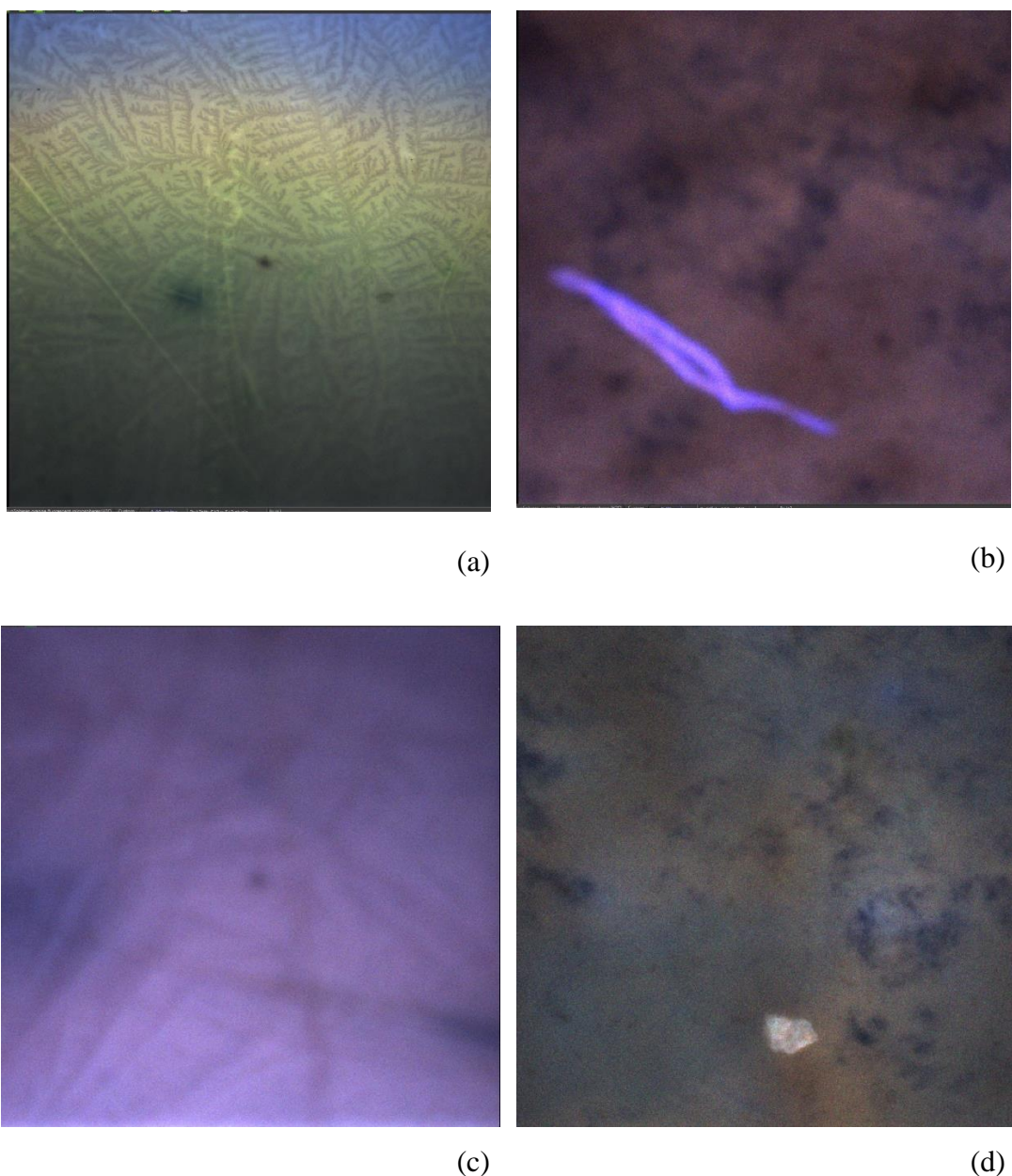


Figure 4.23: CLSM images of TFC after incubation of membranes with E.coli at 37 °C for 18h (a) BisBAL TFC membrane surface after incubation (diluted 10^{-4} with E.coli strain); (b) Pristine TFC membrane surface after incubation (diluted 10^{-4} with E.coli strain); (c) BisBAL TFC membrane surface after incubation (diluted 10^{-5} with E.coli strain); (d) Pristine TFC membrane surface after incubation (diluted 10^{-5} with E.coli strain).

According to Figure 4.23, an active bacterial community was found on the pristine membrane surfaces, whereas a few colonies were scattered on the BisBAL TFC membrane surfaces. In addition, the biofilms on the membrane surfaces mainly consisted of live bacterial cells (green color) and dead bacterial cells (red color) were

rarely observed on BisBAL TFC membrane. As shown in Figs. 8, *E.coli* could easily develop into a biofilm on the control membrane after incubation for 24 h. In contrast, the biofilm formation on BisBAL TFC membrane was substantially inhibited. In actuality, improvement of anti-adhesion ability which could slow down the initial attachment of bacteria on membrane surface might be a more effective approach to reducing biofouling than using bacteriocidal agents which aim at killing/inactivating bacteria already attached on membrane surface. The dead or inactivated bacteria may serve as anchors for the next layer of bacteria, promoting further development of biofouling.

4.2.3 Flux graphs

The flux graph of pristine TFC membrane is given in Figure 4.24. Avarage flux of distilled water was 25 l.m²/h, it reduced significantly and average flux of seawater found 3.5 l.m²/h. Lastly, avarage flux of seawater additive with *E.coli* medium found 2 l.m²/h. Low flux values may be explained with the high accumulation on the membrane surfaces. It can also be estimated from the low flux values that, membrane pores were blocked by the bacteria and seawater.

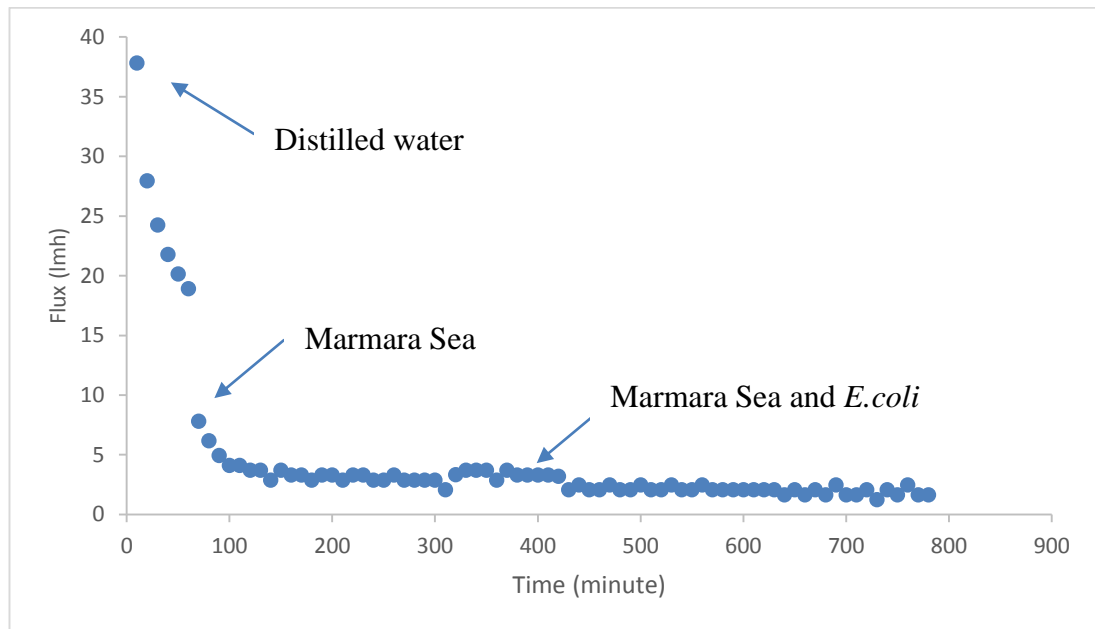


Figure 4.24: Flux of pristine TFC membrane.

Flux graph of prepared BisBAL TFC membrane as it given in Figure 4.25. Avarage flux of distilled water was 10 l.m²/h, it reduced significantly and average flux of seawater found 3.5 l.m²/h. Lastly, avarage flux of seawater additive with *E.coli*

medium found 1.6 l.m²/h. Low flux values may be explained with the accumulation on the membrane surfaces. However BisBAL TFC showed less changing flux reduction than pristine TFC. It may be attributed to the anti biofouling effect of BisBAL TFC membrane.

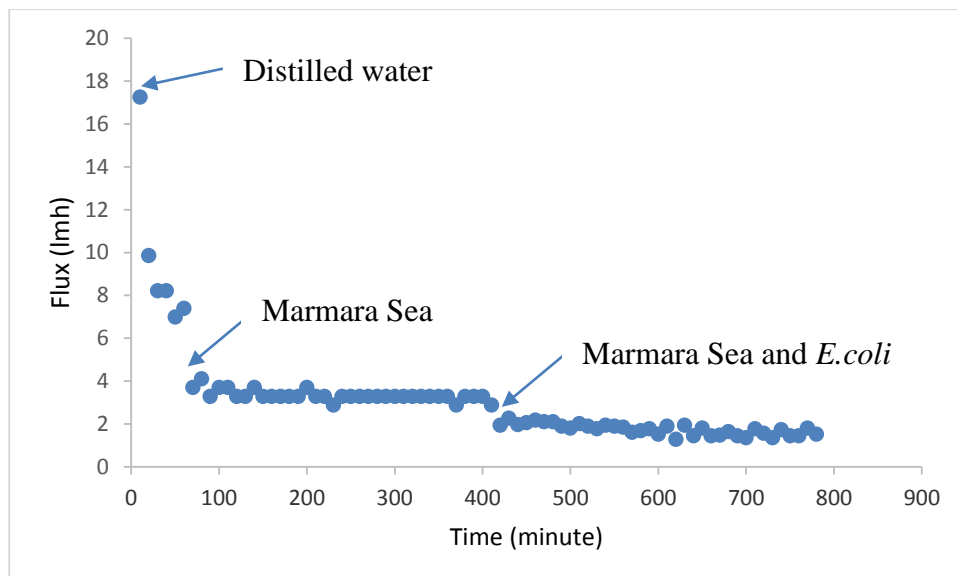


Figure 4. 25: Flux of BisBAL TFC membrane.

5. CONCLUSIONS AND RECOMMENDATIONS

TFC membranes were fabricated through interfacial polymerization method for obtaining high permeabilities, having antibacterial properties, high salt rejections, high mechanical stability values, low contact angle values and low roughness. To reach the aim mentioned above, first support layer of the membrane was prepared, best one was selected. Then TFC membranes were optimized. Finally BisBAL TFC membranes were fabricated in order to examine antibacterial properties.

Results of the performance and characterization tests for support layer of membranes containing PSF as polymers and PVP as the pore-forming agent ; and for the thin film composite membranes prepared with additive BisBAL and pristine are given in Table 5.1 comparatively in order to determine the ingredient ratios for further studies.

Table 5.2: Performances of prepared membranes.

Parameter	SUPPORT LAYER					ACTIVE LAYER	
	%16 PSF	%16 PSF %8PVP10	%16 PSF %8PVP40	%16 PSF %8PVP360	%18 PSF %4.5PVP10 %1.5PV40	Pristine TFC	BisBAL TFC
Permeability (l/m ² h.bar)	109±20	185±28	186±28	47±2	299±28	0.97- 1.42	1.42- 1.68
Contact angle (°)	80.5±3.1	74.4±2.2	82.9±2.3	82.3±1.8	68.5±2.7	29.6±1.6	28.4±2.5
Roughness(nm)	0.365	9.202	0.160	0.305	0.239	0.181	0.128
Average por siz (µm)	0.027	0.025	0.027	0.025	0.020	-	-
Young's Modulu	21.7	5.9	5.4	4.8	6.8	-	-
Elongation (%)	12.3	24.7	23.7	33.0	27.2	-	-
Tensile Strength (3.4	2.7	2.4	3.5	5.8	-	-

From the all results, major findings are listed as follows:

1. Support layer of the membrane preparation experiments (as the rate of PVP increases);

- Viscosity of the polymer solution increased with increasing molecular weight of PVP.
 - Permeability values of the membranes increased with adding PVP. However, increasing molecular weight of PVP caused the decreasing of flux.
 - Contact angle values were similar. It was appeared that while there were some structural changes in morphology of the membranes, contact angle measurements remained the same, suggesting that here the hydrophilicity was mainly controlled by the polymer chemistry.
 - Roughness values were decreasing with increasing molecular weight of PVP.
 - The fingerlike macrovoids were suppressed with increasing PVP molecular weight and structure of membrane was changed a macrovoid structure to a sponge structure.
 - With increasing of molecular weight of PVP, the elongation at break increased and the initial Young's modulus and tensile strength decreased.
 - %18 PSF %4.5 PVP10 %1.5 PV40 was chosen at the end of the experiments as support layer of membrane.
2. TFC PA membrane preparation experiments (with additive BisBAL);
- Optimum monomer concentration was found as 2% MPD and 0.01% TMC for TFC membrane preparation.
 - Flux was higher with additive BisBAL TFC membrane.
 - Contact angle values were similar.
 - Roughness values were similar.
 - It is also hard to say that roughness value directly affect the permeability and filtration performances.
3. Antifouling experiments;
- Addition of BisBAL improved the antibacterial properties of prepared membranes.

- Addition of BisBAL did not change the membrane performance. Also, it can be said that BisBAL additive may have a positive effect to increase membrane performance.
- *E. coli* grew lower on the area surrounding the BisBAL TFC membrane.
- Less changing flux reduction than pristine TFC.

In this work, preparation and characterization of TFC RO membrane having antibacterial properties was reported. Improvement of salt rejection of prepared PA TFC membranes are necessary for the membrane performance. The chemical linkage between TFC and BisBAL can be examined for improvement of membrane performance. Moreover, some other experiments such as preparation of PA TFC membranes with additive BisBAL in different concentrations, examination of residence time of BisBAL on the membrane surface can be experimented. Also, the studies on long-term test should be done in the future.

REFERENCES

- Al-Juboori, R.A., Yusaf, T.** (2012). Biofouling in RO system: Mechanisms, monitoring and controlling, *Desalination* 302 1–23.
- Alpaslan, N., Tanık, A., Dölgen, D.** (2008). Türkiye’de Su Yönetimi Sorunlar ve Öneriler , *TÜSİAD*, T/2008-09 469.
- Al-Tisan, I.A.R., Chandy, J.P., Abanmy, A.R., Hassan, A.M.** (1995). Optimization of seawater reverse osmosis pretreatment: Part III — a microbiological approach, *IDA World Congress*, Vol.4.
- Altuğ, G., Çardak, M., Çiftçi, P.S., Gürün, S.** (2013). First records and microgeographical variations of culturable heterotrophic bacteria in an inner sea (the Sea of Marmara) between the Mediterranean and the Black Sea, Turkey, *Turkish Journal of Biology* 37 184-190.
- Aptel, P., Armor, J., Audinos, R., Baker, R.W., Bakish, R., Belfort, G., Bikson, B., Brown, R.G., Bryk, M., Burke, J.J., Cabasso, I., Chern, R.T., Cheryan, M., Cussler, E.L., Davis, R.H.** (1996). Terminology for membranes and membrane processes (IUPAC Recommendations 1996), *Journal of Membrane Science* 120 149-159.
- Ashhab, A.A., Gillor, O., Herzberg, M.** (2014). Biofouling of reverse-osmosis membranes under different shear rates during tertiary wastewater desalination: Microbial community composition, *Water Research* 67 86-95.
- Badireddy, A., Chellam, S.** (2011). Bismuth dimercaptopropanol (BisBAL) inhibits formation of multispecies wastewater flocs, *Journal of Applied Microbiology* 110, 1426–1437.
- Badireddy, A., Hernandez-Delgadillo, R., Sa’nchez-Na’jera, R., Chellam, S., Cabral-Romero, C.** (2014). Synthesis and characterization of lipophilic bismuth dimercaptopropanol nanoparticles and their effects on oral microorganisms growth and biofilm formation, *Journal Nanopart Res.* Vol. 16. pp. 2456.
- Cadotte, J.E., Petersen, R.J., Larson R.E., Erickson, E.E.** (1980). A new thin-film composite seawater reverse osmosis membrane, *Desalination* 32 25-31.
- Claudio, C., Chellam, S.** (n.d.). Bismuth nanoparticles: antimicrobials of broad-spectrum, low cost and safety, *Nanomedicine* p.p 430-438.

- Codony, F., Domenico, P., Mas, J.** (2003). Assessment of bismuth thiols and conventional disinfectants on drinking water biofilms. *J Appl Microbiol*, pp. 288-93.
- Deng, B., Ding C., Yin, J.** (2014). Effects of Polysulfone (PSf) Support Layer on the Performance of Thin-Film Composite (TFC) Membranes. *Journal of Chemical and Process Engineering*, 1 1-8.
- Denyer, S.P., Hugo, W.B.** (1991). Mechanisms of Action of Chemical Biocides, Their Study and Exploitation, *Blackwell Scientific Publications*, London.
- Domenico, P.** (2002). Method and composition for inhibiting bacteria, US Patent, No: RE37793 E1 dated 16.7.2002.
- Domenico, P., Salo, R., Novick, S., Schoch, P., Van Horn, K., Cunha, B.** (1997). Enhancement of bismuth antibacterial activity with lipophilic thiol chelators, *Antimicrobial Agents And Chemotherapy*. pp. 1697-1703.
- El-Aassar, A., M., A.** (2012). Polyamide Thin Film Composite Membranes Using Interfacial Polymerization: Synthesis, Characterization and Reverse Osmosis Performance for Water Desalination, *Australian Journal of Basic and Applied Sciences*, 6 382-391.
- Fane, A.G., Tang, C.Y., Wang, R.** (2011). Membrane Technology for Water: Microfiltration, Ultrafiltration, Nanofiltration, and Reverse Osmosis, *Elsevier*.
- Feng, C., Wang, R., Shi, B., Li, G., Wu, Y.** (2006). Factors affecting pore structure and performance of poly(vinylidene fluoride cohexafluoro propylene) asymmetric porous membrane, *Journal of Membrane Science* 277 55–64.
- Fritzmann, C., Löwenberg, J., Wintgens, T., Melin, T.** (2007). State-of-the-art of reverse osmosis desalination, *Desalination* 216 1–76.
- Ghosh, A.K., Jeong, B.H., Huang, X., Hoek , E.M.V.** (2008). Impacts of reaction and curing conditions on polyamide composite reverse osmosis membrane properties, *Journal of Membrane Science* 311 34–45.
- Ghosh, A.K., Hoek , E.M.V.** (2009). Impacts of reaction and curing conditions on polyamide composite reverse osmosis membrane properties, *Journal of Membrane Science* 311 34–45.

- Greenlee, L.F., Lawler, D.F., Freeman, B.D., Marrot, B., Moulin, P.** (2009). Reverse osmosis desalination: Water sources, technology, and today's challenges Review, *Water Research* 43 2317-2348.
- Hernandez-Delgadillo, R., Velasco-Arias, D., Diaz, D., Arevalo-Niño, K., Garza-Enriquez, M., Garza-Ramos, M., Cabral-Romero, C.** (2012). Zerovalent bismuth nanoparticles inhibit *Streptococcus mutans* growth and formation of biofilm, *Int J Nanomedicine* 7 2109-13.
- Hirose, M., Ito, H., Kamiyama, Y.** (1996). Effect of skin layer surface structures on the flux behaviour of RO membranes, *Journal of Membrane Science* 121 209–215.
- Idris, A., Yet, L.K.** (2006). The effect of different molecular weight PEG additives on cellulose acetate asymmetric dialysis membrane performance, *Journal of Membrane Science* 280 920–927.
- Ismail, A.F., Padaki, M., Hilal, N., Matsuura, T., Lau, W.J.** (2015). Thin film composite membrane, Recent development and future potential, *Desalination* 356 140–148.
- Ivnitskya, H., Katza, I., Minzc, D., Shimonid, E., Chene, Y., Tarchitzkye, J., Semiath, R., Dosoretza, C.** (2005). Characterization of membrane biofouling in nanofiltration processes of wastewater treatment, *Desalination* 185 255–268.
- Jeong, B.H., Hoek, E.M.V., Yan, Y., Subramani, A., Huang, X., Hurwitz, G., Ghosh, A.K., Jawor, A.** (2007). Interfacial polymerization of thin film nanocomposites: A new concept for reverse osmosis membranes, *Journal of Membrane Science* 294 1–7.
- Jewrajka, S.K., Reddy, A.V.R., Rana, H.H., Mandal, S., Khullar, S., Haldar, S., Joshi, N., Ghosh, P.K.** (2013). Use of 2,4,6-pyridinetricarboxylic acid chloride as a novel co-monomer for the preparation of thin film composite polyamide membrane with improved bacterial resistance, *Journal of Membrane Science* 439 87–95.
- Joo, S.H., Tansel, B.** (2015). Novel technologies for reverse osmosis concentrate treatment: A review, *Journal of Environmental Management* 150 322-335.

- Kang, G., Cao, Y.** (2012). Development of antifouling reverse osmosis membranes for water treatment: A review, *Water Research* 46 584-600.
- Kang, S., Herzberg, M., Rodrigues, D.F., Elimelech, M.** (2008). Antibacterial effects of carbon nanotubes: size does matter! *Langmuir* 24 6409-6413.
- Kirk, R.E., Othmer, D.F.** Encyclopedia of chemical technology. 3rd ed 1980, New York ; Chichester: John Wiley & Sons, Inc. Hoboken, 200.
- Kochkodan, V. Hilal, N.** (2015). A comprehensive review on surface modified polymer membranes for biofouling mitigation, *Desalination* 356 187-207.
- Kucera, J.** (2010). Reverse Osmosis Design, Processes, and Applications for Engineers, 6, New Jersey: John Wiley & Sons, Inc. Hoboken.
- Lau, W.J., Ismail, A.F., Misdan, N., Kassim, M.A.** (2012). A recent progress in thin film composite membrane: a review, *Desalination* 287 190-199.
- Lau, W.J., Ismail, A.F., (2011).** Progress in Interfacial Polymerization Technique on Composite Membrane Preparation, *International Proceedings of Chemical, Biological and Environmental Engineering* Vol.17.
- Lee, K., Arnot, T., Mattia, D.** (2011). A review of reverse osmosis membrane materials for desalination—Development to date and future potential, *Journal of Membrane Science* 370 1-22.
- Li, L., Zhang, S.B., Zhang, X.S., Zheng, G.D.** (2007). Polyamide thin film composite membranes prepared from 3,4_,5-biphenyl triacyl chloride, 3,3_,5,5_-biphenyl tetraacyl chloride and *m*-phenylenediamine, *Journal of Membrane Science* 289 258-267.
- Li, Q., Mahendra, S., Lyon, D.Y., Brunet, L., Liga, M.V., Li, D., Alvarez, P.J.J.** (2008). Antimicrobial nanomaterials for water disinfection and microbial control: Potential applications and implications, *Water Research* Vol. 42, No. 18, 4591-4602.
- Liu, L.F., Yu, S.C., Zhou, Y., Gao, C.J.** (2006a). Study on a novel polyamide-urea reverse osmosis composite membrane (ICICMPD). I. Preparation and characterization of ICIC-MPD membrane, *Journal of Membrane Science* 281, 88-94.
- Liu, L.F., Yu, S.C., Wu, L.G., Gao, C.J.** (2006b). Study on a novel polyamide-urea reverse osmosis composite membrane (ICICMPD). II. Analysis of

- membrane antifouling performance. *Journal of Membrane Science* 283, 133-146.
- Liu, L.F., Yu, S.C., Wu, L.G., Gao, C.J.** (2008). Study on a novel antifouling polyamide-urea reverse osmosis composite membrane (ICIC-MPD) III. Analysis of membrane electrical properties. *Journal of Membrane Science* 310, 119-128.
- Malaeb, L., Ayoub, G.M.** (2011). Reverse osmosis technology for water treatment: State of the art review, *Desalination* 267 1–8.
- Matin, A., Khan, Z., Zaidi, S.M.J., Boyce, M.C.** (2011). Biofouling in reverse osmosis membranes for seawater desalination: Phenomena and prevention, *Desalination* 281 1–16.
- Matsuyama, H., Maki, T., Teramoto, M., Kobayashi, K.** (2003). Effect of PVP Additive on Porous Polysulfone Membrane Formation by Immersion Precipitation Method, *Separation Science and Technology*, Vol. 38-14 3449-3458
- Misdan, N., Lau, W.J., Ismail, A.F.** (2012). Seawater Reverse Osmosis desalination by thin-film composite membrane—Current development, challenges and future prospects, *Desalination* 287 228–237.
- Mulder, M.** (1996). Basic Principles of Membrane Technology. Boston: Kluwer Academic Publishers, Netherlands, pp.6.
- Mutamim, N., Noor, Z., Hassan, M., Yuniarto, A., Olsson, G.** (2013). Membrane bioreactor: Applications and limitations in treating high strength industrial wastewater, *Chemical Engineering Journal*. Vol. 225, pp. 109-119.
- Nath, K.** (2008). Membrane Separation Processes. Prentice-Hall, India, pp.30-33.
- Nguyen, T., Roddick, F.A., Fan, L.** (2012). Biofouling of Water Treatment Membranes: A Review of the Underlying Causes, Monitoring Techniques and Control Measures, *Membranes* 2(4) 804-840.
- Petersen, R.J., Cadotte, J.E.**, (1990). Thin film composite reverse osmosis membrane in: M.C. Porter (Ed.), Handbook of Industrial Membrane Technology, Noyes Publication, New Jersey.

- Ramon ,Z.Y., Hoek, E.M.V.,** (2013). Transport through composite membranes, part 2: Impacts of roughness on permeability and fouling, *Journal of Membrane Science* 425–426 141–148.
- Shannon, M., Bohn, P., Elimelech, M., Georgiadis, J., Marin, B., Mayes A.** (2008). Science and technology for water purification in the coming decades, *Nature* 452 301-310.
- Shawky, H.A., Chae, SR., Lin, S., Wiesner M.R.,** (2011). Synthesis and characterization of a carbon nanotube/polymer nanocomposite membrane for water treatment, *Desalination* 272 46-50.
- Singh, R.,** (2006). Hybrid Membrane Systems for Water Purification: Technology, Systems Design and Operations, *Elsevier*.
- Takao, S.** (1983). Process for Producing Acrylonitrile Separation Membranes in Fibrous Form, US Patent 4,409,162.
- Tarboush, B.J.A., Rana, D., Matsuura, T., Arafat, H.A., Narbaitz, R.M.** (2008). Preparation of thin-film-composite polyamide membranes for desalination using novel hydrophilic surface modifying macromolecules, *Journal of Membrane Science* 325 166-175.
- Uemura, T., Henmi, M.** (2008) Thin-film composite membranes for reverse osmosis, In Li, N.N., Fane, A.G., Winston Ho, W.S., Matsuura, T. Advanced Membrane Technology and Applications 4, New Jersey: John Wiley & Sons, Inc., Hoboken.
- Wang, L., Chen, K., Jiaping, P., Nazih, K.** (2010). Membrane and desalination technologies. *Handbook of Environmental Engineering* Vol. 13, no 2.
- Wilf, M.** (2007). The Guidebook to Membrane Desalination Technology, Balaban Desalination Publication, Italy.
- Vedavyasan, C.V.** (2007). Pretreatment trends - an overview, *Desalination* 203 296–299.
- Yang, H. L., Lin, J.C.T., Huang, C.** (2009). Application of nanosilver surface modification to RO membrane and spacer for mitigating biofouling in seawater desalination, *Water Research* 43 3777-3786.
- Xie, W., Geise, G.M., Freeman, B.D., Lee, H., Byun, G., McGrath, J.E.** (2012). Polyamide interfacial composite membranes prepared from m-phenylenediamine, trimesoyl chloride and a new disulfonated diamine, *Journal of Membrane Science* Vol. 403–404 152–161.

- Url1** <http://www.un.org/waterforlifedecade/pdf/2006_unwater_coping_with_water_scarcity_eng.pdf> date retrieved 15.04. 2015
- Url-2** <<http://www.technologyreview.com/featuredstory/534996/megascale-desalination/>> date retrieved 20.04. 2015
- Url-3** <<http://yunus.hacettepe.edu.tr/~haydar09/wordpress/>> date retrieved 23.04. 2015
- Url-4** <http://www.toray.com/ir/pdf/lib/lib_a265.pdf> date retrieved 18.03. 2015
- Url-5** <<http://education.jlab.org/itselemental/ele083.html>> date retrieved 23.04. 2015

CURRICULUM VITAE

Name Surname: Şeyma Yılmaz

Place and Date of Birth: 21.01.1989, Istanbul

Address: Çöreotu Sok. Örnek Apt. 5/2 Bahçelievler/İSTANBUL

E-Mail: seymayilmazk@gmail.com

B.Sc.: I.T.U. Environmental Engineering

